ROLE OF MEKK2 PHOSPHORYLATION AT THREONINE 263 ON SMYD3-MEDIATED METHYLATION OF LYSINE 260

Rachel Corridore

A THESIS SUBMITTED TO
THE FACULTY OF GRADUATE STUDIES
IN PARTIAL FULFILLMENT OF THE REQUIREMENTS
FOR THE DEGREE OF
MASTER OF SCIENCE

GRADUATE PROGRAM IN BIOLOGY
YORK UNIVERSITY
TORONTO, ONTARIO

APRIL 2024

© Rachel Corridore, 2024

Abstract

MEKK2 is a protein serine/threonine-kinase involved in the activation of many MAP-kinase signalling pathways. In a previous study, SMYD3-mediated methylation at K260 of MEKK2 was demonstrated to promote aberrant input downstream of oncogenic Ras-signaling, promoting Ras-driven PDAC and LAC progression. Our lab has previously characterized the role of MEKK2 phosphorylation at T283 and has recently discovered a novel second phosphorylation site at T263. We show that together, these sites form the bipartite binding group for 14-3-3 adapter proteins. This study focuses on characterizing T263 and T283 as regulatory phosphosites in K260 methylation and implicates 14-3-3 as a promoting factor in facilitating SMYD3-mediated methylation at K260. Our findings provide a potential mechanism of MEKK2 oncogenic function, whereby 14-3-3 preserves phosphorylation at T263 and T283, together promoting K260 methylation and MEKK2 activation. Our study characterizes T263 and T283 of MEKK2 and 14-3-3 phosphoadapter proteins as potential therapeutic targets in PDAC and LAC.

Acknowledgements

I would like to express my gratitude to my supervisor, Dr. Michael Scheid, for granting me the opportunity to pursue this degree and for his invaluable guidance and mentorship over the years. With out his continued support and encouragement, always making time to discuss data and experimental designs, and trusting me with his lab, this would not have been possible. I extend my sincere gratitude to Dr. Chun Peng, for her helpful feedback and expertise, as well as to the rest of the examining committee for their time, consideration, and expertise throughout this process.

I am sincerely appreciative to my lab mates, Ghazal and Shaina, and my colleague David, for their friendship, assistance, and guidance over the years. I would like to thank our laboratory technician, Baodong, for all his guidance and for teaching me how to run my first Western Blot. I would also like to thank my first research practicum student, Sormeh, for all her assistance.

I would like to extend a special thanks to my friends and family, for their unwavering support and encouragement. I am deeply grateful to my parents, Gabe and Mary, for their continued support and raising me to never give up on my dreams. To my sister, Lauren, for always believing in me. And to my partner, Christian, for supporting me and encouraging me every step of the way.

TABLE OF CONTENTS

LIST OF FIGURES

LIST OF TABLES

LIST OF ABBREVIATIONS

CO-IP	Co-immunoprecipitation
DMEM	Dulbecco's Modified Eagle Medium
DMSO	Dimethyl sulfoxide
DNA	Deoxyribonucleic acid
EDTA	Ethylenediaminetetraacetic acid
eGFP	Enhanced green fluorescent protein
FBS	Fetal bovine serum
GDP	Guanosine Diphosphate
GTP	Guanosine Triphosphate
HEK 293T	Human embryonic kidney 293T cells
IP	Immunoprecipitation
KLD	Kinase, Ligase, DpnI
LAC	Lung adenocarcinoma
MAPK	Mitogen-activated protein kinase
MCS	Multiple cloning site
MEKK2	Mitogen-activated protein kinase kinase 2
MEKK3	Mitogen-activated protein kinase kinase 3
PBS	Phosphate buffered saline
PCR	Polymerase chain reaction
PDAC	Pancreatic ductal adenocarcinoma
RE	Restriction enzyme
RT	Room temperature
SD	Standard deviation
SDS-PAGE	Sodium dodecyl-sulfate polyacrylamide gel electrophoresis
SMYD3	SET and MYN-domain containing 3 (lysine methyltransferase)
WT	Wild type

Chapter 1: Introduction and Research Objectives

1.1 Posttranslational Modifications

Proteins commonly undergo reversible modifications known as posttranslational modifications after translation. These reactions involve the addition of a modifying group to one or more amino acids within a target protein. These modifications cause functional alterations to the protein which allow for regulation of cellular processes, such as protein-protein interactions and signalling pathways.[1] Posttranslational modifications and the crosstalk between these protein modifications not only play critical roles in normal cellular processes, but they are also linked to many oncogenic signalling events involved in tumorigenesis.[2] This study focuses on the reversible posttranslational phosphorylation, methylation, and ubiquitination of single amino acid sites.

1.1.1 Phosphorylation

Protein kinases catalyze the transfer of the terminal phosphoryl group of ATP to their specific protein substrate.[3] The addition of the phosphate group occurs at either a serine, threonine, or tyrosine residue. This chemical modification can be reversed by phosphatases, which catalyze the removal of the phosphate group from the substrate protein. Serine and threonine phosphorylation is usually involved in the regulation of processes such as cell-cycle progression, the DNA-damage response, and cellular growth. Phosphorylation of tyrosine residues primarily regulates the activation of signalling cascades that control cellular proliferation and differentiation.[4]

1.1.2 Methylation

In eukaryotic cells, methyl groups are predominately added to basic and positively charged lysine and arginine residues in target proteins. When methylation occurs on the nuclear histone proteins in the cell nucleus, it plays a role in histone modification and transcriptional regulation.[1] However, non-histone proteins are also subject to regulation by methylation at the posttranslational level. The regulatory effect of methylation on protein activity will depend on the site and degree of methylation. Methylation of lysine and arginine residues on non-histone proteins has emerged as an important regulator of cellular signal transduction mediated by many signalling pathways, including the mitogen-activated protein kinase (MAPK) signalling pathway.[5] Unique to methylation, this chemical modification can result in three different methylated states on the same residue, mono-, di-, or tri-methylated. The methylation status of target proteins is controlled by two groups of enzymes, methyltransferases and demethylases.[4,6]

1.1.3 Ubiquitination

Protein ubiquitination occurs in a three-step reaction involving ubiquitin-activating enzyme (E1), ubiquitin-conjugating enzyme (E2), and ubiquitin-protein ligase (E3). This process results in the covalent linkage of a ubiquitin molecule, a short modifier protein, to the ubiquitination site of a protein substrate. Additional ubiquitin molecules can be attached to the lysine residues, ubiquitin attachment sites, in each preceding ubiquitin molecule to form ubiquitin chains. These ubiquitin chains serve as the recognition signal for proteosomes to initiate proteolysis of these polyubiquitinated proteins.[4,7,8] Although ubiquitination often results in the degradation of the ubiquitinated protein through the ubiquitin-proteasome pathway, this modification of the protein can alternatively function to alter protein-protein interactions.[7]

1.2 MAP Kinase Signalling Pathways

Mitogen-activated protein kinases (MAPKs) are serine/threonine kinases that regulate signal transduction pathways in response to various external stimuli. All eukaryotic cells possess multiple MAPK pathways that coordinate to regulate cellular processes such as gene expression, mitosis, proliferation, metabolism, differentiation, motility, survival, and apoptosis. The biological response to MAPK activation depends on the type of stimulus present and the specific MAPK pathway that becomes activated.[9–12] The most extensively studied types of MAPKs are the conventional MAPKs which are categorized into four groups comprised of the extracellular signal-regulated kinases 1/2 (ERK1/2), c-Jun (N)-terminal kinases 1/2/3 (JNK1/2/3), p38 isoforms (α, β, γ, and δ) and ERK5.[12] Each of these MAPK groups are composed of a set of three evolutionarily conserved and sequentially-acting kinases: a MAP kinase kinase kinase (MAPKKK/MEKK/MAP3K), a MAP kinase kinase (MAPKK/MEK/MAP2K), and a MAP kinase (MAPK).[9,10,12]

1.3 MAPK Pathway Activation

MAP kinase pathway activation involves a conserved series of signalling events resulting in phosphorylation of each sequential MAP kinase in the cascade. The general sequence of a MAP kinase signalling cascade involves the sequential activations of a MAP3K followed by a MAP2K, and lastly a MAPK[9,10] Extracellular stimuli such as stress signals, growth factors, mitogens, and cytokines interact with cell surface receptors and cause activation of membrane-bound GTPase proteins of the Ras/Rho family and other membrane-localized protein kinases, such as Src family kinases and Akt. Interaction with these GTPase proteins or phosphorylation by protein kinases are typically responsible for the activation of the MAP3K in the cascade.[11–14] Following activation, the MAP3K serine/threonine kinase will phosphorylate its substrate

MAP2K on a conserved Ser/Thr motif: Ser-X-X-X-Ser/Thr.[15] Once activated, the MAP2K activates the MAPK through dual phosphorylation of the threonine and tyrosine residues within the conserved (Thr-X-Tyr) motif located in the activation loop of the kinase domain.[12,16] MAPKs are serine-threonine kinases that, once activated, facilitate a biological response by causing changes in protein function and gene expression. MAPKs can directly phosphorylate cytoplasmic substrates, causing changes in protein function, or they can translocate to the nucleus where they can regulate the activity of transcription factors controlling gene expression.[11,17]

Signal specificity within the MAPK signalling network is extremely crucial to maintaining normal regulation of cellular processes. The MAPK is equipped with docking sites for the appropriate upstream MAP2K and downstream substrates which promotes signal specificity in MAPK signalling. These docking sites allow high-affinity protein interactions and activation of specific downstream target proteins, ensuring the appropriate biological response is carried out.[11,18,19] Specificity in MAPK signalling is also achieved at the level of extracellular stimulation, as specific MAPKs are activated in response to specific stimuli.[20]

1.4 The Ras-Raf-MEK-ERK MAPK Pathway

The Ras-Raf-MEK-ERK pathway is a mitogen-activated protein kinase (MAPK) pathway that plays a key regulatory role in various cellular processes, including proliferation, differentiation, survival, and migration.[21] The involvement of this MAPK pathway in the survival and development of tumour cells has been widely documented in various cancers.[22] Driver mutations within Ras genes, predominately K-Ras, is the most prevalent oncogenic factor across diverse cancers, accounting for approximately 30% of all cancer types and impacts nearly 10% of cancer patients.[22] An overview of the oncogenic mechanism of the Ras-Raf-MEK-ERK cascade is illustrated in Figure 1.1.

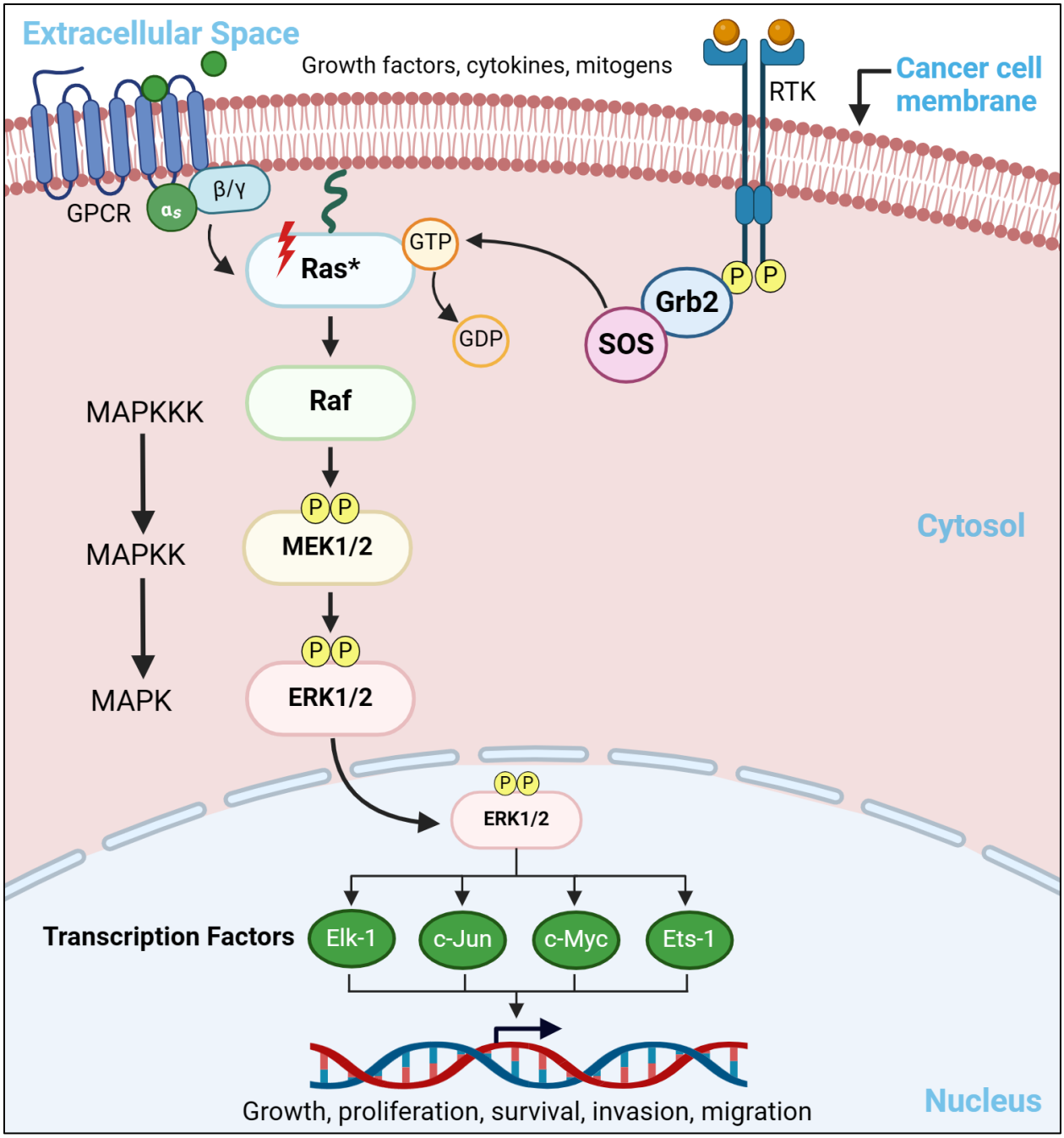

Figure 1.1. Oncogenic Ras-Raf-MEK-ERK signalling and transcriptional targets of ERK1/2. G-protein-coupled receptor (GPCR) and receptor tyrosine (RTK) activation induced by growth factors, cytokines, or mitogens, promotes Ras-GDP to Ras-GTP exchange and activation. Mutated Ras oncoprotein drives oncogenic activation of the Ras-Raf-MEK-ERK cascade. Upon activation, ERK1/2 translocates to the nucleus following dual phosphorylation by MEK1/2. Within the nucleus, ERK1/2 upregulates activation of various transcription factors including Elk-1, c-Jun, c-Myc, and Ets-1, promoting unregulated cellular processes such as growth, proliferation, survival, invasion, and migration, contributing to cancer progression. Created with BioRender.com.

1.4.1 Ras Oncogene and Isoforms

The Ras gene family, including H-Ras, K-Ras, and N-Ras, comprise the most frequently mutated oncogenes in human cancer. With the highest mutation frequencies observed in lung, colorectal, and pancreatic cancer – the top three causes of cancer-related mortality in the United States – the development of Ras-inhibitory drugs remains a primary focus in cancer research.[23] Five Ras mutations account for 70% of all cancers characterized by a Ras mutation: G12D, G12V, G12C, G13D, and Q61R.[24] Specifically, G12D or G12C mutations with in K-Ras have been observed to upregulate MAPK signalling within the Ras-Raf-MEK-ERK cascade. Oncogenic mutations in Ras genes are typically defined by single-base substitutions that allow constitutive Ras-MAPK pathway activation.[25] K-Ras is the most commonly mutated member with the Ras family of GTPases and is considered to be the most common oncogenic driver gene in human cancers.[26] Notably, the K-Ras isoform is mutated in approximately 84% of all Ras-mutated cancers, with nearly 100% K-Ras mutation frequency in pancreatic ductal adenocarcinoma (PDAC), which is considered the most Ras-dependent cancer type.[23] Due to its prevalence and significance in cancer, identifying therapeutic targets and developing therapies to inhibit mutated K-Ras activity in cancers marked by oncogenic K-Ras activation has become a focus in cancer research.

1.4.2 Ras Activation by RTKs

Ras is a small membrane-localized GTP-binding protein that initiates the Ras-Raf-MEK-ERK MAPK signal transduction pathway upon extracellular stimulation. Many growth factors, including epidermal growth factor (EGF), bind extracellularly to transmembrane receptors with intrinsic tyrosine kinase activity.[27] For instance, the EGF-receptor (EGFR) functions as a receptor tyrosine kinase (RTK), to which EGF will bind as a ligand and promote RTK activation.[28] RTKs are generally activated by receptor-specific ligands which, upon binding, will

promote ligand-induced receptor dimerization and trans-autophosphorylation of multiple tyrosine residues in each tyrosine kinase domain.[29] Src homology 2 (SH2) domain-containing signalling proteins, including Grb2, can then bind these tyrosine-phosphorylated residues within the intracellular regions of the activated RTK.[27] Grb2 exists cytoplasmically in a complex with SOS, a guanylnucleotide exchange factor, and converts inactive Ras-GDP to its active Ras-GTP state. The Grb2-SOS complex binds to the activated RTK where Grb2 serves as an adaptor protein to activate SOS and allow the Ras GDP/GTP exchange.[27,30]

1.4.3 Raf Kinases

The Raf family of serine/threonine kinases, including isoforms such as A-Raf, B-Raf, and C-Raf (or Raf-1), function as MAP3Ks and upstream kinases in the MAPK signalling pathway.[31] In quiescent cells, Raf kinases remain in the cytosol as inactive monomers. Raf autoinhibition is maintained through intramolecular interactions between its regulatory and catalytic domains, coupled with binding of a 14-3-3 dimer to specific serine phosphosites.[32] Raf activation is initiated by a direct interaction with active Ras-GTP, recruiting Raf to the membrane.[31] Raf autoinhibition is relieved upon Ras binding, promoting a conformational change requires to allow Raf homodimerization and kinase activation.[32,33] Raf kinases catalyze phosphorylation of S218/222 of MEK1 and S222/S226 of MEK2 with in the activation segments.[34,35]

1.4.4 Mitogen-Activated Protein Kinase/ERK kinase

MEK1/2 is a dual-specificity serine/threonine MAP2K, capable of phosphorylating ERK1/2 at both threonine (T202/185) and tyrosine residues (Y204/187), within its activation loop.[35,36] This dual phosphorylation is essential for the full activation of ERK and subsequent downstream signalling.[37] Upon activation, MEK1/2 phosphorylates its primary substrate ERK1/2 with high

selectivity, ensuring the precise and coordinated activation of ERK1/2 signalling and regulation of cellular processes.[38] However, oncogenic Ras activation results in dysregulation of MEK1/2, leading to aberrant ERK1/2 activation and thereby contributing to tumorigenesis in various cancers such as melanoma, pancreatic, lung, colorectal, and breast cancers.[39]

1.4.5 Extracellular Signal-Regulated Kinase and Oncogenic Functions

ERK1/2 is a serine/threonine MAPK that play a key regulatory role in cell proliferation and is activated in response to mitogenic growth factors including epidermal growth factor (EGF), insulin-like growth factor-1 (IGF-1), and platelet-derived factor (PDGF).[12,36,40] ERK1/2 has also been shown to respond to ligand stimulation of heterotrimeric G protein-coupled receptors (GPCRs), osmotic stress, and cytokines.[12] ERK1/2 is characterized by an extensive substrate specificity, having both nuclear and cytosolic targets, thereby contributing to the regulation of various cellular processes in both normal and oncogenic pathway signalling.[35]

The ERK1 and ERK2 module controls cell proliferation by targeting various effectors including transcription factors that regulate immediate early genes (IEGs) involved in the early stages of the cell cycle and positive regulators of the cell cycle.[12,41] Upon activation and nuclear translocation, ERK1/2 directly phosphorylates nuclear transcription factors such as Elk-1, through docking interactions. Elk-1 is an transcription factor involved in expression of immediate-early (IE) genes, such as c-Jun and c-Fos.[41,42] The expressed c-Jun protein is stabilized through direct phosphorylation by ERK1/2, promoting association with c-Fos, a transcription factor involved in cell cycle progression.[43,44] Together, these proteins form the early response AP-1 (activating protein-1) transcription complexes. AP-1 complexes activate expression of cell cycle regulators, cyclin D1, which, in turn, forms complexes with cyclin-dependent kinases CDK4 and CDK6, allowing G1/S transition and cell cycle progression.[45,46] In

cancer, driver mutations in upstream Ras or Raf genes result in overactivation of the Ras-Raf-MEK-ERK signalling cascade. Consequently, sustained activation of ERK1/2 promotes uninterrupted cell cycle progression and proliferation, contributing to tumorigenesis and cancer progression.[47]

ERK1/2 enhances survival of cancer cells through the promotion of pro-survival signals in response to RTK activation. ERK1/2 signalling regulates the function and expression of various anti-apoptotic proteins, including Mc1-1, a member of the Bcl-2 family proteins.[48] The intrinsic apoptosis pathway is regulated by the Bcl-2 family of pro-survival and pro-apoptotic proteins.[49] Therefore, Mcl-1 upregulation by oncogenic Ras-ERK1/2 activation contributes to survival of cancer cells by supressing the intrinsic apoptotic pathway.[48,49]

The proto-oncogene c-Myc is a transcription factor that regulates numerous signalling pathways involved in cell metabolism, growth, and proliferation.[50] ERK1/2 regulates c-Myc at the posttranslational level through direct phosphorylation at S62, promoting c-Myc stabilization and increasing transcriptional activity.[51,52] Consequently, oncogenic K-Ras-driven ERK1/2 activation promotes c-Myc accumulation, resulting in upregulated c-Myc-mediated expression of genes that regulate cell growth and proliferation, including cell-cycle regulators cyclin D1 and CDK4/6.[50,51] Therefore, dysregulated c-Myc activity contributes to uncontrolled proliferation and survival of cancer cells driven by aberrant K-Ras-ERK signalling.

The Ets-1 proto-oncogene is a member of the Ets family of transcription factors. Ras-mediated ERK1/2 activation results in direct phosphorylation of Ets-1 at T38, increasing Ets-1 transcriptional activity.[53] Ets-1 Ras-responsive elements have been identified in the promoters of genes encoding matrix metalloproteases (MMPs) *MMP1, MMP9, and PLAU*.[54] MMPs are proteolytic enzymes that are known to be involved in cellular invasion and migration, which are

key processes in cancer progression and metastasis.[54,55] MMPs promote cancer invasion by degrading components of the ECM, creating pathways for cancer cells to migrate into surrounding healthy tissues.[56] Consequently, Ets-1 upregulation contributes to the metastatic ability of cancers resulting from oncogenic Ras-ERK1/2 activation.

1.5 MEKK2 and MEKK3 Pathways

MEKK2 (MAP3K2) and MEKK3 (MAPK3K3) are Ser/Thr protein kinases expressed in various types of tissue and belongs to the MEKK/STE11 subgroup of the MAP(3)kinase family.[57] These MAP3Ks initiate the MAPK cascade through integration of various extracellular signals including growth factors, cytokines, cellular stressors and mitogenic signals, allowing regulation of cellular responses to diverse stimuli.[58–61] MEKK2 and MEKK3 share significant amino acid sequence homology and substrate specificity.[62,63] MEKK2/3 stimulate the activation of all four classical MAPKs: JNK 1/2/3, ERK5, ERK1/2, and p38 α/β/δ/γ [12,60,64–66] MEKK2/3 signalling has been documented to result in transcription factor nuclear factor-kappa B (NF-κB) activation downstream of MAPK activation, promoting expression of genes involved in immune responses, inflammation, cell growth, survival and development.[67,68] Therefore, MEKK2 and MEKK3 play crucial roles in regulating many cellular processes including cell growth, proliferation, differentiation, apoptosis, and immune responses.[12,22,60,69] An overview of MEKK2/3 signal integration and activation of various MAPK downstream effectors is illustrated in Figure 1.2.

As discussed, MEKK2/3 become activated upon extracellular stimulation and initiate the activation of various MAPK cascades. MEKK2/3 follow the typical canonical MAPK signalling mechanism, whereby the activated MAP3K will phosphorylate and activate downstream MAP2Ks (also known as MEKs or MKKs), which in turn phosphorylate and activate the final MAPK effectors in the MAPK cascade.[9,10,12]

In the activation of stress-responsive c-Jun N-terminal kinase (JNK), MEKK2/3 initiates the MAPK cascade by signalling to MAPKKs, MKK4 (MEK4) and MKK7 (MEK7) which then directly phosphorylate and activate JNK.[70,71] The JNK signalling pathway is involved in the regulation of many cellular processes, including growth, transformation, and apoptosis.[72]

In response to growth factors, mitogens, cytokines, and stressors, MEKK2/3 phosphorylates MEK5, a specific MAP2K for ERK5, activating ERK5 by phosphorylating its activation loop within the kinase domain.[73–76] MEKK2/3 are the only two of the 19-member MAP3K superfamily to encode the conserved protein binding PB1 domain.[62,63] MEKK2/3 facilitates interaction with MEK5 through their protein binding PB1 domains, establishing a signalling complex, thereby coordinating the transmission of activating signals from MEKK2/3 to ERK5.[77–79] ERK5 activation typically results in the activation of genes that control cell proliferation, growth, differentiation, survival, and migration.[75,76,80]

While ERK1/2 activation is primarily mediated by Raf MAP3Ks upon Ras signalling, MEKK2/3 are also capable of activating the ERK1/2 MAPK pathway through direct phosphorylation of MAP2Ks MEK1/2 in certain cellular contexts, including MEKK2/3 overexpression.[60,69,81] The ERK1/2 MAPK pathway is primarily responsive to growth factors, stress, and mitogenic signals, and typically governs regulation over genes involved in cellular proliferation, growth, survival, and differentiation.[12,69,82,83]

The four p38 isoforms are strongly responsive to various stimuli, including stress and inflammatory cytokines and regulate expression of genes involved in cellular inflammation, differentiation, growth, and apoptosis.[12,84,85] Upstream p38 MAP2Ks are activated by various MAP3Ks, including MEKK2/3, and selectively activate all p38 MAPK isoforms by dual phosphorylation in the conserved TGY motif in the activation loop. MKK3 (MEK3) selectively

phosphorylates and activates p38α, p38δ, and p38γ isoforms, while MKK6 (MEK6) strongly activates all p38α, p38β, p38δ, and p38γ isoforms.[12,84,86]

1.5.1 MEKK2/3 Activation and Regulation

The precise mechanisms through which upstream cellular and membrane-bound receptor elements integrate extracellular signals to induce activation and regulation of MEKK2/3 lack sufficient evidence. However, MAPKKKs are often activated through phosphorylation by upstream kinases or as a result of direct interaction with small GTP-binding proteins of the Ras/Rho family.[12,87] Activation by upstream kinases may be facilitated MAP4Ks, belonging to the Ste20-like family of S/T-kinases, which have been documented to promote JNK activation upon activation of MAP3K signalling.[88] Evidence suggests that MEKK2/3 can form pre-activation complexes with other receptor-proximal upstream signalling proteins, facilitating the integration of various extracellular signals and promote MEKK2/3 activation, leading to downstream MAPK pathway activation.[62,63]

Additionally, G-protein-coupled receptor (GPCR) activation is correlated with activation of the major MAPK pathways.[61] GPCRs are the largest family of membrane proteins and respond to extracellular stimuli such as, stress factors, hormones, and cytokines to mediate majority of cellular processes.[61,89,90] There are many potential mechanisms of MAPK activation by GPCRs, however the activation of specific G-protein subunits promotes downstream signalling cascades that result in phosphorylation and subsequent activation of MEKK2/3.[61,91] The potential mechanisms underlying MEKK2/3 activation by upstream activating elements are illustrated in Figure 1.2.

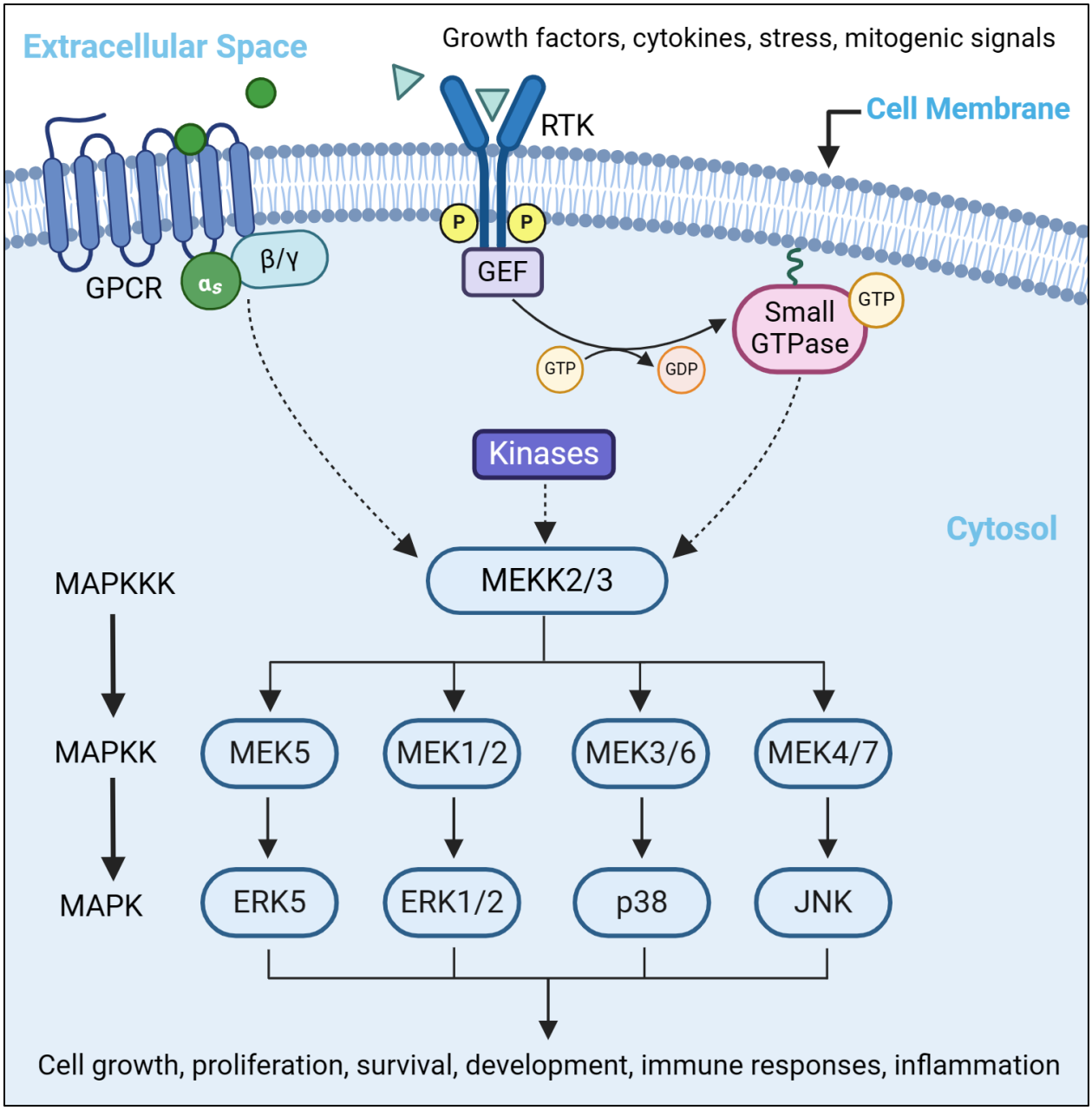

Figure 1.2. MEKK2/3 signal integration and downstream effectors. The available data suggests that MEKK2/3 activation is facilitated by the integration of various extracellular stimuli through G-protein-coupled receptors (GPCRs) and receptor tyrosine kinases (RTKs) or phosphorylation by upstream kinases. Guanine nucleotide exchange factors (GEFs) are generally recruited to the cell membrane upon RTK activation, resulting in the activation of small GTPases which interact with MEKK2/3 to promote activation. MEKK2/3 activate all four major MAPK pathways which regulate various cellular processes. Created with BioRender.com.

However, it is widely understood that MEKK2/3 undergo autoactivation through homodimerization and subsequent autophosphorylation. Upon activating signals, MEKK2 or MEKK3 homodimerize, promoting transautophosphorylation of MEKK2 or MEKK3 regulatory sites S519 and S526 in the activation loop, respectively.[63,64,67,92] Transautophosphorylation of these sites are required for full activation of MEKK2/3 and subsequent initiation of MAPK cascades.[64,92] An MEKK2-interacting protein, identified as Mip1, regulates MEKK2 activity by forming a complex with inactive and non-phosphorylated MEKK2 monomers, inhibiting dimer formation and subsequent activation.[58] Upon extracellular stimuli, such as EGF, the Mip1-MEKK2 complex dissociates, resulting in increased levels of available MEKK2. Therefore, MEKK2 overexpression, detected in various cancers, is sufficient to promote dimerization, resulting in autophosphorylation and activation.[57,58,92] It is likely that Mip1 also regulates MEKK3 dimerization due to its high degree of conservation with MEKK2, however these investigations have not been conducted.

The specific phosphorylation of various serine and threonine residues within the kinase activation loop of MEKK2/3 is induced by distinct activating stimuli to regulate activation of various downstream pathways.[93] For instance, interleukin-1 (IL-1) induces phosphorylation at S526 of MEKK3, promoting activation of MAPK and NF-κB pathways, while lysophosphatidic acid (LPA) stimulation promotes phosphorylation at T516 and S520, leading to IKKβ/NF-κB pathway activation.[64,67,93] While there is limited data regarding mechanisms of MEKK2/3 downregulation, protein phosphatase 2A (PP2A) has been well documented to regulate phosphorylation and activation of MEKK2/3. Following LPA-induced MEKK3 phosphorylation in the activation loop, the catalytic subunit of PP2A binds MEKK3 and dephosphorylates T516 and S520, inactivating MEKK3 and thereby reducing activation of the IKKβ/NF-κB pathway.[93]

Alternatively, PP2A has been documented to act as an allosteric inhibitor to indirectly prevent activating phosphorylation of MEKK2. The regulatory subunit of the trimeric PP2A complex has been detected to directly interact with MEKK2, preventing activating phosphorylation by upstream kinases and other activating signals.[94,95]

1.5.2 MEKK2/3 Promote Tumorigenesis of Various Cancers

Due to the ability of MEKK2/3 to activate various cellular pathways, regulatory mechanisms are crucial to control MEKK2/3 activation and signalling. Consequently, dysregulation of MEKK2/3 can lead to aberrant activation of downstream effectors such as all four classical MAPK pathways and NF-κB.[12,68] Overexpression of MEKK2 has been detected in breast, prostate, colorectal, lung, and pancreatic cancers, while elevated MEKK3 expression has been identified in breast, ovarian, cervical, lung, kidney, and esophageal cancers.[57,62,95–99] The role of MEKK2/3 as oncoproteins in the development and progression of various forms of cancer should be further studied for the development of targeted therapeutic interventions.

MEKK3 upregulation has been detected in esophageal dysplasia, which promotes tumorigenesis of esophageal squamous cell carcinoma (ESCC).[96] In cervical cancer, there is a positive correlation between MEKK3 expression and survivin expression, an anti-apoptotic protein associated with survival of cancer cells, thereby contributing to the development and progression of cervical cancer.[100,101] Similarly, MEKK3 overexpression has been shown to correlate to increased expression of survivin and STAT3, a transcription factor associated with increased development and metastasis of renal cell cancers (RCC).[102,103] Overexpression of MEKK3 is frequently detected in breast and ovarian cancers, leading to increased NF-κB and upregulation of cell survival genes, which in turn promotes cellular resistance to apoptosis.[104,105] In lung

cancers, upregulated MEKK3 is associated with aberrant JNK and p38 activity, resulting in proliferation, migration and invasion of lung cancer cells.[106]

Dysregulation of MEKK2 has been shown to promote migration of invasive breast cancer cells through regulation of cellular adhesion complexes, leading to metastasis.[97,99] Furthermore, MEKK2-MEK5-ERK5 signalling has been implicated in the proliferation and growth of breast cancer cells.[99] Overexpression of MEKK2 is correlated to the tumorigenesis of pancreatic ductal adenocarcinoma (PDAC) and lung adenocarcinoma (LAC), whereby MEKK2 becomes methylated at K260 by overexpressed SMYD3 lysine methyltransferase (KMT), which prevents regulatory control by protein phosphatase PP2A, and promotes MEKK2 signalling to MEK1/2 downstream of oncogenic Ras.[95]

1.6 14-3-3 Adapter Proteins: Binding and Function

14-3-3 proteins comprise a family of eukaryotic phospho-S/T-binding adaptor proteins that regulate all major cellular signalling pathways, including MAPK pathways, thereby modulating diverse cellular processes including cell cycle progression, signal transduction, protein trafficking, and apoptosis.[107–110] 14-3-3 proteins consist of seven isoforms that interact with phosphorylated serine and threonine residues within specific consensus sequences.[107] Majority of 14-3-3 binding sites conform to a Mode I motif, having at least one basic (K/R) residue in the -3 to -5 positions, relative to the phosphoserine or phosphothreonine, followed by a +2 proline.[111,112]

Each 14-3-3 monomeric unit contains one phosphopeptide-binding site located within the amphipathic groove. Consequently, a 14-3-3 dimer can bind two phosphosites simultaneously within the same protein or from two different proteins, acting as a scaffold. While 14-3-3

isoforms can interact with target proteins individually as monomers, they predominantly exist and interact as dimers.[110,113,114]

The role of 14-3-3 interaction depends on its specific target, however 14-3-3 proteins are known to mask nuclear localization or export signals, modify protein conformation to activation or inhibitory states, and inhibit the binding of other interacting proteins, including phosphatases, consequently protecting targets from dephosphorylation.[107,114,115] Consequently, 14-3-3 proteins can contribute to vital processes in cancer progression including apoptosis, cell cycle progression, autophagy, glucose metabolism, and cell motility.[107]

1.6.1 MEKK2/3 Regulation by 14-3-3

As mentioned, MEKK2/3 activation is regulated through phosphorylation at distinct serine and threonine residues.[93] 14-3-3 proteins have been demonstrated to regulate MEKK2/3 activity through their ability to function as scaffolds to facilitate protein-protein interactions.[116] There is evidence to suggest that 14-3-3 proteins interact with specific threonine residues on MEKK2/3 to regulate their activity. Multiple studies conducted by *Matitau et al.* have demonstrated T294 of MEKK3 and the analogous site T283 of MEKK2 as regulatory sites that control the activation of downstream MEKK2/3 effectors.[59,63] In MEKK3 studies, the introduction of a phosphorylation-resistant mutant T294A MEKK3 disturbs the ability for 14-3-3 adaptor proteins to bind, resulting in sustained levels of S526 phosphorylation within the activation loop, promoting amplification of activating signals to downstream NF-κB, in the presence TNF-α stimulation.[59] Thus, it was concluded that T294 phosphorylation promotes 14-3-3 binding, providing a potential mechanism by which MEKK3 signalling is regulated.

Further investigations regarding the role of 14-3-3 in modulating MEKK2 activity demonstrated that 14-3-3 also interacts with MEKK2 at T283. This interaction alters MEKK2 activity by limiting homodimerization and subsequent S519 phosphorylation in the activation loop, resulting in kinase inactivation. Similar to the regulatory control elicited on MEKK3 activity, expression of T283A MEKK2 prevented 14-3-3 interaction, resulting in enhanced stress-activated JNK activity and IL-6 expression, while simultaneously reducing ERK activation and subsequent cellular proliferation rates.[63] These findings indicate that 14-3-3 interacts with MEKK2 at phosphorylated T283 to control MEKK2 activity.

1.7 SMYD3 Methyltransferase Function and Oncogenesis

SMYD3, SET and MYN-domain containing 3, is a lysine methyltransferase (KMT) that has been implicated in the development and progression of various types of cancers.[117] SMYD proteins catalyze the transfer of the methyl group from *S*-adenosyl-L-methionine (SAM), a methyl donor involved in the methylation of many cellular compounds, onto the lysine residue of both histone and nonhistone protein substrates.[118,119] SMYD-mediated lysine methylation influences protein activity, stability, and function, resulting in diverse biological outcomes including regulation of gene expression and cell signalling pathways.[94,119,120]

Experimental findings from tumour biopsies indicate upregulation of SMYD3 in diverse cancer types, including breast, ovarian, prostate, liver, colon, lung, and pancreatic cancer. Elevated SMYD3 levels has been associated with tumour progression and metastasis, resulting in poor disease outcome and increase mortality rate.[121] One mechanism by which SMYD3 contributes to the progression of cancer is through methylation of non-histone proteins involved in cellular signalling, resulting in increased cell proliferation, growth, and migration.[122]

1.7.1 SMYD3-Mediated Methylation of K260 of MEKK2 Promotes Tumorigenesis

Mazur et al. explored the correlation between activating *Kras* mutations (G12D) and upregulated *Smyd3* expression in tumour development using mouse models of PDAC and LAC.[95] SMYD3-mediated K260 methylation enhances MEKK2 input to MEK1/2 increases ERK1/2 activation, which promotes rapid proliferation of cancer cells and overall worsens cancer prognosis.[47] ERK1/2 activation was shown to significantly decrease in $Kras^{G12D}$/*Smyd3*-deficient mouse models, co-occurrent with a significant reduction in pancreatic intra-epithelial neoplasia (PanIN), a precursor to PDAC, and increased lifespan. These results indicate that SMYD3 is required for the progression and worsened prognosis of pancreatic ductal adenocarcinoma (PDAC) following oncogenic K-Ras activation. Similarly, mouse models showed significantly smaller and less advanced lung adenomas following *Smyd3*-deletion, inferring SMYD3 is also responsible for lung adenocarcinoma (LAC) tumorigenesis.[95] MEKK2 methylation status in LKR10 cells (mouse LAC cells) showed decreased methylation *in vitro* upon SMYD3-directed RNA-inference. Further insights into the oncogenic role of SMYD3 and its targeting of synergistic oncogenic signals may be useful in the development of effective treatment for cancers that are characterized by *Smyd3* overexpression.[122]

Mazur et al. characterized K260 of MEKK2 as a target of SMYD3 methylation, preventing MEKK2 inactivation by hindering phosphatase PP2A association, a known key negative regulator of the MAPK pathway.[94] In PDAC and LAC, SMYD3 overexpression leads to aberrant activation of MEKK2, resulting in increased MEKK2 input to MEK1/2 downstream of oncogenic K-Ras signalling within the Ras-Raf-MEK-ERK signalling cascade.[95] They established that amino acids 249-273 of MEKK2 constitutes the binding site for the PP2A complex and methylation at K260 inhibits this interaction, therefore inferring that aberrant

MEKK2 activation is due to the inability of PP2A to negatively regulate activating phosphorylation events on MEKK2 and downstream targets.[95] Additionally, they confirmed that SMYD3 was the only KMT out of eleven tested that could methylate MEKK2. SMYD3 can catalyze MEKK2 methylation using unmethylated, mono-, or di-methylated K260 as substrates to generate the fully saturated trimethylated state at K260.[95]

1.7.2 Importance of Identifying SMYD3 Targets in Cancer Progression

PDAC is acknowledged as the most lethal form of pancreatic cancer characterized by an average 5-year survival rate of less than 10%, with the majority of patients diagnosed at an advanced late-stage or metastatic state.[123,124] Similarly, LAC stands as the predominant histological subtype among non-small cell lung cancers (NSCLC), exhibiting elevated rates of mortality and proclivity for metastasis.[125]

Growing evidence has linked SMYD3 to tumorigenesis in several cancer types where it acts as an activator of multiple oncogenic mechanisms.[126] As discussed, one of the ways SMYD3 promotes oncogenesis is through its involvement in cellular signalling pathways by targeting non-histone proteins that are crucial regulators of normal cell proliferation, growth, migration, and survival.[122] Recent studies have shown that expression of SMYD3 is robustly elevated in diverse human cancers, suggesting its role as a putative oncogene.[127] Therefore, investigating therapeutic targets in SMYD3-mediated cancer progression provides opportunities for developing targeted therapeutic interventions.

1.8 Hypothesis and Research Objectives

The first aim of this study is to characterize T263 as a novel secondary phosphosite on MEKK2 and 14-3-3-binding site. As mentioned, Matitau et al. have demonstrated that MEKK2 interacts with 14-3-3 through a phosphorylation-dependent association at T283, altering MEKK2 activity and signalling the MAPK pathway.[63] Since T283 is an established phosphosite and 14-3-3 binding site, it was postulated that T263, located 20 amino acids upstream from T283, may also be a 14-3-3-binding phosphosite. The sequence surrounding T263 is consistent with a Mode I 14-3-3 binding motif, containing a -3 basic lysine residue and a +2 proline [KXXpTXP].[111,112]

The second aim of this study is to determine whether SMYD3-mediated methylation of MEKK2 at K260 conferred regulatory control over T263 and T283 phosphorylation status and signalling to downstream MEK and ERK in the MAPK cascade. Direct interactions between neighbouring methylation and phosphorylation sites represent a distinct class of post-translational modification (PTM) crosstalk, referred to as a 'methyl-phospho' switch.[128] Methylation at lysine residues is an emerging mechanism to control phosphorylation at surrounding phosphorylation sites.[129] Recent studies have recognized the significance of "methyl switches" in regulating PTMs of neighbouring residues.[129] This type of post-translational regulation is characterized by the stimulation or inhibition of neighbouring modifications as a result of methylation at one lysine residue.[129] The crosstalk between phosphorylated and methylated residues allows for fine-tuned control of protein function and downstream signalling events.[5] An overview of the objectives of this study are illustrated in Figure 1.3.

As such, I hypothesize that T263 is a novel 14-3-3 phospho-binding site on MEKK2 and SMYD3-mediated methylation of MEKK2 at K260 will alter the phosphorylation status of neighbouring T263, altering downstream MAPK pathway activation.

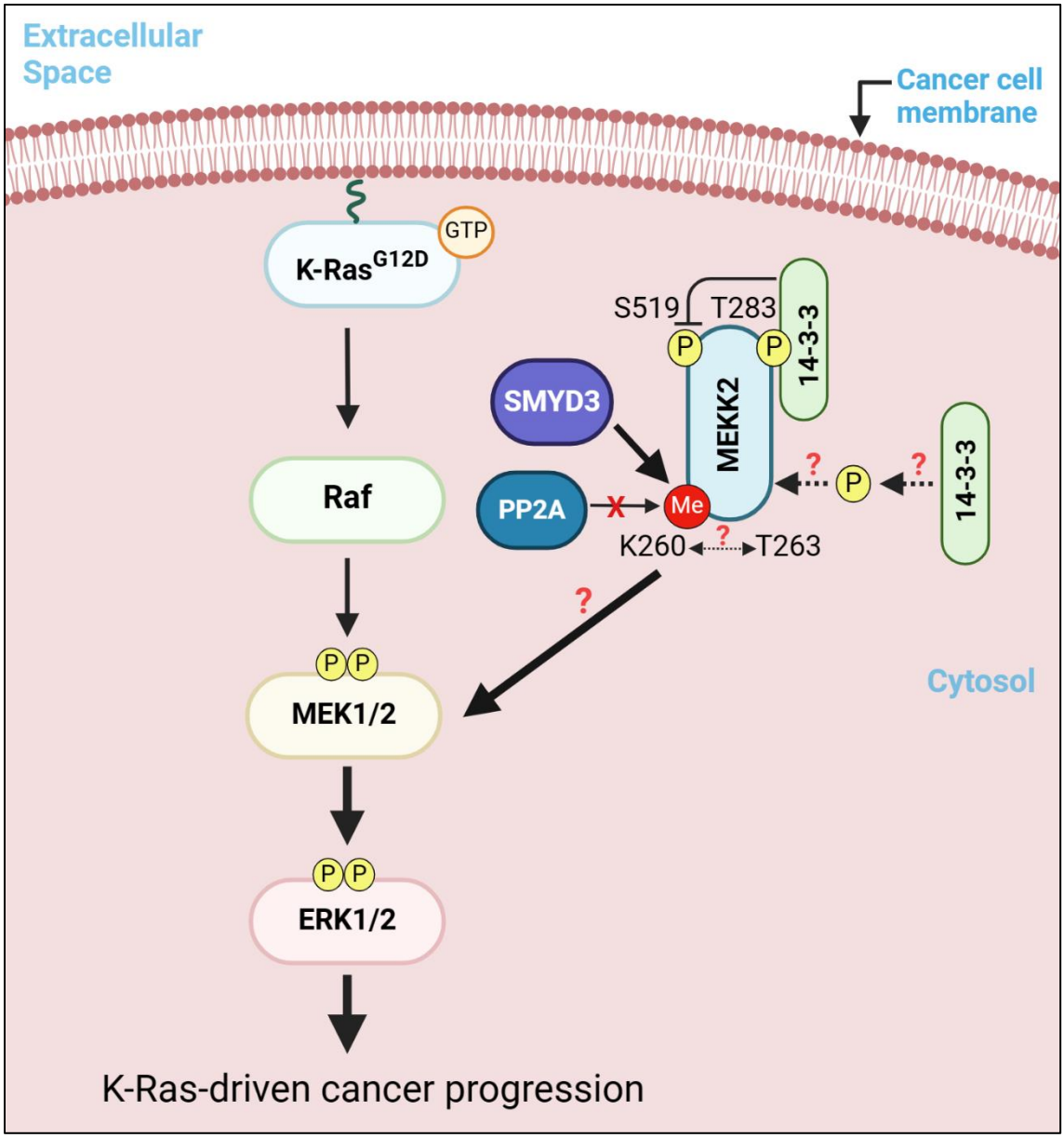

Figure 1.3. Determining the role of T263 of MEKK2 in K-Ras-driven tumorigenesis. Oncogenic activation of the Ras-Raf-MEK-ERK pathway is initiated by a G12D driver mutation in K-Ras. Overexpressed SMYD3 methylates K260 of MEKK2, preventing PP2A association, and promotes MEKK2 input to MEK1/2 downstream of oncogenic Ras signalling. The objectives of the study aim to characterize T263 as a novel phosphosite that binds 14-3-3 and its phosphorylation status is influenced by neighbouring K260 methylation. Created with BioRender.com.

Chapter 2: Procedures, Protocols, and Methodology

2.1 Mutagenesis and DNA Amplification

Plasmids: pCMV10-FLAG-MEKK2 *M. musculus* was generated by previous members of the Scheid lab using p3xFLAG-CMV-10 vector backbone. LV102-FLAG-MEKK2 *H. sapiens* construct was obtained from GeneCopoeia (catalog no. EX-Z4520-Lv102-50). pMSCV-FLAG-SMYD3 *H. sapiens* was a gift from Julien Sage (Addgene plasmid #85650). pcDNA™4/myc-His C vector backbone was obtained from Invitrogen™ (ThermoFisher Scientific V863-20). pcDNA™4-FLAG-SMYD3 was generated by subcloning FLAG-SMYD3 from pMSCV-FLAG-SMYD3 into the pcDNA™4/myc-His C vector backbone. All constructs contain ampicillin/carbenicillin resistance gene controlled by a bacterial promoter.

Polymerase Chain Reaction (PCR) and Mutagenesis: Mutations of pCMV10-FLAG-MEKK2 and LV102-FLAG-MEKK2 were generated using Q5® Site-Directed Mutagenesis Kit (NEB E0554S) and were sequence-verified by The Centre for Applied Genomics (TCAG). Forward and reverse primers were prepared by Invitrogen and were diluted 10-fold to obtain a stock concentration of 100µM. The following reagents were assembled in PCR tubes on ice: Q5® Hot Start High-Fidelity 2X Master Mix, 10µM forward primer, 10µM reverse primer, 1-25ng/µl template DNA, and nuclease-free water, according to the Q5® Mutagenesis protocol (NEB). Samples were placed in a thermocycler (Eppendorf Mastercycler®) on the following settings: Initial Denaturation at 98°C for 30 seconds; 25 cycles and a final extension at 72°C for 2 minutes. Each cycle consists of denaturation at 98°C for 10 seconds, annealing at 50-72°C (based on annealing temperature of primers) for 30 seconds per kb (based on kilobase pair size of template DNA), and extension at 72°C for 25 seconds per kb. The PCR products were subjected

to a Kinase, Ligase and DpnI (KLD) reaction consisting of the following reagents: PCR product, 2X KLD Reaction Buffer, 10X KLD Enzyme Mix, and nuclease-free water (NEB E0554S), yielding the ligated mutated construct.

Transformation:

High-Efficiency Transformation: This procedure was used following any plasmid ligation step (ie. KLD reaction and subcloning). 50µl of NEB® 5-alpha (DH5α strain) competent *E. coli* cells (subcloning efficiency; NEB catalog no. C2988) were inoculated with the construct on ice for 30 minutes. DH5α *E. coli* cells were heat shocked at 42°C for 30 seconds and then placed on ice for 5 minutes. The bacteria-plasmid mixture was incubated in SOC Outgrowth Medium (NEB E0554S) at 37°C for 1 hour. Transformed bacteria was resuspended on a prepared carbenicillin-containing LB-agar selection plate and was cultured for 16-20 hours at 37°C (inverted). Colonies were isolated and grown in 5mL Lennox Luria Broth (LB) from Sigma-Aldrich (catalog no. L3022) containing 1µg/ml carbenicillin (Sigma-Aldrich C1613). Inoculations were incubated at 37°C for 16-20 hours on a VWR S-500 Orbital Shaker.

Low-Efficiency Transformation for Amplifying Large Quantities of Plasmid DNA: 50µl of competent DH5α *E. coli* cells were inoculated with 1µl of plasmid DNA on ice for 5 minutes. Cells were then heat shocked at 42°C for 30 seconds and were incubated on ice for an additional 5 minutes. Cells were plated on a carbenicillin-containing LB-agar selection plate and were cultured for 16-20 hours at 37°C (inverted). One colony was isolated and grown in 5ml Lennox Luria Broth (LB) from Sigma-Aldrich (catalog no. L3022) containing 1µg/ml carbenicillin (Sigma-Aldrich C1613) and was incubated at 37°C for 16-20 hours on a VWR S-500 Orbital

Shaker. The 5mL culture was then resuspended in 100ml of LB + carbenicillin and was incubated at 37°C for 16-20 hours on shaker.

Miniprep: This procedure was used to isolate small amounts of plasmid DNA for the purpose of sequence verification of mutant constructs. Following the high-efficiency transformation protocol, cells were pelleted using an Eppendorf 5415D Centrifuge set to the following settings: 3000 rpm, 4°C, 5 minutes. Plasmid DNA was purified from DH5α *E. coli* cells with PureLink™ HiPure Plasmid Miniprep Kit (ThermoFisher Scientific Invitrogen™ K210011), according to the manufacturer's protocol.

Midiprep/Maxiprep: This procedure was used to isolate large amounts of plasmid DNA for transfections. Following the low-efficiency transformation protocol, cells were pelleted using an Eppendorf 5415D Centrifuge set to the following settings: 3000 rpm, 4°C, 15 minutes. Plasmid DNA was purified from DH5α *E. coli* cells with QIAGEN Plasmid Midi Kit (catalog no. 12143) or QIAGEN Plasmid Maxi Kit (catalog no. 12162), according to the manufacturer's protocol.

Plasmid Purity and Concentration: Purity and concentration of plasmid DNA from Mini/Midi/Maxipreps was determined using the ThermoFisher Scientific NanoDrop™ 2000 Spectrophotometer. Concentrations were recorded in µg/µl. Purity was assessed using the 260/280 ratio, with a ratio of approximately1.8 indicating the presence of pure DNA.

Sequence Verification: Following miniprep of plasmid DNA, samples were prepared by combining 0.2-2µg of plasmid DNA, 10µM of sequencing primer (only when using custom primers, otherwise TCAG standard primers were selected and added at their facility) and nuclease-free water in PCR tubes to a total volume of 7µl. The samples were mailed to The Centre for Applied Genomics (TCAG, SickKids Hospital, Toronto, Ontario). Construct

sequences, uploaded to Genesifter, were compared to the wildtype sequence of gene insert using the Align Sequences Nucleotide BLAST tool (Basic Local Alignment Search Tool) from Nation Center for Biotechnology Information (NCBI).

2.2 Subcloning of Plasmid DNA

Restriction Enzyme Digestion: pMSCV-SMYD3 was restriction enzyme (RE) digested with NotI (NEB catalog no. R0189S) and BglII (NEB R0144S). pcDNA4/myc-His-C was RE digested with NotI and BamHI (NEB R0136S). Digestions were performed by combining plasmid DNA, restriction enzymes, 10x NEBuffer™ r3.1 (NEB B6003S), and milliQ water, to a total volume of 50µl. Reactions were incubated at 37°C for 1 hour, then heat inactivated at 65°C for 15 minutes to stop digestion.

Agarose Gel Electrophoresis: 1% w/v agarose gels were made by mixing agarose (BioRad catalog no. 1613102) with TAE buffer pH 8.3 composed of 40mM Tris-base (BioShop TRS001), 20mM acetic acid, 1mM EDTA and milliQ water. The mixture was heated to dissolve the agarose and SYBR® Green I nucleic acid gel stain (Sigma-Aldrich S9430) was added once slightly cooled. Gels were casted in a flat gel casting tray and well-combs were inserted. Solidified agarose gels were placed in the Sub-Cell GT Cell apparatus from BioRad and filled with TAE buffer. DNA samples and 1kb DNA ladder (NEB N3232S) were loaded into wells and current was applied using a VWR AccuPower Model 300 electrophoresis power supply unit at a constant voltage of 175V (volts) for 45 minutes.

Gel Extractions: DNA fragments were visualized on an agarose gel under UV light. Specific bands of interest were excised from the gel using a clean blade. DNA was then purified from the

gel using PureLink™ Quick Gel Extraction kit from ThermoFisher Scientific (Invitrogen™ K210012), according to the manufacturer's protocol.

Ligations: To ligate the RE digested and purified FLAG-SMYD3 gene insert into the pcDNA4-myc-His C vector backbone, the following components were combined on ice: 10X T4 DNA ligase buffer (NEB B0202), vector DNA, insert DNA, T4 DNA ligase (NEB M0202), and milliQ water. Insert DNA to vector DNA was added at a ratio of 3:1. Two negative controls were performed as follows: T4 DNA ligase was not added to the reaction in control 1, which yielded no colonies post-transformation, and only vector DNA was added to the reaction in control 2 (no insert DNA) to assess for vector self-ligation. The reactions were incubated for 2 hours at room temperature (RT) and subsequently transformed following the *high-efficiency transformation* protocol described above, using carbenicillin-containing LB-agar selection plates. To confirm successful insertion of FLAG-SMYD3, the subcloned construct was RE (NotI) digested and then analyzed for size (kb) using agarose gel electrophoresis (see methods above).

2.3 Cells Lines and Cell Culture Conditions

Cell Lines: Human Embryonic Kidney (HEK) 293T cells were obtained from American Type Culture Collection (ATCC). HEK 293Ta lentiviral packaging cells were purchased from GeneCopoeia (catalog No. LT008). HAP1 parental and custom HAP1 *mekk2* knock-out cells were generated using CRISPR/Cas-9 gene-editing and purchased from Horizon Discovery.

Cell Culture: 293T and 293Ta cells were cultured in Dulbecco's Modified Eagle's Medium (DMEM) from ThermoFisher Scientific (Gibco™ 11995065) supplemented with 10% fetal bovine serum (FBS) from ThermoFisher Scientific (Gibco™ 12483020) and 1% penicillin and streptomycin (Pen Strep) from ThermoFisher Scientific (Gibco™ 15140122). HAP1 cells were

cultured in Iscove's Modified Dulbecco's Medium (IMDM) from ThermoFisher Scientific (Gibco™ 12440053). Cells were incubated at 37°C with 5% CO_2.

Passaging: When cells reached 70-80% confluency in a 100mm dish, spent media was aspirated and cells were washed once with 10ml of 1X phosphate-buffered saline (PBS) pH 7.4 from ThermoFisher Scientific (Gibco™ 10010023). Cells were incubated with 1ml of 0.25% Trypsin-EDTA (1X) from ThermoFisher Scientific (Gibco™ 25200056) at 37°C with 5% CO_2 for 2 minutes (293T and 293Ta cells) or 5 minutes (HAP1 cells). Cells were resuspended with 9ml of appropriate media and plated to a ratio of 1:10 for general maintenance.

Long-Term Storage/Freezing: Once cells reached 70-80% confluency in a 100mm dish, cells were washed with 1X PBS, trypsinized, and pelleted at 1200 rpm, RT, for 3 minutes. Spent media was aspirated and cells were resuspended in freezing media consisting of DMEM (293T and 293Ta cells) or IMDM (HAP1 cells), 20% FBS, and 10% dimethyl sulfoxide (DMSO) cryoprotectant from Sigma-Aldrich (catalog no. D5879). Cells were stored in 1ml aliquots in cryogenic vials and stored at -80°C until further use.

Thawing: Cells were thawed in a water bath set to 37°C. 1ml of thawed cells were plated in a 100mm dish with 9ml of appropriate media. The media was aspirated and replaced after 24 hours.

2.4 Expression of Exogenous DNA in Mammalian Cells

Transfection: This procedure was used to achieve transient expression of wild type and mutant FLAG MEKK2 from various constructs in HEK 293T cells. Cells were seeded at a ratio of 1:10 in 6-well plates or 100mm dishes and grown to 70-80% confluency. The following components were equilibrated to RT prior to transfection: Opti-MEM® I (Reduced Serum Medium) from

ThermoFisher Scientific (Gibco™ 31985070), polyethyleneimine (PEI; transfection reagent) from Sigma-Aldrich (catalog no. 408727), and plasmid DNA. Per one well of a 6-well plate, cells were suspended in 2ml of medium. 2.5µg of plasmid DNA was diluted in 125µl of Opti-MEM® I and incubated at RT for 5 minutes. 7.5µl of PEI was diluted in 125µl of Opti-MEM® I. For 100mm dishes: cells were suspended in 10ml of medium. 15µg of plasmid DNA was diluted in 750µl of Opti-MEM® I and incubated at RT for 5 minutes. 45µl of PEI was diluted in 750µl of Opti-MEM® I. For both conditions, DNA and PEI mixtures were combined and incubated at RT for 20 minutes to allow DNA-PEI complexes to form. DNA-PEI complexes were added dropwise into the culture medium, avoiding direct contact with the cells. Cells were incubated for 24 hours at 37°C with 5% CO_2. The culture medium was aspirated, and the cells were rinsed once with 1X PBS. Fresh medium, supplemented with 10% FBS and 1% antibiotics, was carefully added to the cells. The cells were incubated for another 24 hours under the same conditions, after which they were subjected to treatment or immediate harvest, Figure 2.2.

Co-Transfection: To transfect two plasmids simultaneously in mammalian cells, the standard transfection procedure was followed with the modification that total plasmid DNA consisted of an equal mixture of DNA from both plasmids. For SMYD3 co-transfections with MEKK2 constructs in HEK 293T cells, 7.5µg (100mm dishes) or 1.25µg (6-well plates) of pcDNA4-Flag-SMYD3 was co-transfected with an equal amount of MEKK2 plasmid DNA in the SMYD3-positive condition. In the SMYD3-negative condition, pcDNA4-myc-His C empty vector was co-transfected with MEKK2 using the same method.

2.5 Generation of HAP1/MEKK2-Stable Cell Line

Puromycin Selection Assay: HEK 293Ta cells were seeded at a 1:10 ratio and were grown to 70-80% confluency in a 6-well plate. Once confluent, each well was incubated with varying concentrations of puromycin from ThermoFisher Scientific (Gibco™ A1113803), and cell death was assessed. The following concentrations of puromycin were used: 0.25µg/ml, 0.5µg/ml, 0.75µg/ml, 1µg/ml, 1.5µg/ml, 2µg/ml. The concentration in which cell death was first observed was used to select for puromycin-resistance following viral transduction (ie. 1µg/ml).

Lentiviral Particle Production: Lenti-Pac™ HIV Expression Packaging Kit from GeneCopoeia (catalog no. LT021) was used to produce MEKK2-containing lentiviral particles in HEK 293Ta cells. The kit contained a pseudo type packaging mix (TSP) consisting of lentiviral packaging plasmids, eGFP (enhanced green fluorescent protein) positive control plasmid, EndoFectin™ Lenti transfection reagent, and TiterBoost™ Reagent (500X). HEK 293Ta cells were seeded at a 1:10 ratio in 6-well plates and were grown to 70-80% confluency. LV102-Flag-MEKK2 constructs were co-transfected with packaging plasmids at a 1:1 ratio, using EndoFectin™ Lenti diluted in Opti-MEM® I. For the positive control, packaging plasmids were co-transfected with the eGFP positive control plasmid at a 1:1 ratio. For the negative control, packaging plasmids were solely transfected. After 24 hours, TitberBoost™ was added at a 1:500 ratio to the culture medium to boost lentiviral production. Following 48 hours from initial transfection, the culture medium was harvested which contained lentiviral pseudoparticles released from the transfected HEK 293Ta cells. The medium was taken up into a 5ml syringe and filtered through a 0.45µm PES low protein-binding filter. The resulting viral supernatant was used to transduce HAP1/- cells, Figure 2.1.

Lentiviral Transduction and Polyclonal Selection: Particular modifications to transduction methods were as outlined in Chapter 3.7 Generally, HAP1/- cells were seeded at a 1:10 ratio in 6-well plates or 100mm dishes and grown to 50-60% confluency. Viral supernatant was added to the culture medium and incubated for 76 hours at 37°C with 5% CO_2. Spent medium was aspirated and washed once with 1X PBS, and fresh culture medium containing 1-2µg/ml of puromycin was added. Clonal expansions were lysed and pooled together upon reaching 80-90% confluency, yielding a polyclonal population of transduced cells that may exhibit varying levels of MEKK2 expression. Lentiviral transduction of HAP1/- cells with MEKK2 constructs is illustrated in Figure 2.1.

Isolation of Monoclonal Cells: Following selection and clonal expansion, 6mm round filter papers soaked with 0.25% Trypsin-EDTA (1X) were place over 6 individual colonies, for each transduced construct. Monoclonal cells were then transferred into individual wells of a 6-well plate by placing the filter paper directly into the IMDM culture medium. Colonies adhered to the well and were expanded to 80% confluence, and then sub-cultured into 100mm dishes.

2.6 Cell Treatments and Stimulations

SMYD3 Inhibition: BAY-6035 is a potent and selective inhibitor of SMYD3 which prevents SMYD3-mediated methylation of MEKK2. BAY-6035 powder (Sigma-Aldrich SML2325) was suspended in DMSO to a stock concentration of 5mM. Following 48 hours of transfection, HEK 293T cells were incubated with 250nM of BAY-6035 at 37°C with 5% CO_2 for 2 hours prior to harvest. BAY-6035 was added directly to the spent medium, with gentle agitation of the dish.

Stimulation: HAP1/- and HAP1/MEKK2-stable cells were seeded at a ratio of 1:10 and grown to 75-80% confluency in IMDM culture media. Cells were starved for 16 hours prior to

stimulation by aspirating the culture media and rinsing the cells with 1X PBS and supplementing the cells with a starvation media that lacked FBS. The starvation media was composed of IMDM and 1% Pen Strep and contained 2µg/ml puromycin to maintain selection. The cells were either stimulated with 10% FBS (serum), 10ng/ml TNF-α (cytokine) from ThermoFisher (Gibco™ PHC3016) or 100ng/ml IGF-1 (growth factor) from ThermoFisher (Gibco™ PHG0078). Stimulant was added to the starvation medium, and cells were incubated for 0 min, 5 min, 10 min, or 20 min at 37°C with 5% CO_2. After the specific incubation period, the cells were immediately lysed. For 0 min, cells were not stimulated and were immediately lysed.

2.7 Cell Lysis and Immunoprecipitation

Cell Lysis and Harvest: Spent medium was aspirated and cells were washed twice with cold 1X PBS. Cell lysis buffer (RIPA) with protease and phosphatase inhibitors were added to the cells (1ml per 10^7 cells), and cell lysate was transferred into microcentrifuge tubes, on ice. RIPA buffer was composed of 140mM NaCl, 10mM Tris-HCl (pH 8.0), 1% Triton X-100, 0.1% sodium deoxycholate, 0.1% SDS and diluted in milliQ water. Protease inhibitors added were 10ug/ml Pepstatin A (ThermoFisher Scientific 78436), 0.2mM AEBSF (ThermoFisher Scientific 78431), 10ug/ml Leupeptin (ThermoFisher Scientific 78435), and 1ug/ml Aprotinin (ThermoFisher Scientific 78432). Phosphatase inhibitors added were 1mM sodium fluoride phosphatase inhibitor, and 20mM β-glycerophosphate phosphatase inhibitor (Sigma-Aldrich G9422). Sonication was applied in three 5 second intervals until the lysate become clear to disrupt cell membranes and facilitate protein release. Lysate was centrifuged at 12,000 rpm for 10 minutes at 4°C. Supernatant was transferred into new microcentrifuge tubes and the pellet was discarded. Cell lysates were total protein normalized using the Pierce™ BCA Protein Assay Kit (ThermoFisher Scientific 23225), according to the manufacturer's protocol. To prepare lysate

samples to load into SDS-PAGE, 150µl of lysate was transferred into new microcentrifuge tubes and was boiled with 50µl of 4X Sample Buffer (3:1 lysate to 4X Sample Buffer), containing 200mM Tris-HCl (pH 6.8), 40% glycerol, bromophenol blue, 8% SDS, 10% β-Mercaptoethanol, and milliQ water, at 95°C for 5 minutes.

Immunoprecipitation: Anti-FLAG® M2 Affinity Gel (Sigma-Aldrich A2220) agarose beads were maintained in a 1:1 bead to gel slurry and upon IP, were washed and resuspended in RIPA buffer. 20µl of packaged gel volume was added to the cell lysates and incubated at 4°C for 1 hour to overnight on a rotator. IP samples were centrifuged at 12,000 rpm for 1 minute at 4°C and supernatant was aspirated. The pelleted beads were washed with RIPA buffer three times. For any IP's involving HEK 293T cells, protein elution FLAG-tagged proteins occurred by boiling the beads with 200µl of 1X Sample Buffer at 95°C for 5 minutes. For any IP's involving HAP1 cells, elution was performed by combining 150µg/ml of 3X FLAG Peptide (Sigma-Aldrich F4799) with RIPA buffer to achieve a total volume of 100µl, which was then combined with the washed beads and rotated at 4°C for 1 hour. The beads were pelleted at 12,000 rpm for 1 minute and supernatant was transferred to new microcentrifuge tubes. 4X Sample Buffer was added to the supernatant at a ratio of 3:1 (supernatant to 4X Sample Buffer) and was boiled at 95°C for 5 minutes, Figure 2.2.

2.8 Protein Gel Electrophoresis

NuPAGE Gel Casting Protocol: Handcast gels were prepared using Mini-PROTEAN® gel casting apparatus from BioRad. 10% resolving gel consisted of 30% Acrylamide/Bis solution (BioRad 1610156), 7x Bis Tris Buffer (2.5M Bis-Tris (Sigma-Aldrich B9754) and 1.5M HCl), Tetramethylethylenediamine (TEMED) (BioRad 1610801), 10% Ammonium Persulfate (APS)

(BioRad 1610700), and milliQ water. Once APS was added, resolving gel was pipetted into the gel casting apparatus and topped with 70% ethanol. Once the acrylamide had polymerized (20-30 minutes), the ethanol was removed, and 4% stacking gel was layered on top of the resolving gel. 10-well or 15-well combs were added into the stacking gel and gels were allowed to polymerize for an additional 20-30 minutes. Gels were stored at 4°C for future use.

SDS-PAGE: Proteins were separated on a 10% polyacrylamide gel using sodium dodecyl-sulfate polyacrylamide gel electrophoresis. Proteins were boiled in SDS-containing Sample Buffer during sample preparation, as previously descried, to denature proteins and confer a uniform negative charge on the proteins, allowing proteins to be separated by mass. Electrode gel cassettes were assembled in the Mini-PROTEAN Tetra Vertical Electrophoresis Cell (BioRad). The outer chamber of the electrophoresis cell was filled with 1X XT MOPs running buffer consisting of 20X XT MOPs (BioRad 1610788) diluted in milliQ water and 5mM of sodium bisulfate reducing agent (Sigma-Aldrich 243973). Between 10-50mg/ml of protein was loaded into each well and Precision Plus Protein Dual Color Standards (BioRad 1610374) 10-250kD protein ladder was loaded into the first lane of each gel. The inner chambers were filled with 1X XT MOPs buffer, and the cell lid was assembled. A constant voltage of 120V was applied to the gels for 1 hour or until the dye front ran off the gel, Figure 2.2.

2.9 Fluorescent Western Blotting

Figure 2.2 provides an illustration of all below methods.

Transfer: Proteins were transferred from the acrylamide gels following SDS-PAGE to Immobilon-P Polyvinylidene Fluoride (PVDF) Membrane (Millipore Sigma IPVH00010). Transfer membranes were cut to the size of the gel and preactivated by soaking in 100%

methanol for 5 minutes. Membranes were then soaked in Bis-Tris transfer buffer pH 7.2 composed of 25mM bicine, 25mM Bis-Tris, 1mM EDTA, and 10% methanol. Fisherbrand™ Pure Cellulose Chromatography Paper (Fisher Scientific 05-714-4) was used as transfer paper and was cut to the exact size of the transfer membranes. Once the gel had finished running, the gel and transfer papers were briefly soaked in transfer buffer and assembled on a Semiphor Semi-dry transfer unit from Amersham Pharmacia Biotech. Transfer buffer was lightly applied to the base and lid of the transfer unit. The order of the transfer assembly are as follows: 4 pieces of transfer paper, PVDF membrane, gel, and 4 more pieces of transfer paper, all soaked in bis-tris transfer buffer. Current was calculated based on area of covered surface on transfer machine multiplied by 0.8milliamps (mA). Constant current was applied to the transfer machine for 1 hour.

Blocking: Membranes were incubated in 3% powder skim milk dissolved in 1X PBS for 1 hour to overnight at 4°C.

Immunoblotting: Primary antibodies were suspended in a solution composed of 50% blocking solution and 50% Western Wash buffer (1X PBS, 0.1% Tween-20, 0.01% SDS). Membranes were incubated with primary antibodies with rocking for 2 hours at RT over overnight at 4°C. Membranes were washed 3 times for 5 minutes with Western Wash buffer. Fluorescent secondary antibodies were suspended in Western Wash buffer and incubated with membranes for 1 hour at RT in dark (covered with aluminum foil). Membranes were washed again prior to imaging. Working concentrations of primary and secondary antibodies are listed in Table 2.1 and Table 2.2, respectively.

Detection: Fluorescent secondary antibodies with fluorophores emitting at 700nm and 800nm were detected using the Odyssey® Infrared Imaging System, Model 9120.

2.10 Microscopy

Fluorescence Microscopy: An Olympus microscope was used to visualize enhanced green fluorescent protein expression (eGFP) in HAP1 *mekk2* knockout cells following lentiviral transduction the eGFP gene (GeneCopoeia catalog no. LT001-02). Images were captured with a QImaging 2000R camera connected to the QCapture Pro program.

2.11 Statistical Analysis

All statistical analysis was performed using GraphPad Prism version 10.0.0 for Windows, GraphPad Software, Boston, Massachusetts USA, www.graphpad.com. Graphical representations of data were generated by GraphPad Prism. Significance was set to the following conditions: ns; $p > 0.05$, *; $p \leq 0.05$, **; $p \leq 0.01$, ***; $p \leq 0.001$, ****; $p \leq 0.0001$. Statistical tests performed included one-way ANOVA and two-way ANOVA followed by Dunnett's or Šídák's multiple comparisons tests, respectively.

2.12 Antibodies

Table 2.1. Primary antibodies used for immunoblotting.

Primary Antibody	**Concentration**	**Catalog No.**
Mouse monoclonal anti-FLAG® M2	1:10,000	Sigma-Aldrich F3165
Rat monoclonal anti-HA High Affinity	1:10,000	Roche 11 867 423 001
Rabbit anti-P-p44/42 MAPK (T202/Y204) (Erk1/2)	1:1000	Cell Signaling Technology 9101S Cell Signaling Technology 4370S
Mouse anti-p44/42 MAPK (Erk1/2)	1:1000	Cell Signaling Technology 4696S
Rabbit anti-14-3-3 (pan)	1:1000	Cell Signaling Technology 8312S
Rabbit monoclonal anti-Myc-Tag (Sepharose® Bead)	1:20 (IP)	Cell Signaling Technology 55464S
Rabbit anti-MEKK2	1:1000	Cell Signaling Technology 19607S
Rabbit monoclonal anti-Dme-Lysine	1:1000	Cell Signaling Technology 14117S
Rabbit monoclonal anti-Tme-Lysine	1:1000	Cell Signaling Technology 14680S
Rabbit anti-phosphor-T263 MEKK2	1:20,000	GenScript Custom
Rabbit anti-phosphor-T283 MEKK2	1:10,000	Open BioSystems Custom

Table 2.2. Fluorescent secondary antibodies used for detection using Odyssey® Infrared Imaging System.

Secondary Antibody	**Concentration**	**Catalog No.**
IRDye® 680LT Goat anti-Rabbit IRDye® 680RD Goat anti-Rabbit	1:10,000	LI-COR 926-68021 LI-COR 926-68071
IRDye® 800CW Goat anti-Rat	1:10,000	LI-COR 926-32219
IRDye® 800CW Goat anti-Mouse	1:10,000	LI-COR 926-32210

2.13 Lists of Common Reagents

All aqueous acids, bases, and alcohols were purchased from Science Store located in the Petrie Science and Engineering Building, York University.

Table 2.3. Common reagents purchased from BioShop Canada.

Name	**Catalog No.**
Ethylenediaminetetraacetic acid (EDTA)	EDT002
Sodium Acetate (NaCH2COOH)	SAA304
Sodium Chloride (NaCl)	SOD004
Sodium Dodecyl Sulfate (SDS)	SDS001
Tris (tris(hydroxymethyl)aminomethane)	TRS001
Tris-hydrochloride (HCl)	TRS004
Tween®-20	TWN510

Table 2.4. Common reagents purchased from BioRad.

Name	**Catalog No.**
Ammonium persulfate	1610700
Precision Plus Protein Dual Colour Standards	1610374
20X XT MOPs Running Buffer	1610788
10X PBS (Phosphate Buffered Saline)	1610780

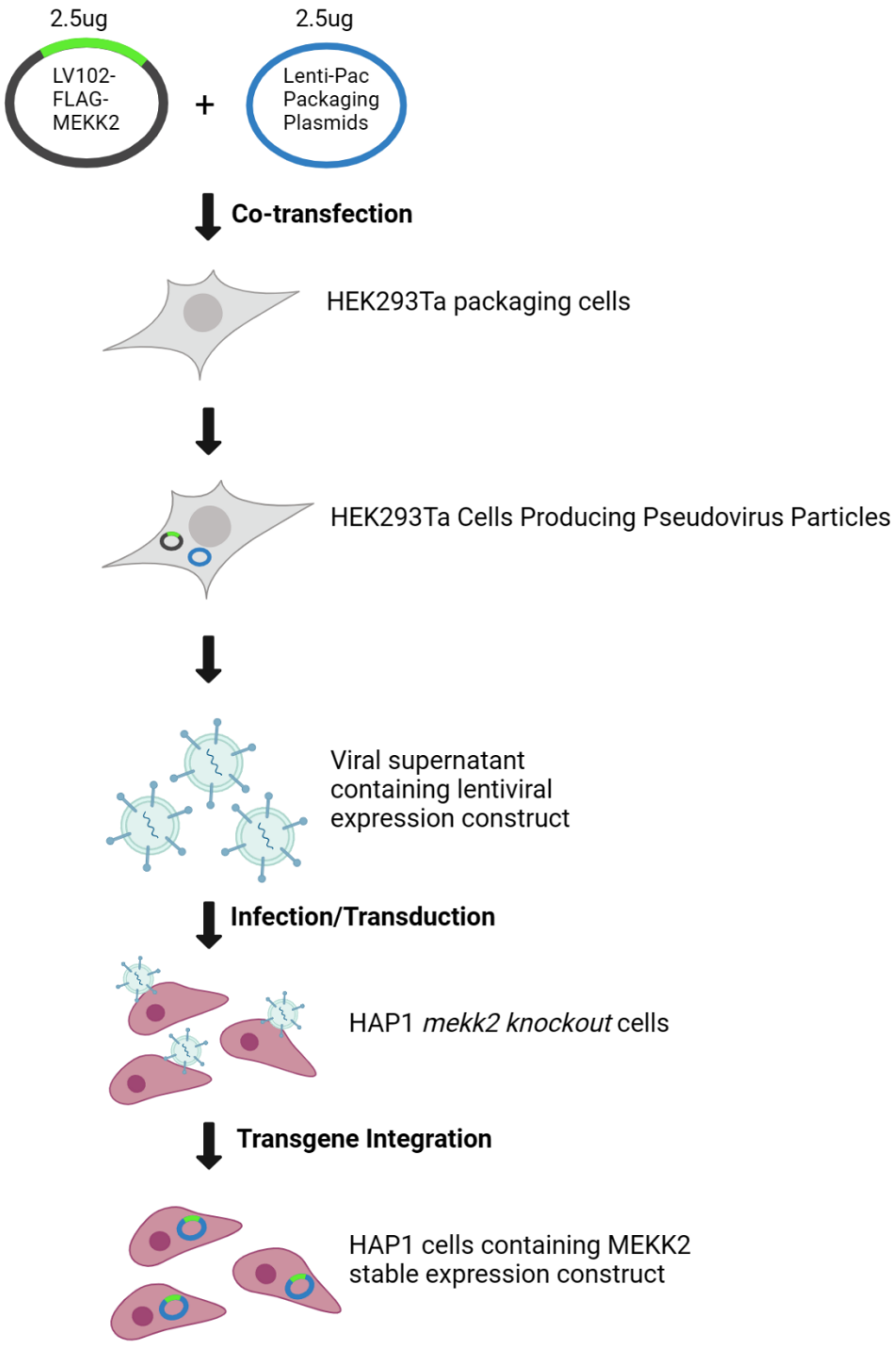

Figure 2.1. Illustration of Lentiviral Transduction and HAP1/MEKK2-Stable Cell Line Generation. Created with BioRender.com.

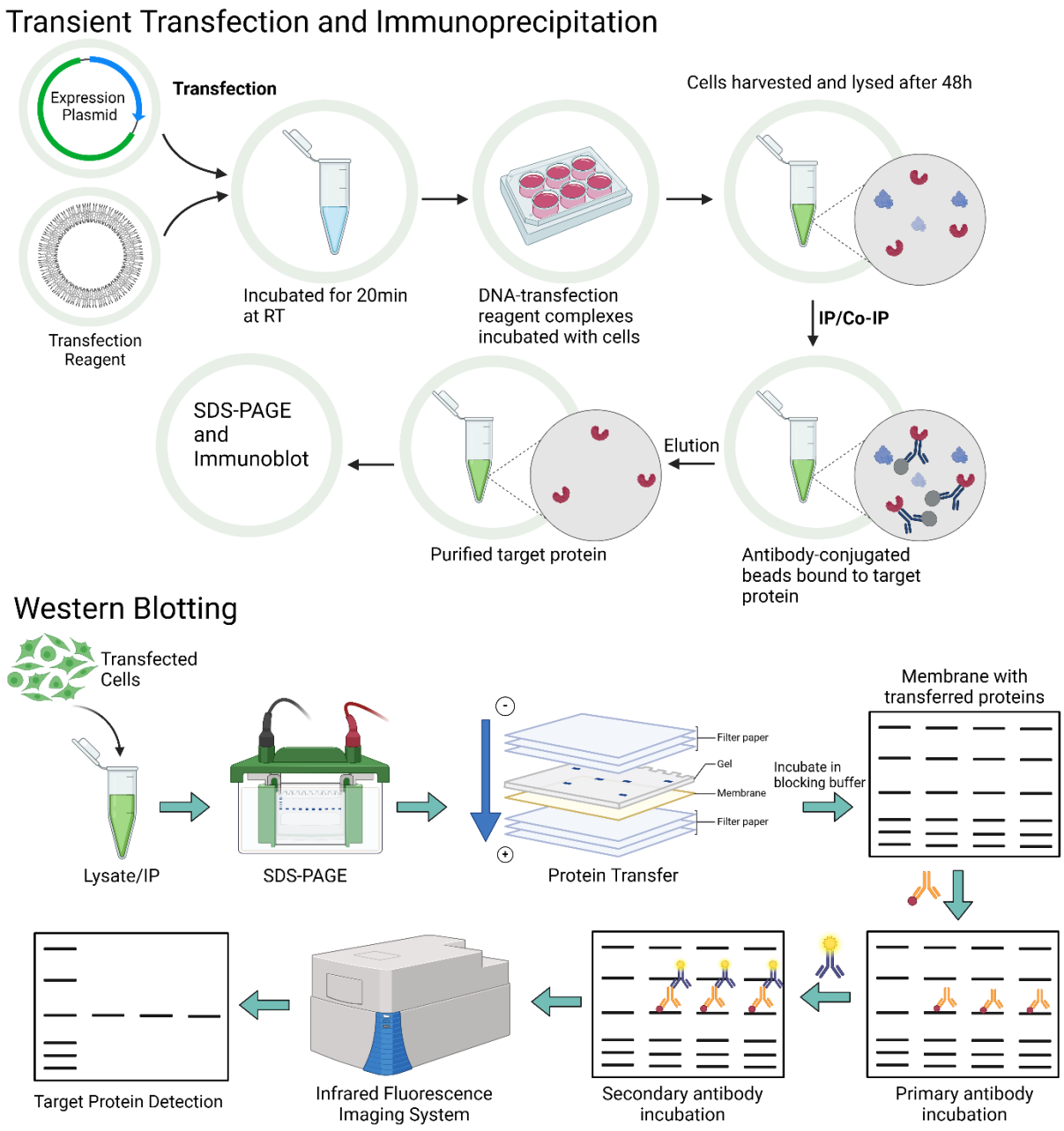

Figure 2.2. Illustration of Transient Transfection, Immunoprecipitation and SDS-PAGE, and Western Blotting Techniques. Created with BioRender.com.

Chapter 3: Discoveries, Findings, and Results

3.1 Demonstrating T263 as a Novel Phosphosite and 14-3-3 Binding Site

Previous work from our lab showed that T283 of MEKK2 is a phosphorylation site that binds to the phosphor-adapter protein 14-3-3.[63] Each monomeric unit of 14-3-3 can interact with a single phosphopeptide. Therefore, 14-3-3 dimerization enables interaction with two phosphosites simultaneously as a bipartite complex.[114] Baodong Wu and Dr. Michael Scheid conducted initial experiments to identify the presence of a second phosphorylation site on MEKK2. These experiments demonstrated that mutation of T263 resulted in complete loss of 14-3-3 co-immunoprecipitation (Wu and Scheid, unpublished observations). This promoted Wu and Scheid to generate a phosphor-specific antibody to T263 to investigate the ability of this site to undergo phosphorylation.

Initial experiments were conducted by Wu and Scheid, in which HEK 293T cells were transfected with pCMV10-FLAG empty vector (FLAG vector) and pCMV10-FLAG-MEKK2, containing wild-type (WT) or harbouring substitution mutations of the *M. musculus* MEKK2 gene. Cells were lysed, immunoprecipitated (IP), and Western Blots were performed. Blots were probed for total FLAG MEKK2, phosphor-T263, phosphor-T283, and endogenous 14-3-3. All MEKK2 point mutations were made using Q5 site-directed mutagenesis and include T263A MEKK2 and T283A MEKK2, threonine to alanine substitution, preventing phosphorylation at these residues. K385M MEKK2, a kinase dead mutant resulting from a loss of function mutation of a critical lysine residue within the active site, was also investigated.

The results of this experiment primarily showed that T263 phosphorylation was lost upon T263A mutation, Figure 3.1A The T263A MEKK2 mutant displayed a 90% reduction in T283

phosphorylation and the T283A MEKK2 mutant displayed a 60% reduction in T263 phosphorylation, relative to WT MEKK2, suggesting that these two sites interfere with or regulate each other's phosphorylation. This result was partially replicated in Figure 3.1B, displaying an 80% reduction in phosphor-T283 signal in the T263A mutant. K385M MEKK2 did not produce a significant change in either T263 or T283 phosphorylation and 14-3-3 co-immunoprecipitation was maintained in K385M MEKK2, inferring that kinase activity is not required for 14-3-3 interaction, Figure 3.1A.

There was no observed 14-3-3 co-immunoprecipated with either T263A MEKK2 and T283A MEKK2, despite being present in the lysate, Figure 3.1A. Upon replication of the experiment in triplicate transfections of both T263A MEKK2 and T283A MEKK2, Figure 3.1B, both mutants displayed complete loss of 14-3-3 co-IP relative to WT MEKK2. Therefore, 14-3-3 co-IP's with WT MEKK2 and K385M MEKK2 but does not interact with either T263A or T283A MEKK2.

A subsequent peptide competition assay was performed in support of the first objective, which was to demonstrate T263 as a novel phosphosite and the second site of the 14-3-3 bipartite binding group. Custom peptides were generated by GenScript to correspond to the animo acids surrounding T263 of MEKK2. HEK 293T cells were transfected with only either FLAG vector or WT MEKK2, lysed, and incubated with either T263-phosphorylated or T263-nonphosphorylated antigen peptides. Proteins were then immunoprecipated with anti-FLAG. Western Blots were probed for total FLAG MEKK2, phosphor-T263, and endogenous 14-3-3.

When no peptide was added to the IP, 14-3-3 was able to co-IP with WT MEKK2, Figure 3.2A, B. Upon addition of the phosphorylated peptides, a significant 80% reduction in T263 phosphorylation signal was observed, Figure 3.2A. Furthermore, the addition of non-

phosphorylated peptides did not significantly alter T263 phosphorylation status of WT MEKK2. To achieve further confidence, the experiment was repeated and a 60% reduction in T263 phosphorylation was observed, Figure 3.2B. The data from both replicate studies was analyzed for statistical significance by performing one-way ANOVA followed by Dunnett's multiple comparisons test, using GraphPad Prism, and significance was set to $p \leq 0.05$. It was found that the difference between the means representing T263 phosphorylation signal of WT MEKK2 + no-peptide and WT MEKK2 + phosphorylated-peptide groups was statistically significant, $p \leq 0.01$, Figure 3.2C. As expected, the difference between the means of WT MEKK2 + no-peptide and WT MEKK2 + non-phosphorylated peptide T263 was not statistically significant, $p > 0.05$.

Furthermore, the complete loss of 14-3-3 co-IP in Figure 3.2A and B, demonstrates that T263-phosphorylated peptides outcompete WT MEKK2 in binding to 14-3-3. Additionally, 14-3-3 co-IP was maintained in the non-phosphorylated T263 peptide condition, indicating WT MEKK2 outcompetes non-phosphorylated T263 peptides in binding 14-3-3. Despite slightly faint 14-3-3 signal in WT MEKK2 + non-phosphorylated peptide lanes, Figure 3.2B, strong co-IP signal was observed in Figure 3.2A to indicate no significant change in 14-3-3 interaction with MEKK2. Overall, the loss of T263 phosphorylation and 14-3-3 co-IP following T263A MEKK2 mutation, Figure 3.1, and upon competition with T263-phosphorylated peptides, Figure 3.2, provides evidence to characterize T263 as a novel phosphosite on MEKK2 and a novel site of phosphorylation-dependent 14-3-3 interaction.

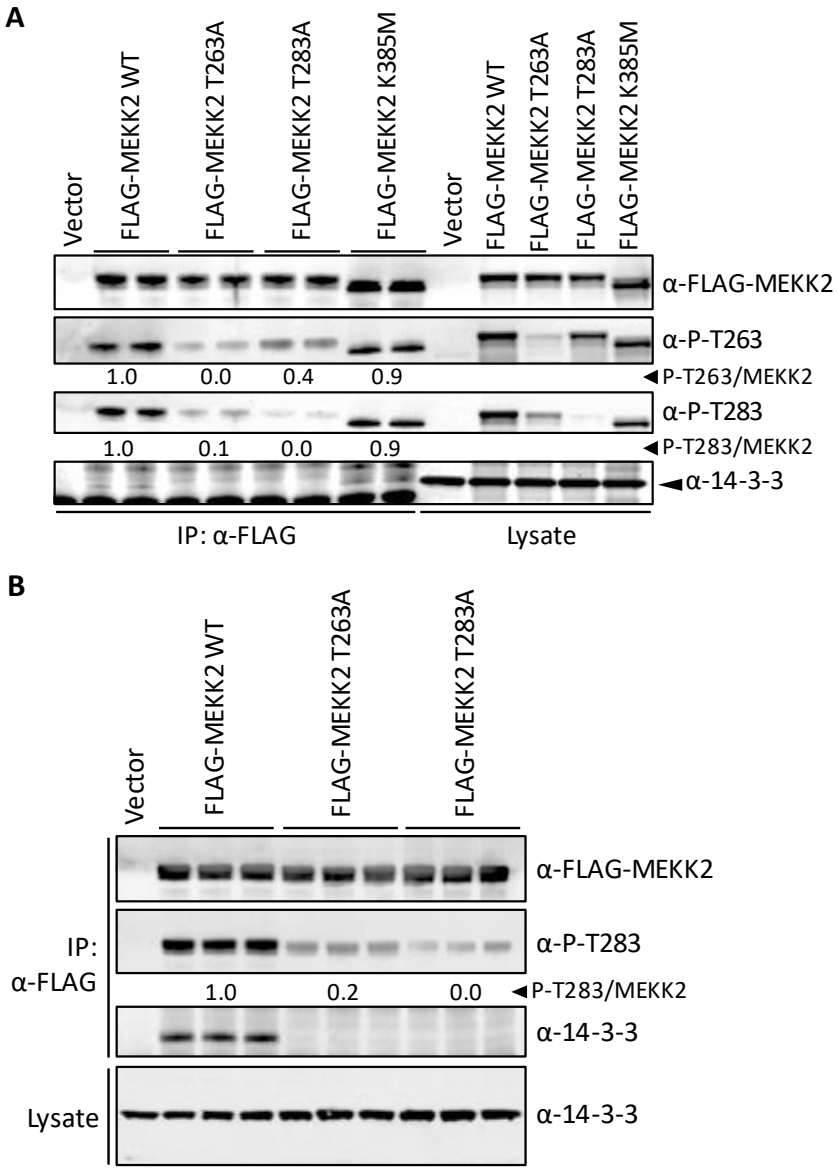

Figure 3.1. T263 is a novel phosphorylation site on MEKK2 and 14-3-3 interacts at T263 and T283. A) FLAG vector (p3xFLAG-CMV-10), WT FLAG MEKK2, T263A FLAG MEKK2; threonine 263 substituted to alanine, T283A FLAG MEKK2; threonine 283 substituted to alanine, or K385M FLAG MEKK2; kinase dead, lysine 385 substituted to methionine, were transfected into HEK 293T cells for 24 h, lysed, immunoprecipitated with anti-FLAG conjugated beads, and fractioned by SDS-PAGE. MEKK2 and mutants were detected by anti-FLAG, anti-phosphor-T263, and anti-phosphor-T283. Endogenous 14-3-3 was detected using pan-specific 14-3-3 antibody. Fluorescent secondary antibodies were detected by Odyssey infrared imaging; band density was measured using ImageJ software. Phosphor-signal to total MEKK2 ratios are representative of the average band intensity between duplicates for each MEKK2 variant, normalized to WT MEKK2. *IP*, immunoprecipitated; *P*, phosphorylated. Performed by Baodong Wu, Scheid Lab. B) FLAG vector, WT FLAG MEKK2, T263A FLAG MEKK2, or T283A FLAG MEKK2 were transfected in HEK 293T cells and immunoprecipitated as in A. MEKK2 and mutants were detected by anti-FLAG, anti-phosphor-T283, and pan-14-3-3 immunoblotting. Phosphor-signal to total MEKK2 ratios are representative of the average between triplicates for each MEKK2 variant, normalized to WT MEKK2. Performed by Baodong Wu, Scheid Lab.

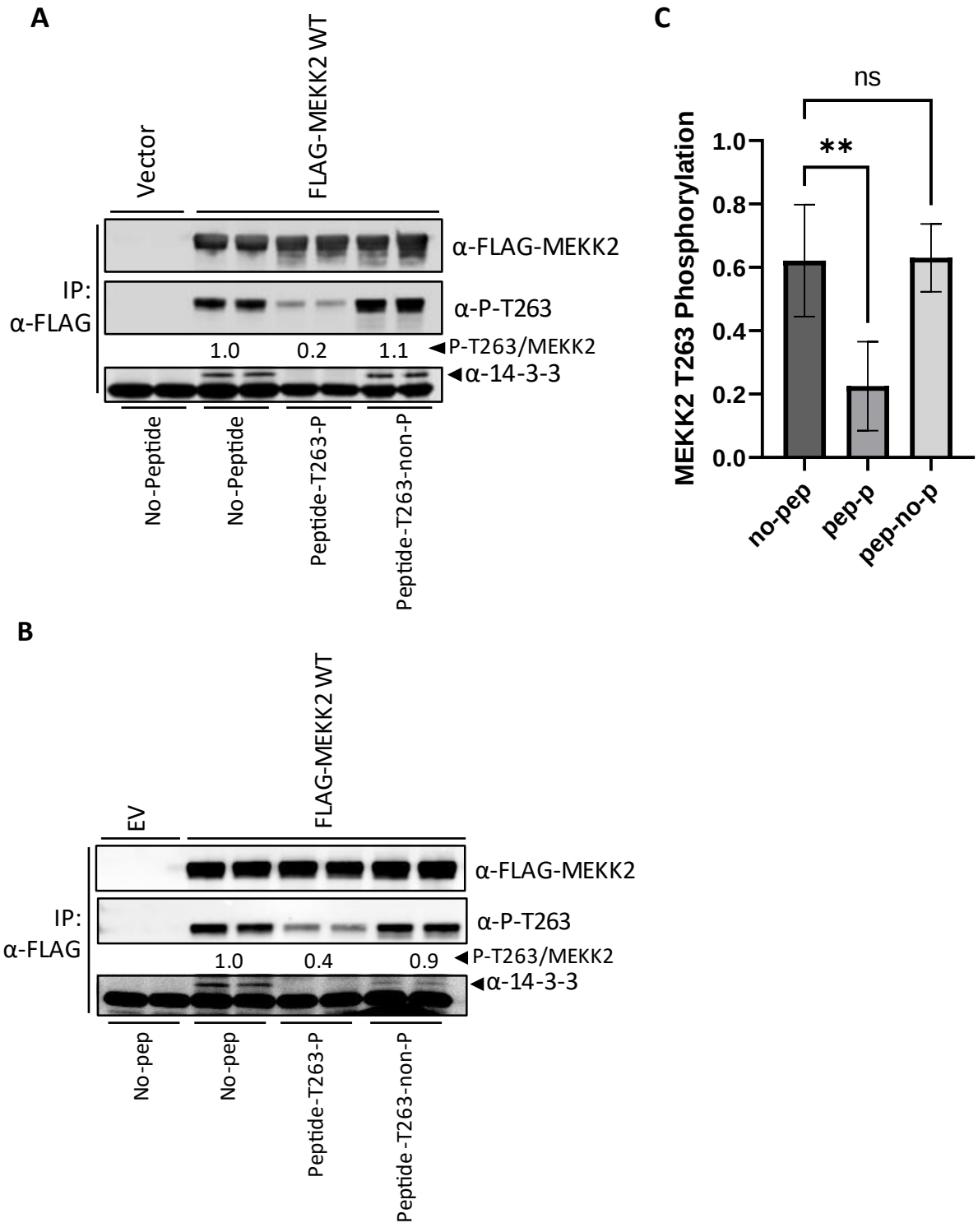

Figure 3.2. T263 phosphorylation and 14-3-3 association assay by peptide competition. A) FLAG vector and WT FLAG MEKK2 were transfected into HEK 293T cells for 24 h and lysed. Either no peptides (no-pep), T263-phosphorylated peptides (peptide-T263-p; pep-p) or non-phosphorylated peptides (peptide-T263-non-P; pep-no-p) were added to the lysate. A co-IP was performed using anti-FLAG conjugated beads and proteins were fractioned by SDS-PAGE. MEKK2 was detected by anti-FLAG and anti-

phosphor-T263 immunoblotting. Endogenous 14-3-3 was detected using pan-specific 14-3-3 antibody. Fluorescent secondary antibodies were detected by Odyssey infrared imaging; band density was measured using ImageJ software. Phosphor-signal to total MEKK2 ratio is representative of the averaged band intensity between duplicates for each MEKK2 variant, normalized to the no-peptide condition. Performed by Baodong Wu, Scheid Lab. B) Experiment repeated as in A. Performed by Rachel Corridore. C) Statistical analysis of T263 phosphorylation signal among no-peptide, pep-p, and pep-no-p groups. One-way ANOVA followed by Dunnett's multiple comparisons test was performed using GraphPad Prism. Data reported as Mean±SD, n=4; (**) $p \leq 0.01$, statistically significant; (ns) not significant, $p > 0.05$. Significance was set to $p \leq 0.05$.

3.2 Endogenous SMYD3 Inhibition

Mazur et al. (2014) demonstrated that SMYD3, a lysine methyltransferase, methylates K260 of MEKK2.[95] K260 is 3 amino acids upstream of our novel MEKK2 phosphorylation site at T263. Therefore, our next objective was to determine if SMYD3-mediated K260 MEKK2 methylation has a regulatory role on T263 and T283 phosphorylation status. HEK 293T cells were transfected with FLAG vector, WT MEKK2, T263A MEKK2, T283A MEKK2, and K385M MEKK2. Two hours prior to harvest, cells were incubated with 250nM of SMYD3-inhibitor BAY-6035, a potent and selective inhibitor which prevents the methylation of MEKK2 by SMYD3.[130] Cells were lysed and proteins were examined by Western blot. Blots were probed for total FLAG MEKK2, phosphor-T263, and phosphor-T283.

Phosphorylation signal at T263 increases slightly by 20% in WT MEKK2 with the addition of BAY-6035, while no change is observed in T283 phosphorylation, Figure 3.3A. In T263A MEKK2, loss of T283 phosphorylation was observed in equal amounts before and after BAY-6035 addition, with slight background signal present in those lanes. In T283A MEKK2, T263 phosphorylation decreases by 10%. In kinase dead K385M MEKK2, T263 phosphorylation increases by 30% and T283 phosphorylation increases by 40%. To further investigate the changes seen in K385M MEKK2, the experiment was repeated in triplicates using only WT MEKK2 and K385M MEKK2, Figure 3.3B. WT MEKK2 once again displayed insignificant changes in phosphorylation with endogenous SMYD3 inhibition, however no significant changes in T263 and T283 phosphorylation status in K385M MEKK2 was observed in this replicate experiment.

Consistent with our previous findings, loss of either T263 or T283 phosphorylation interfere with one another, Figure 3.3A. A significant reduction in T263 phosphorylation in T283A MEKK2 was observed, which was similarly observed in T263A MEKK2 with near complete loss of T283 phosphorylation.

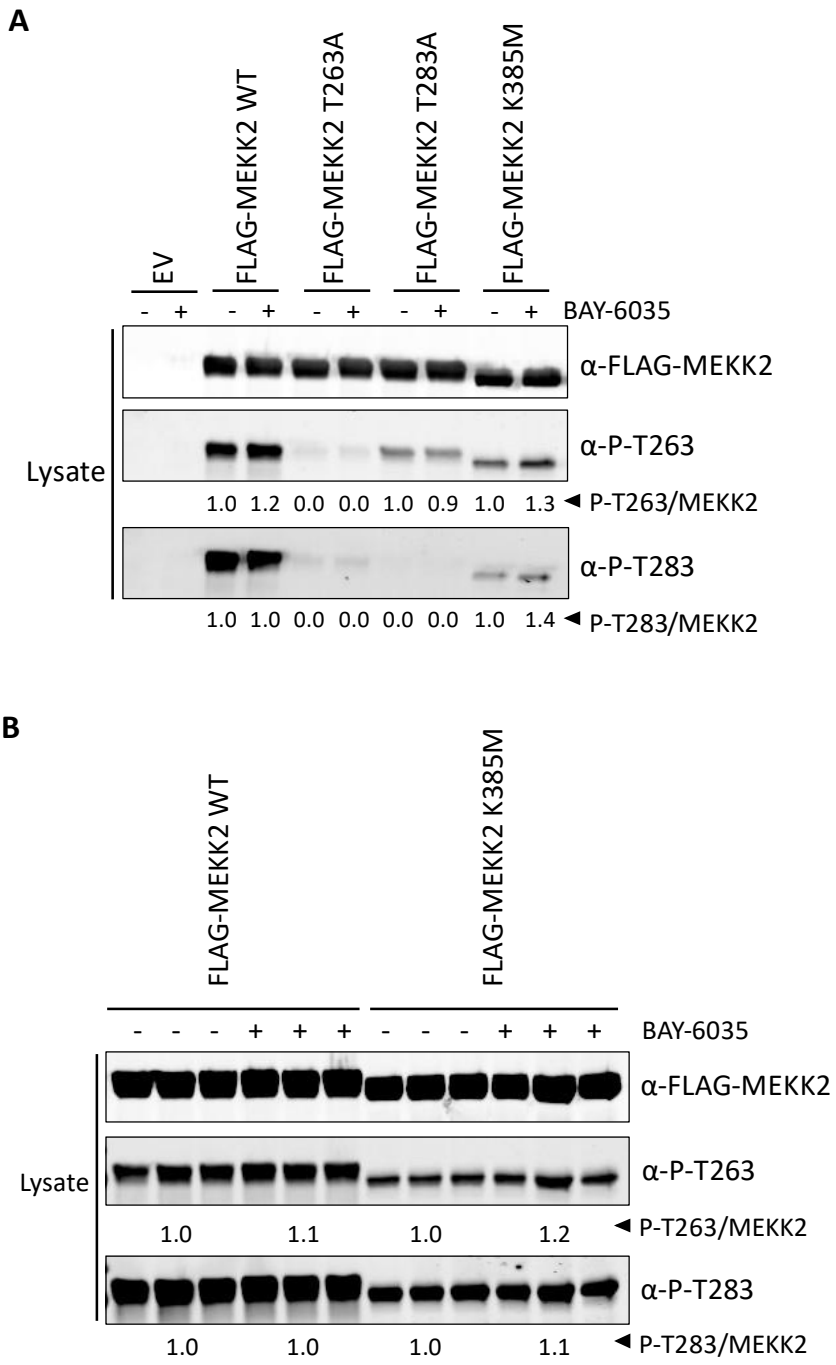

Figure 3.3. SMYD3 inhibition does not impact MEKK2 phosphorylation at T263 and T283. A) EV; empty vector (FLAG vector), WT MEKK2, T263 MEKK2, T283 MEKK2, and K385M MEKK2 were transiently expressed in HEK 293T cells for 48 h. Indicated cells were incubated with 250nM BAY-6035 for 2 h prior to cell harvest and lysis. Lysate proteins were separated by SDS-PAGE and immunoblotted with anti-phospho-Thr-263, anti-phospho-Thr-283, and anti-FLAG. Fluorescent secondary antibodies were detected by Odyssey infrared imaging; the density of each band was determined using ImageJ. P-T263 and P-T283 to total FLAG-MEKK2 ratios were normalized to the no BAY-6035 condition for each transfected plasmid. B) WT MEKK2 and K385M MEKK2 were transfected in HEK 293T in triplicates as described in A.

3.3 SMYD3-Mediated Methylation at K260 Likely Does Not Regulate MEKK2 Phosphorylation at T263 and T283

After observing minimal changes in T263 and T283 phosphorylation following endogenous SMYD3 inhibition, our next set of experiments involved the generation of a SMYD3 expression-vector to perform MEKK2 and SMYD3 co-transfections.

Central to this project was the subcloning of the pMSCV-Flag-SMYD3 plasmid into the pcDNA4/myc-His C vector. Upon initial co-transfection experiments using pMSCV-Flag-SMYD3, no SMYD3 signal was detected by anti-FLAG immunoblotting (not shown). It was deduced that the lack of expression may have been caused by the LTR promoter within the pMSCV vector. Therefore, a vector backbone containing a CMV promoter, supported in HEK 293T cells, was opted for.[131]

As described in Chapter 2.2 pcDNA4/myc-His C empty vector backbone, 5.1kb in size, was double-digested with BamHI and NotI restriction enzymes within the MCS, Figure 3.4A. This digestion produced a 5.1kb fragment with 5' overhangs at both ends, with the only excised nucleotides originating from the original vector being those located within the MCS. Subsequently, pMSCV-Flag-SMYD3, 8.7kb in size, was RE-digested with BglII and NotI. This resulting 6.7kb fragment corresponded to the pMSCV backbone, and the 2kb fragment corresponded to the FLAG-SMYD3 insert, Figure 3.4B. The BglII cut produced a 3' overhang on one end of the SMYD3 insert, which would ultimately ligate with the compatible 5' BamHI overhang from the pcDNA backbone, destroying the RE sites upon ligation. Simultaneously, the compatible 5' NotI overhangs from the opposite end of the SMYD3 insert and pcDNA would ligate, leaving the NotI RE site intact. Successful ligation was confirmed through NotI digestion

of the ligated plasmid, producing a 7.1kb fragment comprised of the 5.1kb pcDNA backbone and 2kb FLAG-SMYD3 insert, confirming a subcloned pcDNA4/myc-His-Flag-SMYD3 plasmid had been generated, Figure 3.4C.

To determine the effect of SMYD3 expression on MEKK2 phosphorylation status, pcDNA4-Flag-SMYD3 was co-transfected with WT MEKK2, T263A MEKK2, T283A MEKK2, and K385M MEKK2 in HEK 293T cells, Figure 3.5. A FLAG-IP was performed to detect di-methylation signal. Phosphorylation signals were observed within the lysate and compared under conditions of SMYD3 expression and its absence. Firstly, these results confirmed that pcDNA4-Flag-SMYD3 produces robust SMYD3 expression in HEK 293T cells, as demonstrated by very saturated FLAG-SMYD3 signal. Upon initial observation, it appeared that SMYD3 expression resulted in significantly increased phosphorylation signals in all MEKK2 variants. However, after quantifying band density and normalizing the phosphorylation to total MEKK2 ratios to the MEKK2 no-SMYD3 condition for each variant, it was determined that there were only minor changes in phosphorylation with SMYD3 expression. T263 phosphorylation increased by 20% in WT MEKK2, 20% in T283A MEKK2, and no change in K385M MEKK2. T283 phosphorylation increased by 40% in WT MEKK2, 10% in T263A MEKK2, and no change again in K385M MEKK2.

Furthermore, these increases in MEKK2 phosphorylation in SMYD3-positive lanes is observed in conjunction with increased total MEKK2 signal in both lysate and IP, suggesting that increased phosphorylation signal may be attributed to increased total MEKK2 upon SMYD3 co-expression. Lastly, di-methylation signal was solely observed in K385M MEKK2 upon SMYD3 expression, using a pan-specific di-methyl lysine antibody. These results indicate K385M MEKK2 is di-methylated to a small degree only upon SMYD3 expression.

The absence of di-methylation signal upon SMYD3 expression in WT MEKK2 was unexpected. Consequently, the following experiments were designed to detect FLAG-immunoprecipitated FLAG MEKK2 in both di-methylated and tri-methylated states. K260R MEKK2 and F258R MEKK2, methylation-resistant mutants of MEKK2, were generated by site-directed mutagenesis to characterize K260 as the sole MEKK2 methylation site. The lysine (K) and the -2 phenylalanine (F) residues are essential for substrate methylation by SMYD3 lysine-methyltransferase, rendering these MEKK2 mutant methylation-resistant.[132]

As demonstrated in Figure 3.6A and B, WT MEKK2, K260R MEKK2 and F258R MEKK2 were co-transfected with FLAG SMYD3 in HEK 293T cells. A FLAG-IP was performed, and proteins were immunoblotted for FLAG MEKK2, FLAG SMYD3, pan-di-methylation and pan-tri-methylation, and phosphor-T263, and phosphor-T283. Primarily, K260R MEKK2 and F258R demonstrated complete loss of methylation signal relative to WT MEKK2, indicating SMYD3-mediated methylation of MEKK2 is occurring at K260, and F258 is required for K260 methylation.

Next, we asked whether K260 methylation influences T263 and T283 phosphorylation status. FLAG MEKK2 signal intensity varied between SMYD3 conditions, consistently appearing more saturated in the SMYD3-positive condition for each MEKK2 construct. To address this variation and accurately analyze the effect of SMYD3 on MEKK2 phosphorylation, phosphorylation to total MEKK2 ratios were averaged between triplicate transfections and normalized to the no-SMYD3 condition for each MEKK2 construct. When observing changes in phosphorylation in WT MEKK2 upon SMYD3 co-expression, a 30% reduction was observed in T263 phosphorylation and a similar 40% reduction was observed in T283 phosphorylation, Figure 3.6A. The experiment was repeated as illustrated in Figure 3.6B, where a similar 30% reduction

again observed in T263 phosphorylation. However, T283 phosphorylation appeared to decrease by 80% in the SMYD3-positive condition. This observation might be attributed to the loss of protein in lane 6, one of the three replicate transfections, which could have influenced the overall average signal intensity for T283 phosphorylation, resulting in a lower phosphorylation-to-total protein ratio.

Despite complete loss of methylation in K260R MEKK2, T263 phosphorylation appeared to increase by 40% upon SMYD3 addition in Figure 3.6A. However, T283 phosphorylation was observed to decrease by 20%. In F258R MEKK2, there was only a 10% reduction observed in T263 phosphorylation, while a similar 20% reduction was observed in T283 phosphorylation, Figure 3.6B. Overall, while these findings are inconclusive, they suggest that SMYD3-mediated K260 methylation appears to have limited influence on the regulation of T263 and T283 phosphorylation in MEKK2.

MEKK3 (MAP3K3) shares significant sequence homology with MEKK2 and is phosphorylated at homologous sites; T274 and T294, Figure 3.7A. As in MEKK2, the MEKK3 phosphorylation sites are also 20 amino acids apart and the lysine 271 residue is -3 to T274. As demonstrated in Figure 3.6B, F258 of MEKK2 is required for SMYD3-mediated K260 methylation. It was hypothesized that the lack of a -2 phenylalanine residue relative to K271 in MEKK3 would prevent methylation at this lysine residue. To further confirm the observed MEKK2 methylation was occurring at K260, WT MEKK2 and WT MEKK3 were co-transfected with pcDNA4-Flag-SMYD3 and immunoprecipitated with anti-FLAG, Figure 3.7B. Through Western Blot analysis, di-methylation and tri-methylation signal was detected in correspondence with the WT MEKK2 + SMYD3 group but was completely absent in MEKK3 + SMYD3 group. Since only MEKK2 is capable of undergoing SMYD3-mediated methylation, these findings provide further evidence

that SMYD3-mediated methylation of MEKK2 occurs at K260 and the -2 phenylalanine is crucial for methylation to occur. This result also demonstrates a divergence in control between MEKK2 and MEKK3, despite highly similar cell signalling roles and activation mechanisms.[13] Furthermore, as demonstrated in Figure 3.7B, T263 and T283 phosphorylation levels remained relatively unchanged in response to SMYD3 expression in WT MEKK2. Furthermore, this experiment showed that MEKK3 is phosphorylated at the T263-equivalent site (T274) and that methylation at K271 is not required for T274 and T294 phosphorylation. Additionally, these findings provide further evidence to confirm that K260 methylation has limited influence on MEKK2 phosphorylation at T263 and T283.

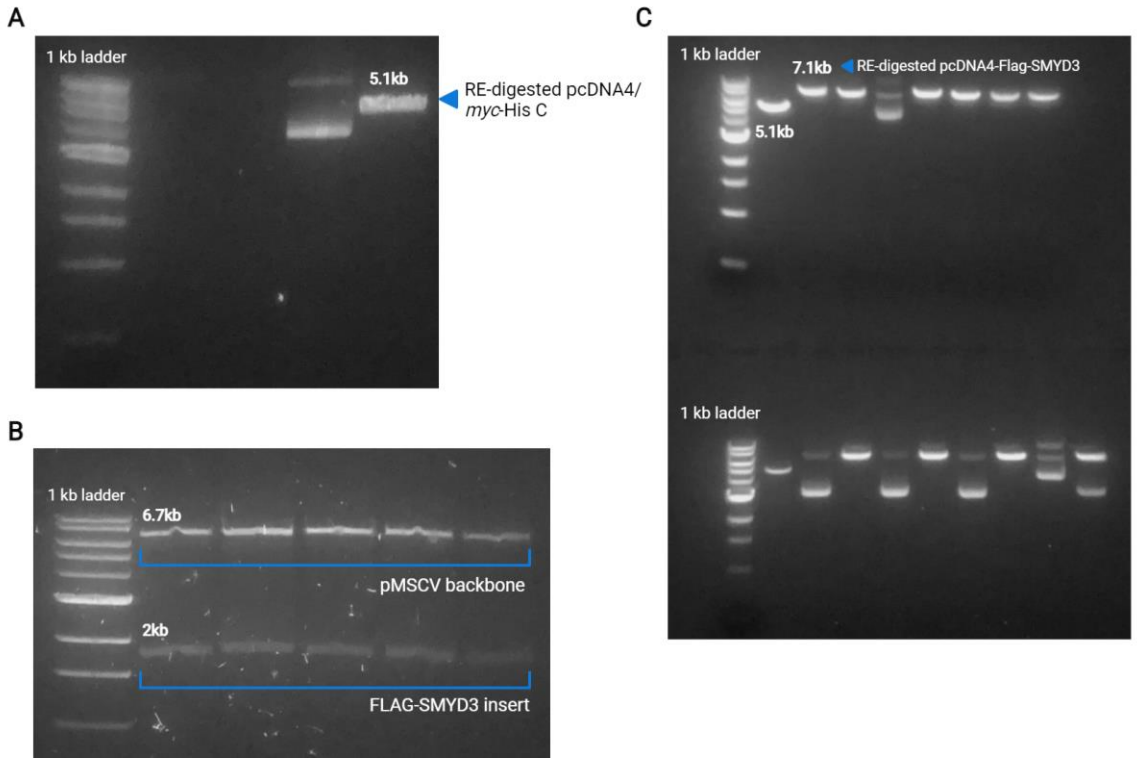

Figure 3.4. pMSCV-Flag-SMYD3 subcloning into pcDNA4 backbone. A) 5.1kb DNA fragment corresponding to pcDNA4/myc-His C double-digested with BamHI and NotI within the MCS. Linearized fragment was excised from the 1% agarose gel. pMSCV-SMYD3 was a gift from Julien Sage (Addgene plasmid #85650; RRID: Addgene_85650). RE; restriction enzyme, MCS; multicloning site. B) pMSCV-Flag-SMYD3 was double-digested with BglII and NotI. RE-digestion produced 6.7kb fragment corresponding to the pMSCV vector backbone and a 2kb fragment corresponding to the FLAG-SMYD3 insert. 2kb DNA fragments from each lane were excised from the 1% agarose gel. Lanes 2-6 represent DNA from five independent miniprep samples of pMSCV-Flag-SMYD3. C) Post-ligation NotI single-digestion of pcDNA4-Flag-SMYD3. RE-digestion yielded a linearized 7.1kb fragment, indicating successful ligation of the 5.1kb pcDNA4 vector and 2kb FLAG-SMYD3 insert. Top: Lane 1 represents the vector-only control 2, as described in 2.2 Lanes 2-9 represent DNA from eight selected colonies. Bottom: Lane 1 represents the vector-only control 2, as described in 2.2 Lanes 2-10 represent DNA from an additional nine selected colonies.

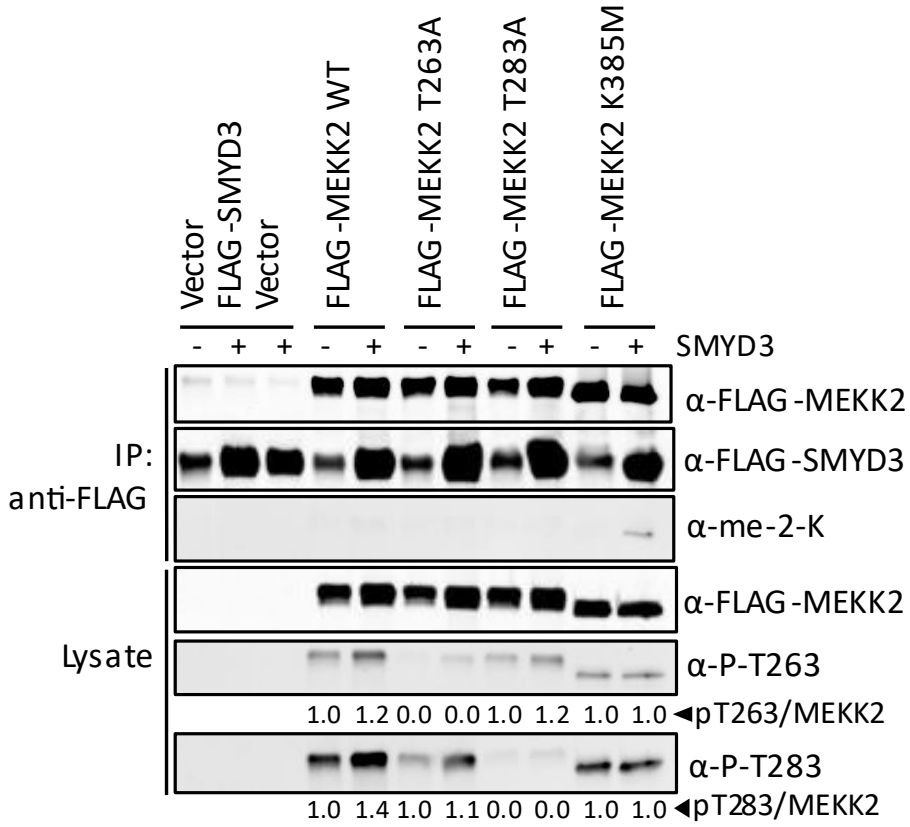

Figure 3.5. pcDNA4-Flag-SMYD3 co-transfection with MEKK2 and mutants. FLAG vector, WT MEKK2, T263A MEKK2 T283A MEKK2, and K385M MEKK2 were transiently expressed in HEK293T cells for 48 h. Indicated cells (+) were co-transfected with pcDNA4-Flag-SMYD3. Whole-cell lysates were total-protein normalized using BCA Protein Assay Kit. Lysate and immunoprecipitated proteins were separated by SDS-PAGE and immunoblotted with anti-phospho-Thr-263, anti-phospho-Thr-283, anti-di-methyl-lysine and anti-FLAG primary antibodies. Fluorescent secondary antibodies were detected by Odyssey infrared imaging. Band quantification was performed using ImageJ. Phosphorylation to total MEKK2 ratios were normalized to the no-SMYD3 condition for each MEKK2 variant.

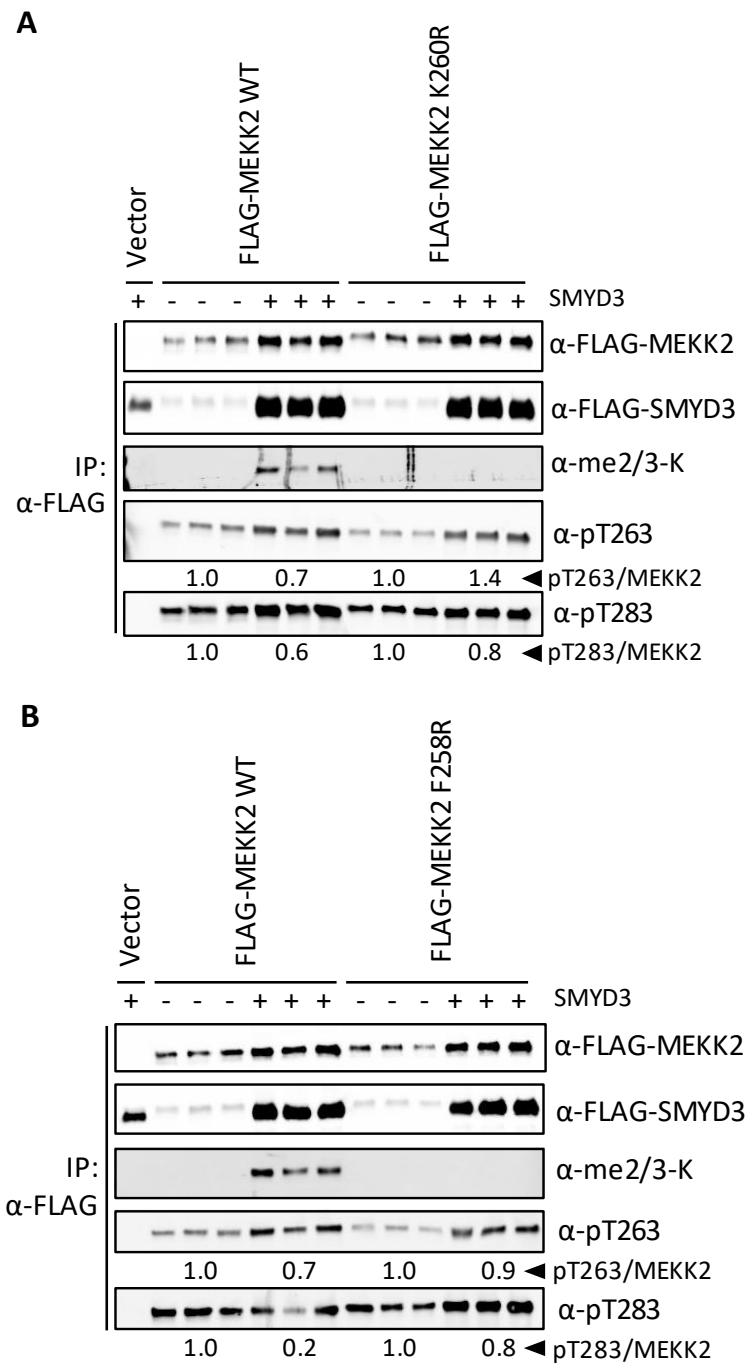

Figure 3.6. Effect of loss of methylation on T263 and T283 phosphorylation. FLAG vector, WT MEKK2 and K260R MEKK2; methylation-resistant (A) or F258R MEKK2; methylation-resistant (B) were transiently expressed in HEK293T cells for 48 h. Indicated cells (+) were co-transfected with pcDNA4-Flag-SMYD3.Whole-cell lysates were total-protein normalized using BCA Protein Assay Kit. Immunoprecipitated proteins were separated by SDS-PAGE and immunoblotted with anti-phospho-Thr-263, anti-phospho-Thr-283, anti-FLAG, anti-di-methyl-lysine, and anti-tri-methyl-lysine primary antibodies. Fluorescent secondary antibodies were detected by Odyssey infrared imaging. Band quantification was performed using ImageJ. Phosphorylation to total MEKK2 ratios were averaged between triplicates and normalized to the no-SMYD3 condition for each MEKK2 variant.

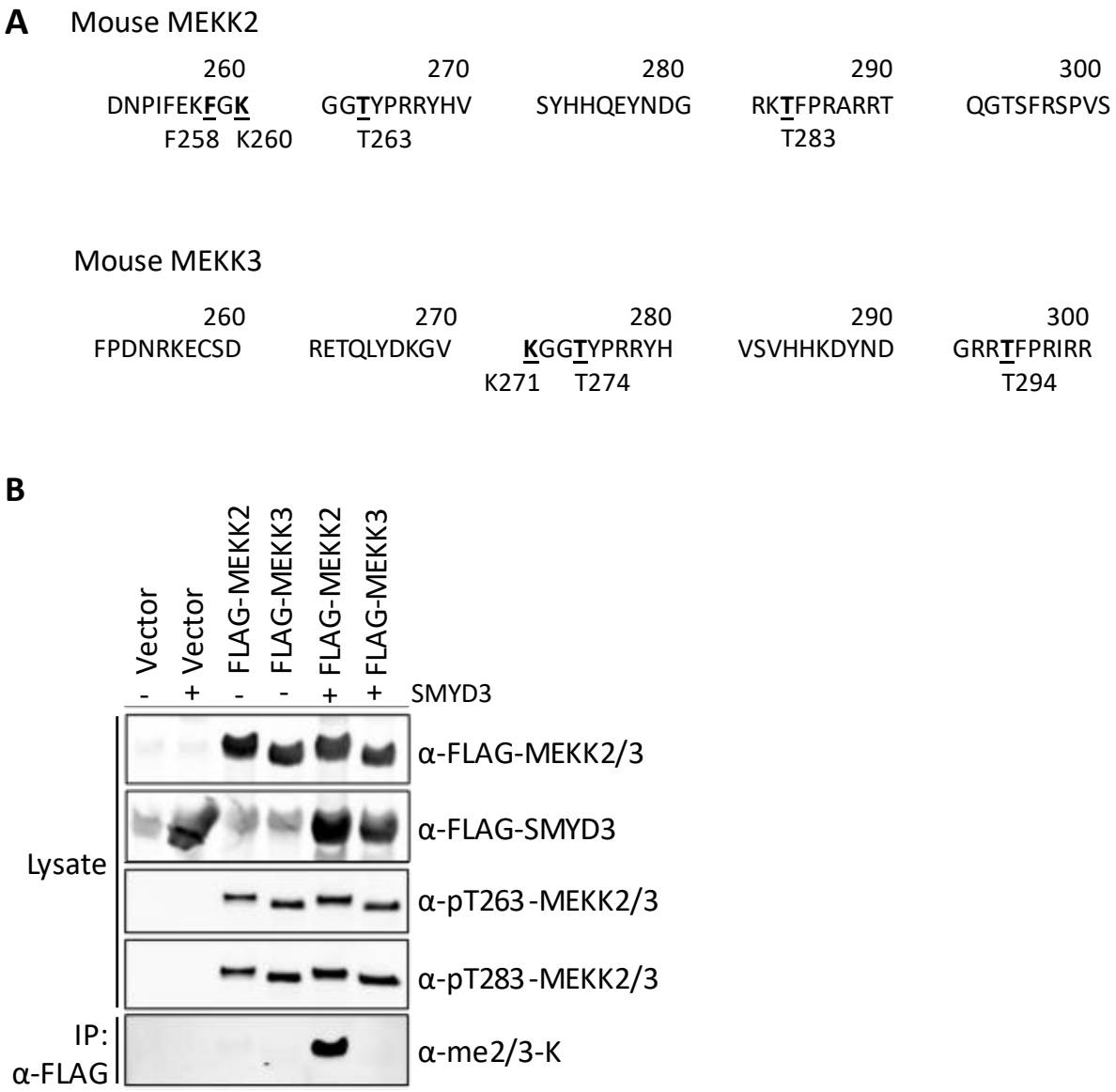

Figure 3.7. MEKK3 is not methylated by SMYD3. A) *M. Musculus* MEKK2 amino acid sequence; UniProt M3M2_MOUSE Q61083. *M. Musculus* MEKK3 amino acid sequence; UniProt M3K3_MOUSE Q61084. Homologous sites labelled. B) FLAG vector, WT MEKK2, and WT MEKK3 were transiently expressed in HEK293T cells for 48 h. Indicated cells (+) were co-transfected with pcDNA4-Flag-SMYD3. Whole-cell lysates were total-protein normalized using BCA Protein Assay Kit. Immunoprecipitated proteins were separated by SDS-PAGE and immunoblotted with anti-FLAG, anti-phospho-T263, anti-phospho-T283, anti-di-methyl-lysine, and anti-tri-methyl-lysine primary antibodies. Fluorescent secondary antibodies were detected by Odyssey infrared imaging. Assisted by Sormeh Mehrabi, Scheid Lab.

3.4 Addressing Increased Total MEKK2 Signal Upon SMYD3 Co-Transfection

Ubiquitination sites can be predicted based on the sequence patterns and motifs that surround the site. Sequence patterns surrounding ubiquitination sites in human and mice include enriched hydrophobic residues at positions -4 to +4 and enriched positively charged arginine residues in the flanking regions.[133] In the previous section (Section 3.3 a trend had become apparent where a significant increase in total FLAG MEKK2 signal was consistently observed upon co-transfection of pcDNA-Flag-SMYD3, as demonstrated in Figure 3.5 and Figure 3.6. When comparing total FLAG MEKK2 signal between the SMYD3-negative to SMYD3-positive condition for each transfected MEKK2 variant, there was a significant increase in FLAG MEKK2 signal. Based on these observations, it was hypothesized that K260 could serve as a primary site of MEKK2 ubiquitination. Lysine methylation at ubiquitination sites can stabilize protein activity by inhibiting the binding of E3 ubiquitin ligase, preventing protein degradation via the ubiquitin-proteasome pathway.[129] Consequently, an excess of accessible SMYD3, following co-transfection, could lead to enhanced MEKK2 methylation at K260, potentially inhibiting ubiquitination at this locus and consequent degradation of MEKK2. Elevated MEKK2 activity could have severe implications in the dysregulation of MAPK pathways and tumorigenesis. Therefore, we asked whether K260 is ubiquitination site, and whether SMYD3-mediated methylation at K260 prevents ubiquitination.

To test this hypothesis, HA-tagged ubiquitin (HA-Ub) and FLAG SMYD3 were co-transfected with WT MEKK2 or K260R MEKK2 in HEK 293T cells, Figure 3.8. The K260R MEKK2 mutant replaces lysine with an arginine residue, rendering this mutant ubiquitination-resistant as arginine lacks the necessary functional groups for ubiquitin attachment.[134] Proteins were immunoprecipitated with anti-FLAG and subsequently immunoblotted with anti-HA and anti-

FLAG antibodies. Upon expression, HA-Ub was observed to co-IP with both WT MEKK2 and K260R MEKK2. Importantly, the observed levels of HA-Ub remained unchanged in WT MEKK2 following SMYD3 expression. If SMYD3-mediation at K260 was preventing MEKK2 ubiquitination, complete loss of HA-Ub association with WT MEKK2 would have been observed. These results primarily indicate that MEKK2 is ubiquitinated however, this ubiquitination does not occur at K260, as indicated by association of HA-Ub with K260R MEKK2.

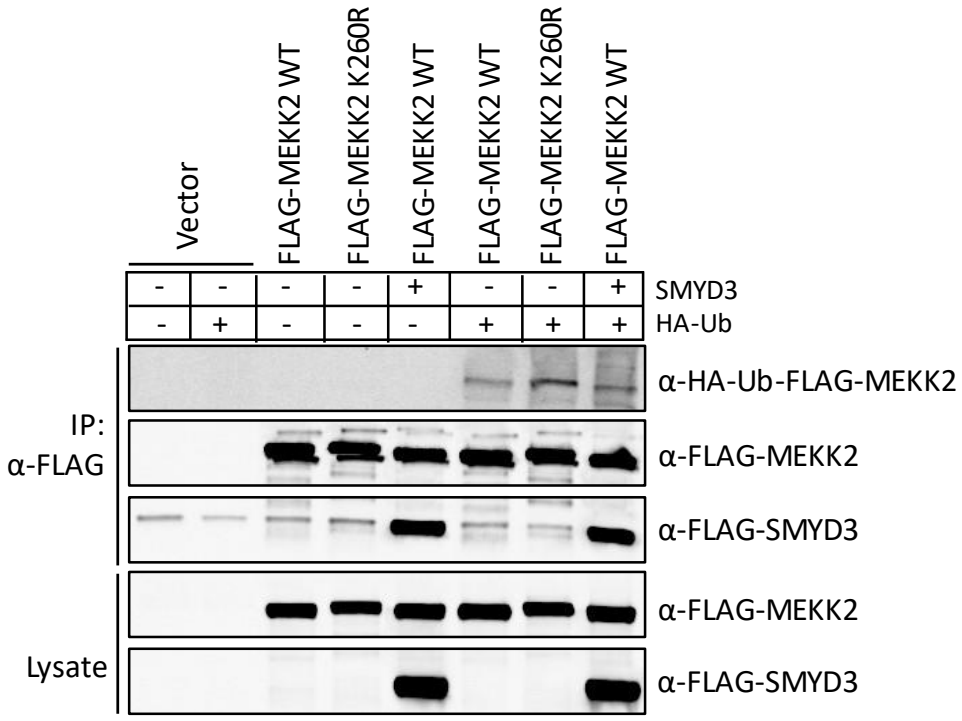

Figure 3.8. MEKK2 ubiquitination is not specific to K260. FLAG vector, WT MEKK2 and K260R MEKK2 were transiently expressed in HEK293T cells for 48 h. Indicated cells (+) were co-transfected with either pcDNA4-Flag-SMYD3 or HA-Ub. Whole-cell lysates were total-protein normalized using BCA Protein Assay Kit. Immunoprecipitated proteins were separated by SDS-PAGE and immunoblotted with anti-FLAG. Fluorescent secondary antibodies were detected by Odyssey infrared imaging.

3.5 MEKK2 Methylation at K260 is Regulated by T263 and T283 Phosphorylation

Following the observation that K260 methylation has minimal impact on T263 and T283 phosphorylation, we next asked if phosphorylation at these sites influences K260 methylation. The effect of T263 and T283 phosphorylation on K260 methylation was determined through Western Blot analysis. A double mutated T263/283A MEKK2 (T2A) variant was prepared, which is phosphorylation-resistant at both phosphosites. This MEKK2 mutant was generated by site-directed mutagenesis to determine whether loss of phosphorylation at both sites conferred an augmented affect on K260 methylation than the single T263 and T283 MEKK2 mutants.

WT MEKK2, T263A MEKK2, T283A MEKK2, and T2A MEKK2 were co-transfected with pcDNA4-Flag-SMYD3, Figure 3.9A. Following harvest, the cells were lysed, FLAG-immunoprecipitated, and immunoblotted for FLAG MEKK2, di-methylation and tri-methylation. Upon signal quantification, a significant 80% reduction in methylation signal was observed in T263A MEKK2. Similarly, a 60% reduction in methylation was observed in T283A MEKK2 and T2A MEKK2. These data were analyzed for statistical significance by performing one-way ANOVA followed by Dunnett's multiple comparisons test, using GraphPad Prism, and significance was set to $p \leq 0.05$. The analysis demonstrated a statistically significant difference in the mean values representing K260 methylation between WT MEKK2 and each phosphorylation-resistant MEKK2 variant, Figure 3.9B. The data set was derived from three independent co-transfections (n=3), and the p-value was found to be less than 0.001 for T263A MEKK2 and less than 0.01 for T283A MEKK2 and T2A MEKK2, indicating statistical significance. These results indicate that K260 methylation is regulated by T263 and T283 phosphorylation as the absence of phosphorylation at either or both of these sites negatively regulates K260 methylation.

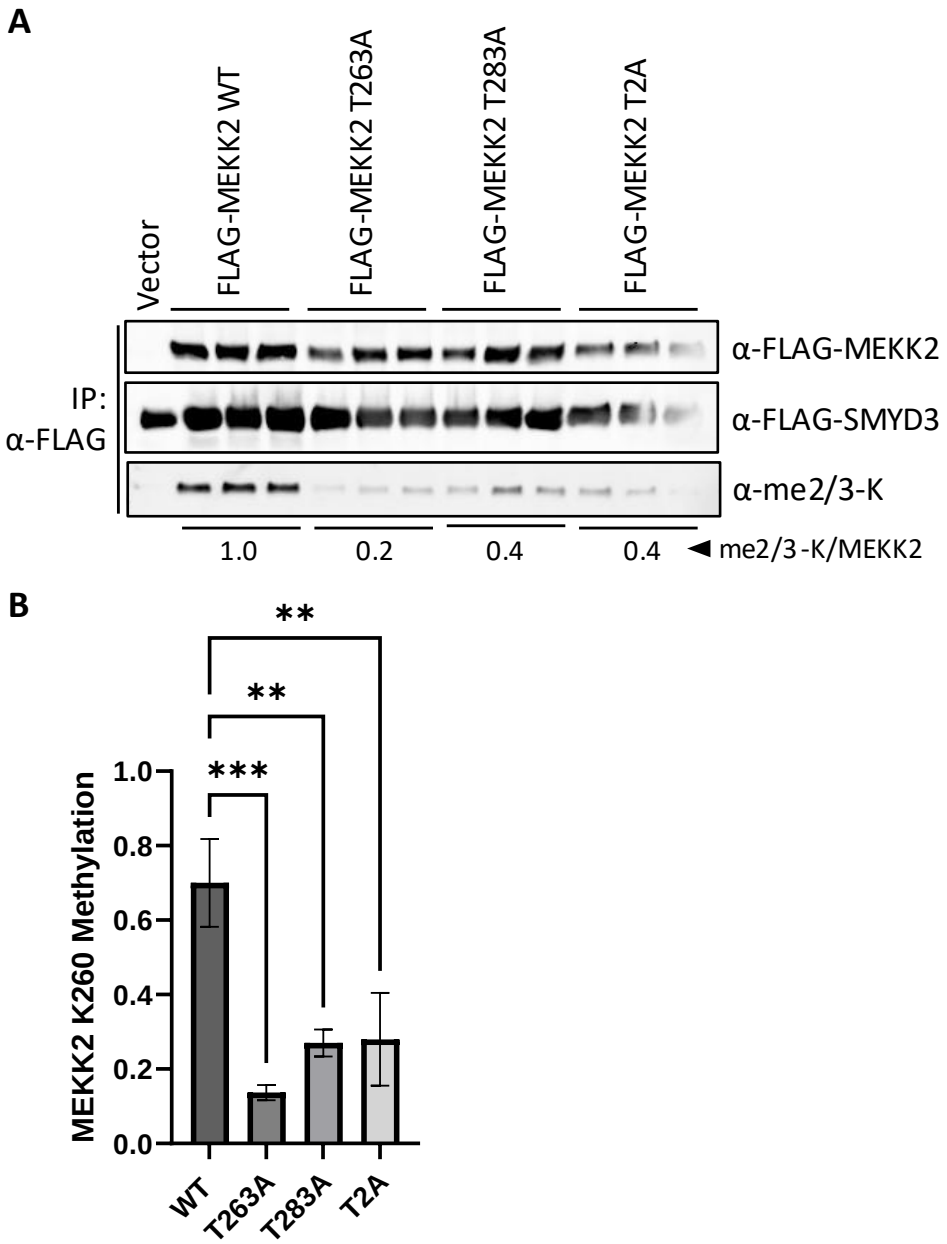

Figure 3.9. SMYD3-mediated methylation at K260 requires T263 and T283 phosphorylation. A) FLAG vector, WT MEKK2, T263A MEKK2, T283A MEKK2, and T2A MEKK2 were transiently expressed in HEK293T cells for 48 h. All cells were co-transfected with pcDNA4-Flag-SMYD3. Whole-cell lysates were total-protein normalized using BCA Protein Assay Kit. Immunoprecipitated proteins were separated by SDS-PAGE and immunoblotted with anti-FLAG, anti-di-methyl-lysine, and anti-tri-methyl-lysine primary antibodies. Fluorescent secondary antibodies were detected by Odyssey infrared imaging. Band density was quantified using ImageJ. Methylation to total MEKK2 signal was averaged between triplicates and normalized to WT. B) Statistical analysis of K260 methylation in WT MEKK2, T263A MEKK2, T283A MEKK2, and T2A MEKK2 from A. One-way ANOVA followed by Dunnett's multiple comparisons test was performed using GraphPad Prism. Data reported as Mean±SD, n=3; (**) $p \leq 0.01$, (***) $p \leq 0.001$. Significance was set to $p \leq 0.05$.

3.6 Investigating a Direct Interaction Between MEKK2 and SMYD3

To investigate whether SMYD3 directly interacts with MEKK2 when methylating K260, WT MEKK2 and all mutants were subjected to analysis by protein purification. WT MEKK2, T263A MEKK2, T283A MEKK2, T2A MEKK2, K260R MEKK2, F258R MEKK2, and K385M MEKK2 were co-transfected with pcDNA4/myc-His-Flag-SMYD3. Cell lysates were subjected to protein purification using Myc-conjugated agarose beads and subsequently immunoblotted with anti-FLAG and anti-14-3-3 antibodies. The 14-3-3 signal in lysate in these experiments serves as a loading control, as 14-3-3 signal in the Myc-IP was not detected.

As demonstrated in Figure 3.10, FLAG MEKK2 signal from all MEKK2 variants was observed to co-IP with Myc-FLAG-SMYD3. This co-IP occurred following protein purification through Myc-immunoprecipitation, affirming the interaction between the respective MEKK2 variants and SMYD3. In WT MEKK2, T263A MEKK2, and T283A MEKK2, FLAG MEKK2 co-IP signal was enriched by over 2-fold upon co-transfection of SMYD3, relative to background signal observed prior to SMYD3 addition., Figure 3.10A. T2A MEKK2 co-IP signal was observed to increase by 90% upon SMYD3 addition. Similarly, FLAG MEKK2 co-IP signal corresponding to methylation resistant K260R MEKK2 was enriched by 70%, however F258R MEKK2 only displayed a 10% enrichment after quantification, Figure 3.10B. Interestingly, K385M MEKK2 displayed a 50% loss of co-IP signal. Overall, enrichment in FLAG MEKK2 co-IP signal in SMYD3-positive lanes suggests a direct interaction between MEKK2 and SMYD3, regardless of T263 and T283 phosphorylation or K260 methylation status.

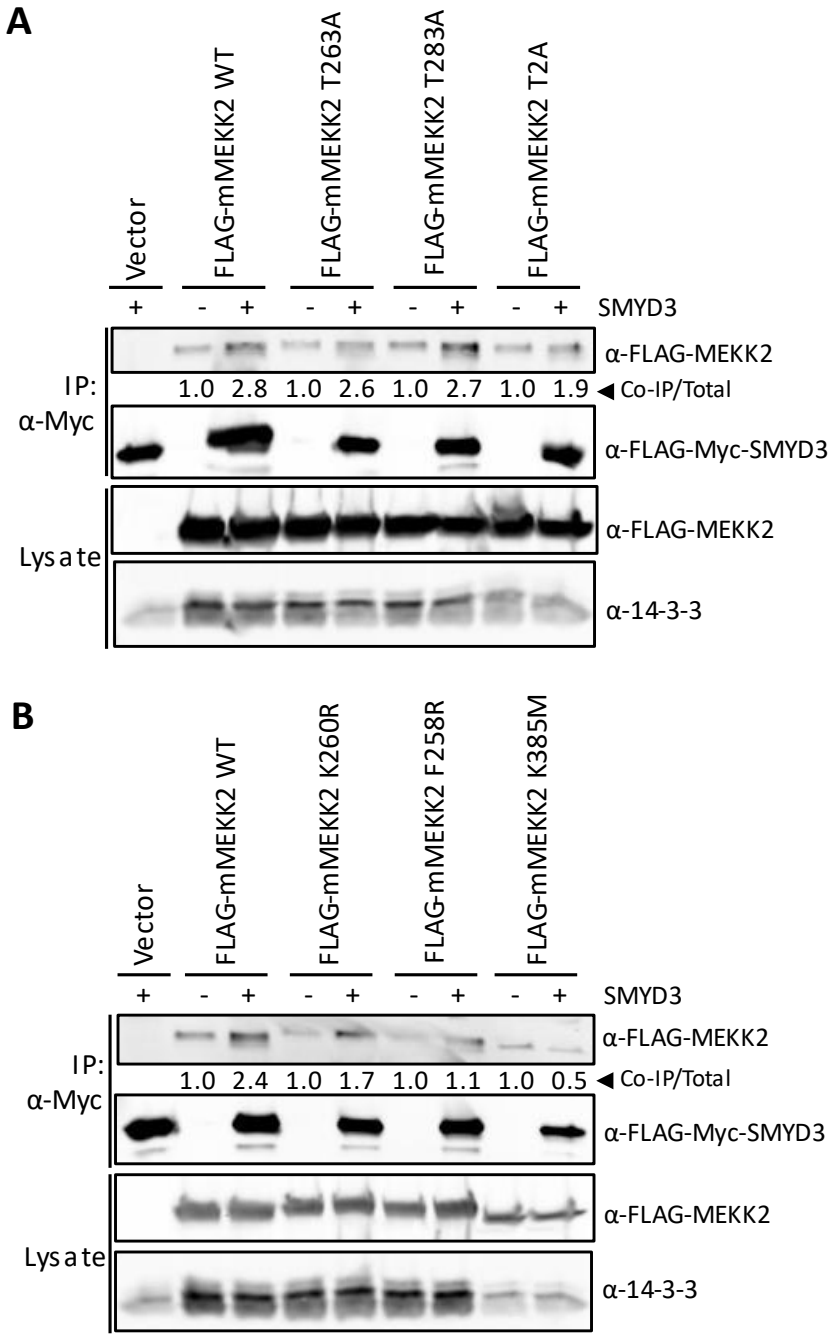

Figure 3.10. Analyzing a direct interaction between SMYD3 and MEKK2 through co-immunoprecipitation. A) WT MEKK2, T263A MEKK2, T283A MEKK2, and T2A MEKK2 were transiently expressed in HEK293T cells for 48 h. Cells co-transfected with pcDNA4-Flag-SMYD3 are indicated by (+). Whole-cell lysates were total-protein normalized using BCA Protein Assay Kit. Proteins were immunoprecipitated with Myc-conjugated agarose beads and were separated by SDS-PAGE and immunoblotted with anti-FLAG and pan anti-14-3-3 antibodies. Fluorescent secondary antibodies were detected by Odyssey infrared imaging. Band quantification was performed using ImageJ. Co-immunoprecipated MEKK2 to total MEKK2 ratio was normalized to the no-SMYD3 condition for each MEKK2 construct. B) K260R MEKK2, F258R MEKK2, and K385M MEKK2 were transiently expressed in HEK 293T cells for 48 h. Myc-IP and Western Blot analysis performed as described in A.

3.7 Generation of Stable MEKK2-Expressing HAP1 Clones from HAP1/- MEKK2 Knockouts

To investigate the role of endogenous MEKK2 in downstream signalling to ERK1/2, HAP1 cells with a whole-genome deletion of MEKK2 were generated using CRISPR/Cas-9 genome-editing technology by Horizon Discovery. Since HAP1 cells are a haploid cell line, these cells have undergone a complete deletion of the sole *mekk2* gene copy in their whole genome, rendering these cells MEKK2 knockouts. CRISPR/Cas-9 utilizes a guide RNA molecule that recognizes its complementary target DNA sequence and directs Cas-9 protein to create a break in the DNA. In the case of DNA deletions, the cell then employs its own repair mechanisms to join the broken DNA ends together through a process called non-homologous end joining (NHEJ).[135]

HEK293Ta cells have a high transfection efficiency and support production and packaging of lentiviral vectors.[136] Lentiviral particle production, as described in Chapter 2.5 requires co-expression of lentiviral expression plasmids, containing the gene of interest, with lentiviral packaging plasmids. HEK 293Ta cells efficiently produce viral packaging proteins, facilitating the assembly and release of lentiviral pseudoparticles into the cell medium, which then becomes the viral supernatant used to transduce HAP1/- cells. These pseudoviral particles contain the transgene and viral proteins that are vital to transduce HAP1/- cells and integrate the gene of interest into the host cellular genome.

Firstly, a lentiviral expression plasmid containing *H. Sapiens* WT MEKK2, LV102-Flag-MEKK2, was obtained from GeneCopoeia. MEKK2 mutations were generated using site-directed mutagenesis and expression was verified by transient transfection in HEK 293T cells. Cells were transfected with WT MEKK2, T263A MEKK2, T283A MEKK2, K260R MEKK2, F258R MEKK2, K385M MEKK2, Figure 3.11A. Cell lysates were subjected to Western Blot

analysis and were immunoblotted with anti-FLAG, anti-phosphor-T263, and anti-phosphor-T283.

T263A MEKK2, T283A MEKK2, and K260R MEKK2 produced strong FLAG MEKK2 signal. Weak FLAG MEKK2 signal was observed for WT MEKK2 and K385M MEKK2, while no signal was observed for F258R MEKK2. The absence of FLAG signal for F258R MEKK2 indicated that the mutagenesis had failed and was re-attempted. In Figure 3.11B, FLAG signal corresponding to F258R MEKK2 was observed, which indicated that the second mutagenesis attempt had been successful. As with prior mutagenesis using the pCMV10-Flag-MEKK2 plasmid, the K260R/K385M MEKK2 mutagenesis failed within the LV102-Flag-MEKK2 vector. Thus, suggesting that these mutations in combination could affect protein function or stability, demonstrated by a lack of expression. It was observed that the working stock of LV102-Flag-MEKK2 plasmid had potentially deteriorated or become compromised. This degradation was inferred by the complete loss of FLAG MEKK2 signal corresponding to WT MEKK2. Consequently, LV102-Flag-MEKK2 plasmid DNA from the originally obtained stock was amplified and purified from DH5-α *E. coli* cultures. Plasmid DNA, obtained from four individual colonies originating from the transformation, were labelled A-D and subsequently transfected in HEK 293T cells, Figure 3.11C. It was evident that plasmid DNA from samples B-D produced the strongest FLAG MEKK2 and phosphorylation signals, therefore these LV102-Flag-MEKK2 plasmids were combined and used for stable cell line generation.

The first method used to generate stable MEKK2 add-back HAP1/- cell lines was the culturing of a polyclonal population of puromycin-resistant cells. As described in Chapter 2.5 HAP1/- cells were transduced with WT or mutant MEKK2-containing lentiviral particles and selected with 1µg/ml of puromycin. The selected cells, which contained the pac gene originating from the

LV102 vector, were allowed to proliferate over a period of 1-2 weeks. The polyclonal expansions were then pooled together, lysed, and analyzed by Western Blot for expression of recombinant MEKK2, Figure 3.12A. Unfortunately, no FLAG MEKK2 signal was detected in any of the stable cell line attempts which included HAP1/- + WT, HAP1/- + T263A, HAP1/- + T283A, HAP1/- + T2A, HAP1/- + K260R, HAP1/- + F258R, HAP1/- + K385M. To increase selection efficiency, the polyclonal stable generation method was repeated using double the amount of puromycin and lentiviral supernatant, Figure 3.12B. The results similarly demonstrate no detection of FLAG MEKK2 or phosphor-T263 signal from any of the stable transfection attempts, indicating that stable cell lines had not been generated by either of our first two attempts.

Polyclonal cell lines are derived from multiple transduced cells which are pooled together to produce a heterogenous population of cells that yield variable levels of protein expression.[137] The lack of FLAG MEKK2 signal may have been caused by variability in protein expression levels between colonies that were pooled together, yielding overall lower concentrations of MEKK2 protein. Therefore, a new method was used that aimed to generate a monoclonal population of MEKK2-expressing cells that share a common progenitor cell, thereby producing similar levels of protein expression, using colony isolation techniques. As described in Chapter 2.5 six monoclonal colonies, for each transduced MEKK2 construct, were isolated and expanded. These clones were lysed and analyzed by Western Blot for FLAG MEKK2 expression, Figure 3.12C. As demonstrated, FLAG MEKK2 signal was not detected from any of the HAP1/- MEKK2 add-back cells however, faint T263 phosphorylation signal produced by cells originating from colony 4 of K260R MEKK2 was observed. These results indicate that this method also had a poor transfection efficiency, yielding no to low levels of MEKK2 expression.

To further investigate the cause of the lack of MEKK2 expression, a GFP expression assay was performed in native HAP1/- cells to determine the efficacy of the lentiviral particle production and transduction methods, as described in Chapter 2.10 A lentiviral plasmid containing eGFP, enhanced green fluorescent protein, was transfected into HEK 293Ta cells and viral supernatant was produced as previously described. Roughly $50x10^3$ HAP1/- cells were transiently transduced with either 0ul, 50ul, 150ul, or 300ul of viral supernatant and 10µg/ml of polybrene, which was used to improve transduction efficiency by promoting adherence of viral particles to HAP1/- cells. Cells were investigated under fluorescent microscopy after 76 hours, Figure 3.13A. Strong eGFP fluorescence was detected upon addition of 300ul of viral supernatant to HEK 293Ta cells, indicating the lentiviral particles are effective at transducing HAP1/- cells.

In Figure 3.13B, stable expression of WT MEKK2 recombinant protein in HAP1/- cells was confirmed. HAP1/- MEKK2 add-backs were generated by transducing $50x10^3$ HAP1/- cells with 300ul of viral supernatant, carrying either WT MEKK2 or T2A MEKK2, and selecting for puromycin-resistance. As a control, $50x10^3$ HAP1/- cells were transiently transduced using the protocol previously described but did not undergo the selection process and were harvested after 76 hours. Following FLAG-immunoprecipitation, transient FLAG MEKK2 signal was detected after transient transduction of HAP1/- cells with WT MEKK2 and T263A MEKK2 and T263 phosphorylation signal was detected corresponding to WT MEKK2. Following selection and potential integration of the MEKK2 transgene, FLAG MEKK2 signal corresponding to both WT MEKK2 and T263A MEKK2 significantly declined. However, levels of T263 phosphorylation signal corresponding to WT MEKK2 remained unchanged between the transient transduction and stable transduction HAP1/- groups. In Figure 3.13C, FLAG MEKK2 signal corresponding to WT MEKK2 was increased approximately 10-fold by harvesting HAP1/- add-backs from 10

individual 100mm dishes. However, FLAG-MEKK2 signal from T2A MEKK2 was not observed to increase to this degree. Overall, these results indicate that HAP1/- MEKK2 add-back stable cells had been generated that strongly express recombinant WT FLAG MEKK2 protein.

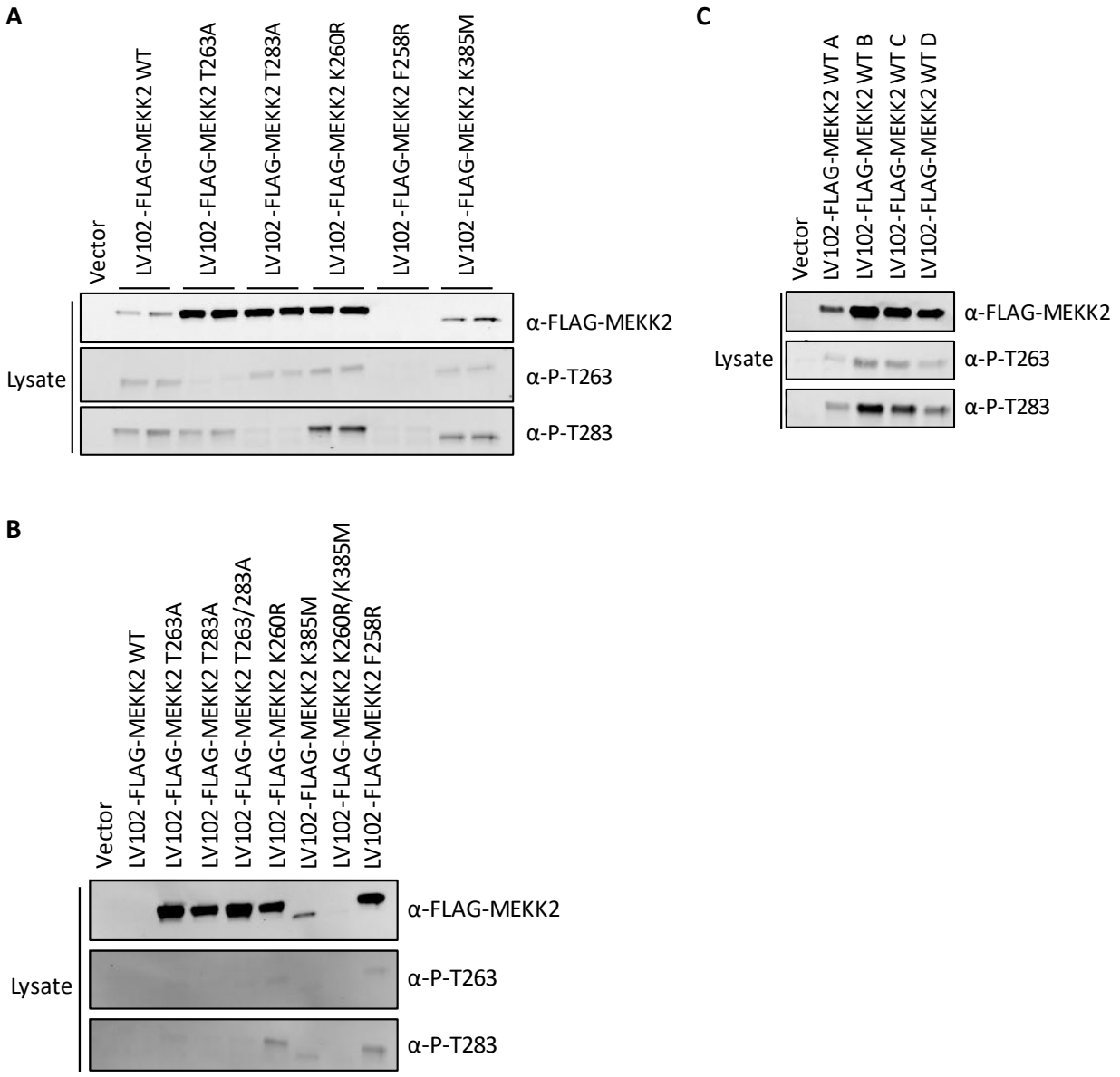

Figure 3.11. LV102-Flag-MEKK2 expression verification troubleshooting. A) Indicated *H. Sapiens* MEKK2 plasmids were transiently expressed in HEK293T cells for 48 h. Whole-cell lysates were total-protein normalized using BCA Protein Assay Kit. Whole-cell lysates were probed with anti-phospho-Thr-263, anti-phospho-Thr-283, and anti-FLAG. Fluorescent secondary antibodies were detected by Odyssey infrared imaging. B) Transfection and Western Blot prepared as described in A. C) WT MEKK2 was transformed into competent DH5-α E. coli and grown on an ampicillin-resistant LB-agar plate for 20 hours. Four colonies were selected and grown in LB-media with continued ampicillin-selection for 20 hours. LV102-Flag-WT MEKK2 plasmids were isolated from bacterial cultures originating from the 4 individual colonies and were transiently expressed in HEK293T cells.

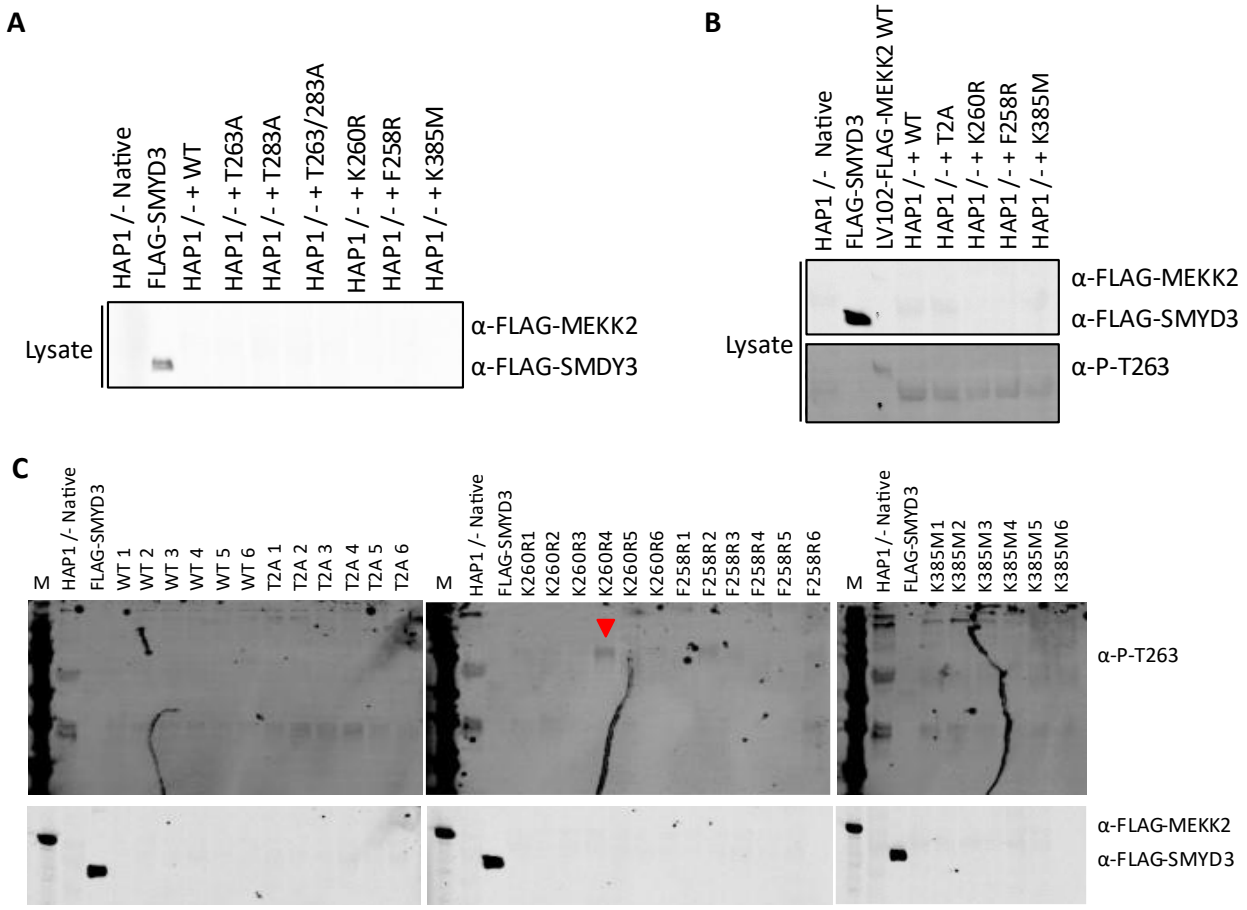

Figure 3.12. Polyclonal and monoclonal stable MEKK2 expression attempts. A) HAP1/- *MEKK2 knock-out* cells were transduced with 100ul of lentivirus containing FLAG-WT, T263A, T283A, T2A, K260R, F258R, K385M MEKK2 in 100mm dishes for 76 h. Following 5 days of selection in 1µg/ml puromycin, clonal cells were lysed and pooled. The polyclonal HAP1/- cells were subjected to Western Blot analysis and probed for FLAG to detect transient MEKK2 expression. HAP1/- native; non-transduced cells. B) HAP1/- *MEKK2 knock-out* cells were transduced with 200ul lentivirus containing FLAG-WT, T2A, K260R, F258R, K385M MEKK2 in 100mm dishes for 76 h. Following 5 days of selection in 2µg/ml puromycin, colonies were lysed and pooled. Polyclonal HAP1/- cells were subjected to Western Blot analysis and probed for FLAG and pT263 to detect transient MEKK2 expression. C) HAP1/- *MEKK2 knock-out* cells were transduced with 30ul of lentivirus containing FLAG-WT, T2A, K260R, F258R, K385M MEKK2 in 6-well plates for 76 h. Transduced cells were lysed and sub-cultured into three 100mm plates, per construct. Cells were plated in IMDM culture medium containing 2µg/ml puromycin. Monoclonal cells were isolated and expanded in 6-well plates to 80% confluency, then were sub-cultured into two 100mm dishes, per construct. Once clones reached 80% confluency, cells were lysed and subjected to Western Blot analysis, and probed for FLAG and pT263 to detect transient MEKK2 expression. Faint pT263 detected in K260R MEKK2 clone 4, indicated by the red arrow.

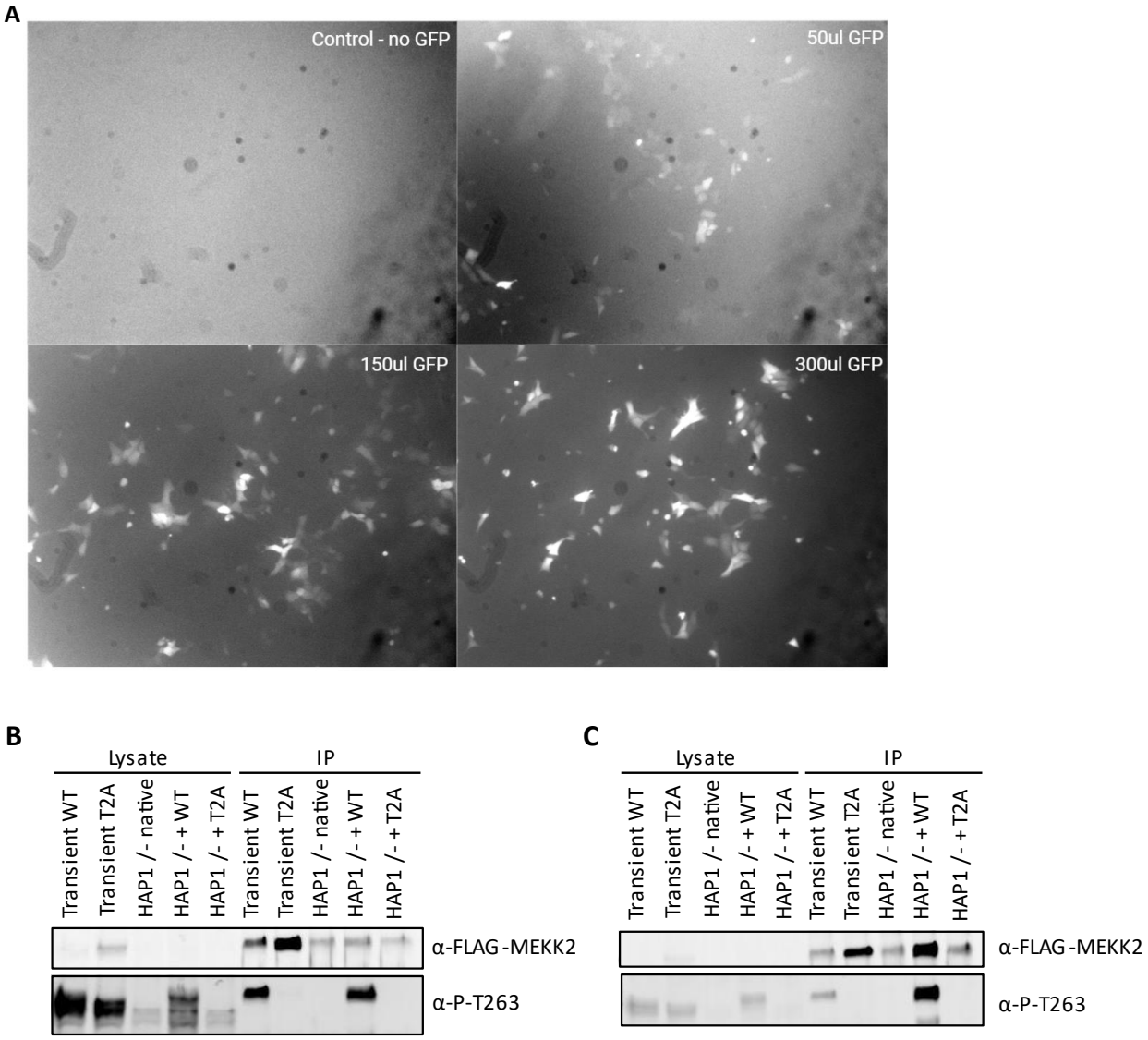

Figure 3.13. Confirmation of recombinant MEKK2 expression in HAP1/MEKK2-stable cells. A) $50x10^3$ HAP1 *MEKK2 knock-out* cells were transduced with 0ul, 50ul, 150ul, or 300ul of eGFP-containing lentiviral supernatant in 6-well plates in a culture medium containing IMDM, 10% heat-inactivated FBS, and 10µg/ml polybrene. eGFP expression was investigated after 76 h using fluorescence microscopy. B) $50x10^3$ HAP1 *MEKK2 knock-out* cells were transduced with 300ul WT MEKK2 or T263A MEKK2-containing lentiviral supernatant in 100mm dishes, in a culture medium containing IMDM, 10% heat-inactivated FBS, and 10µg/ml polybrene. Transient cells were lysed and FLAG-immunoprecipitated after 76 h. HAP1/- + WT and HAP1/- + T2A stable cells were incubated with 2µg/ml of puromycin. Following selection, polyclonal expansions were harvested at 80-90% confluency and subjected to Western Blot analysis. Proteins were immunoblotted with anti-FLAG and anti-P-T263. C) Transduction and polyclonal expansion as performed as in B, HAP1/- + WT and HAP1/- + T2A add-backs were harvested from ten 100mm dishes.

3.8 Stimulation of HAP1 Cell Lines

HAP1/- WT MEKK2 stable-expressing cells were subjected to growth factor and cytokine stimulation to explore the effect of MEKK2 stimulation on phosphorylation at T263 and T283, and subsequent activation of downstream effector proteins, ERK1/2. For this series of experiments, HAP1/- MEKK2 knockout native cells and HAP1/- + WT MEKK2 add-backs were stimulated with either Fetal Bovine Serum (FBS), Insulin-like Growth Factor 1 (IGF-1), or Tumour Necrosis Factor-α (TNF-α), as described in Chapter 2.6 Levels of T263 and T283 phosphorylation and ERK1/2 phosphorylation were measured by Western Blot analysis at different time points: 0 min, 5 min, 10 min, and 20 min.

First, TNF-α was used to stimulate HAP1/- native cells and HAP1/- + WT MEKK2 cells for increasing durations of time. HAP1/- cells were incubated with 10ng/ml of TNF-α for either 0 min, 5 min, 10 min, or 20 min, and were analyzed by Western Blot for changes in MEKK2 phosphorylation and downstream ERK1/2 phosphorylation. As illustrated in Figure 3.14, FLAG MEKK2 signal appeared just beneath non-specific bands. Therefore, to accurately isolate and quantify only FLAG-MEKK2 signal, the averaged value corresponding to background signal from the HAP1/- native lanes was subtracted from each total FLAG signal from each of the HAP1- + WT MEKK2 lanes. Following quantification of band density corresponding to T263 and T283 phosphorylation, no significant change in phosphorylation was observed at either site at any time point during TNF-α stimulation. After 5 minutes of TNF-α stimulation in HAP1/- + WT MEKK2 cells, ERK1/2 phosphorylation was observed to reach a peak, displaying a 50% increase relative to unstimulated HAP1/- native cells.

Next, 100ng/ml of IGF-1 was used to stimulate HAP1/- cells using methods described in the previous experiment. In Figure 3.15A, FLAG MEKK2 signal again appeared just beneath non-specific bands, as observed in Figure 3.14. This suggested that anti-FLAG immunoblotting was not efficient in detecting MEKK2. Nonetheless, FLAG MEKK2 signal was isolated and quantified as previously described and MEKK2 phosphorylation was analyzed. The observed changes in T263 and T283 phosphorylation were remarkably similar between both sites. There was an approximate 50% increase in phosphorylation observed after 5 minutes of IGF-1 stimulation, reaching a peak at 10 minutes where a 2.4-fold increase was observed, followed by a decline to approximately basal levels observed in unstimulated HAP1/- + WT MEKK2 cells at the 20-minute mark. Interestingly, ERK1/2 phosphorylation was observed to decrease following IGF-1 stimulation in both native and WT MEKK2 add-back cells. However, another common observation was noted between both cell types, where ERK1/2 phosphorylation reverted to baseline levels, as observed in unstimulated HAP1/- native cells, after 10 minutes of IGF-1 stimulation.

To further investigate the substantial increase in MEKK2 phosphorylation observed after 10 minutes of IGF-1 stimulation, the experiment was replicated using similar methods. To eliminate background interference during FLAG immunoblotting, an anti-MEKK2 antibody was used to probe for MEKK2 immunoprecipitation. As demonstrated in Figure 3.15B, T263 phosphorylation remained at approximately baseline levels between 0 to 20 minutes of IGF-1 stimulation in HAP1/- + WT MEKK2 cells. When observing ERK1/2 phosphorylation, HAP1/- native cells displayed an initial 30% reduction in phosphorylation after 5 minutes of IGF-1 stimulation, followed by a 40% increase in phosphorylation at 10 minutes of IGF-1 stimulation and a 70% increase following 20 minutes of stimulation, relative to baseline level. Interestingly,

ERK1/2 phosphorylation originated 50% lower in HAP1/- + WT MEKK2 add-back cells prior to stimulation compared to unstimulated than HAP1/- native cells and only increased by approximately 20% following 20 minutes of IGF-1 stimulation. The experiment was repeated once more and ERK1/2 phosphorylation was observed through Western Blot analysis, as demonstrated in Figure 3.15C. In HAP1/- native cells, ERK1/2 phosphorylation again initially decreased at 5 minutes post-stimulation. However, in contrast to the prior study, phosphorylation continued to decrease after 10 minutes of stimulation. Phosphorylation levels were then observed to return to baseline level following 20 minutes. In the MEKK2 add-back cells, ERK1/2 phosphorylation was also observed to initially decrease at 5 minutes post-stimulation, ultimately returning to unstimulated levels following 20 minutes of IGF-1 stimulation.

Levels of ERK1/2 phosphorylation following IGF-1 stimulation from the three replicate studies were analyzed for statistical significance by performing two-way ANOVA followed by Šídák's multiple comparisons test, using GraphPad Prism, and significance was set to $p \leq 0.05$. The analysis demonstrated a statistically significant difference in the mean values representing ERK1/2 phosphorylation levels between unstimulated HAP1/- native cells and unstimulated HAP1/- MEKK2 add-back cells. However, the analysis confirms that changes observed in ERK1/2 phosphorylation at any other time point between cell types are not statistically significant.

To understand the baseline effects of starvation and reintroduction of serum on the HAP1/- cells, HAP1/- native cells and HAP1/- + WT MEKK2 were each cultured in 100mm dishes and were starved for 20 hours prior to FBS stimulation. Cells were lysed and proteins were immunoprecipated with anti-FLAG and probed for MEKK2 phosphorylation and 14-3-3 interaction. In Figure 3.16A, both T263 and T283 phosphorylation signals are observed to

steadily increase over the 20 minutes of FBS stimulation. T263 phosphorylation was observed to increase by 2.3-fold, while T283 phosphorylation increased by 90%, following 20 minutes of FBS stimulation. Although 14-3-3 was not detected in the lysate (not shown), and thus co-IP signal quantification was not possible, stronger 14-3-3 co-IP signal was observed in HAP1/- + WT MEKK2 prior to FBS stimulation (0 minutes). These results could serve as additional support of the interaction between MEKK2 and 14-3-3, however these results were not reproduced and therefore any augmentation in 14-3-3 interaction upon reintroduction of MEKK2 is inconclusive. When observing the effects of FBS on ERK1/2 phosphorylation, HAP1/- native cells demonstrated a steady increase of phosphorylation over 20 minutes of FBS stimulation. However, HAP1/- MEKK2 add-back cells displayed an initial peak in ERK1/2 phosphorylation prior to stimulation, which continued to sharply decrease through out the duration of stimulation.

The experiment was repeated in Figure 3.16B, where T263 phosphorylation was observed to only increase by 30% after 20 minutes of FBS stimulation, with an observed 20% decrease observed at 10 minutes. However, T283 phosphorylation signal increased by 2.5-fold after 20 minutes of FBS stimulation, demonstrating a similar trend as observed in Figure 3.16A. These results generally suggest that T263 and T283 phosphorylation increase in HAP1/- + WT MEKK2 add-back stable cells following 20 minutes of FBS stimulation.

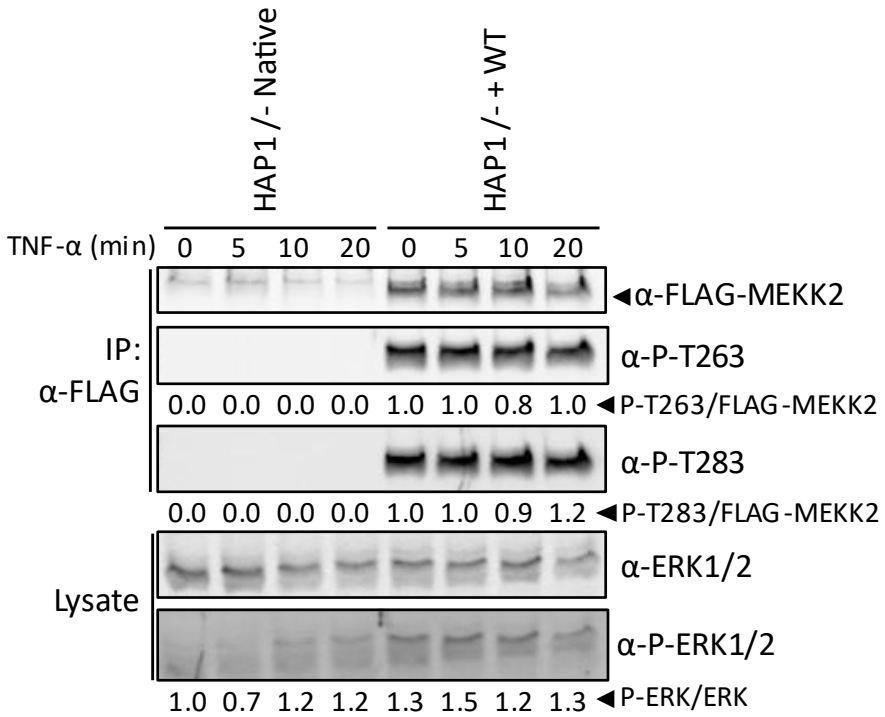

Figure 3.14. Cytokine stimulation of HAP1/- MEKK2 add-back cells. HAP1/- native and HAP1/- + WT MEKK2 cells were each cultured in five 100mm dishes and grown to 75% confluency. Cells were incubated with 10ng/ml of TNF-α for either 0, 5, 10, or 20 minutes. Cell lysis was performed immediately following the end of the desired stimulation duration. Whole-cell lysates were total-protein normalized using BCA Protein Assay Kit. FLAG-immunoprecipitated proteins were separated by SDS-PAGE and immunoblotted with anti-FLAG, anti-phospho-Thr-263, anti-phospho-Thr-283, anti-ERK1/2, and anti-phospho-ERK1/2. Fluorescent secondary antibodies were detected by Odyssey infrared imaging. Band quantification was performed using ImageJ. Total FLAG MEKK2 signal was isolated by subtracting the averaged value corresponding to background signal from the HAP1/- native lanes from each total FLAG signal from each of the HAP1- + WT MEKK2 lanes. MEKK2 phosphorylation to total MEKK2 ratios were normalized to the unstimulated HAP1/- + WT MEKK2 condition. ERK1/2 phosphorylation to total ERK1/2 ratios were normalized to the unstimulated HAP1/- native condition.

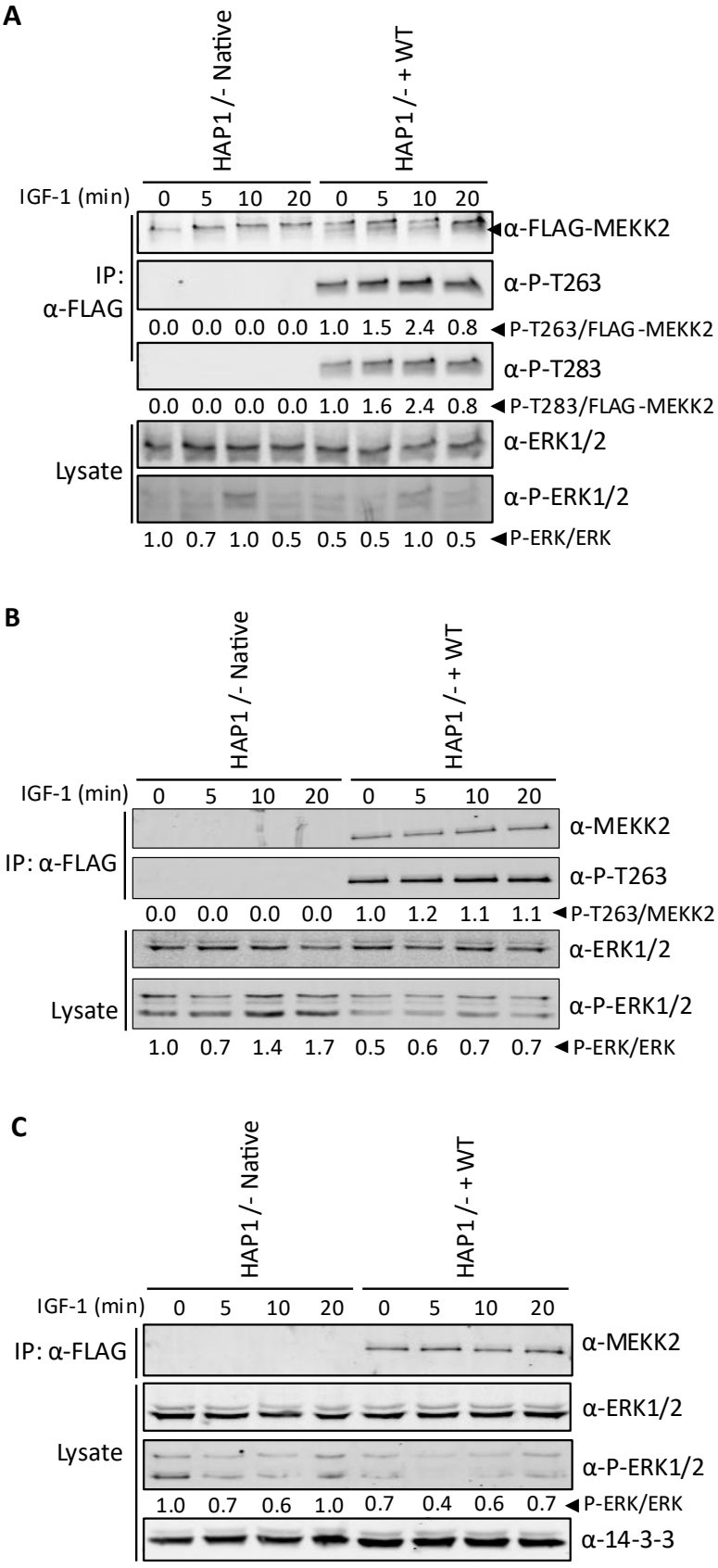
A
HAP1 /- Native
HAP1 /- + WT
IGF-1 (min)
0 5 10 20 0 5 10 20
IP: α-FLAG
α-FLAG-MEKK2
α-P-T263
0.0 0.0 0.0 0.0 1.0 1.5 2.4 0.8
P-T263/FLAG-MEKK2
α-P-T283
0.0 0.0 0.0 0.0 1.0 1.6 2.4 0.8
P-T283/FLAG-MEKK2
Lysate
α-ERK1/2
α-P-ERK1/2
1.0 0.7 1.0 0.5 0.5 0.5 1.0 0.5
P-ERK/ERK
B
HAP1 /- Native
HAP1 /- + WT
IGF-1 (min)
0 5 10 20 0 5 10 20
IP: α-FLAG
α-MEKK2
α-P-T263
0.0 0.0 0.0 0.0 1.0 1.2 1.1 1.1
P-T263/MEKK2
Lysate
α-ERK1/2
α-P-ERK1/2
1.0 0.7 1.4 1.7 0.5 0.6 0.7 0.7
P-ERK/ERK
C
HAP1 /- Native
HAP1 /- + WT
IGF-1 (min)
0 5 10 20 0 5 10 20
IP: α-FLAG
α-MEKK2
Lysate
α-ERK1/2
α-P-ERK1/2
1.0 0.7 0.6 1.0 0.7 0.4 0.6 0.7
P-ERK/ERK
α-14-3-3

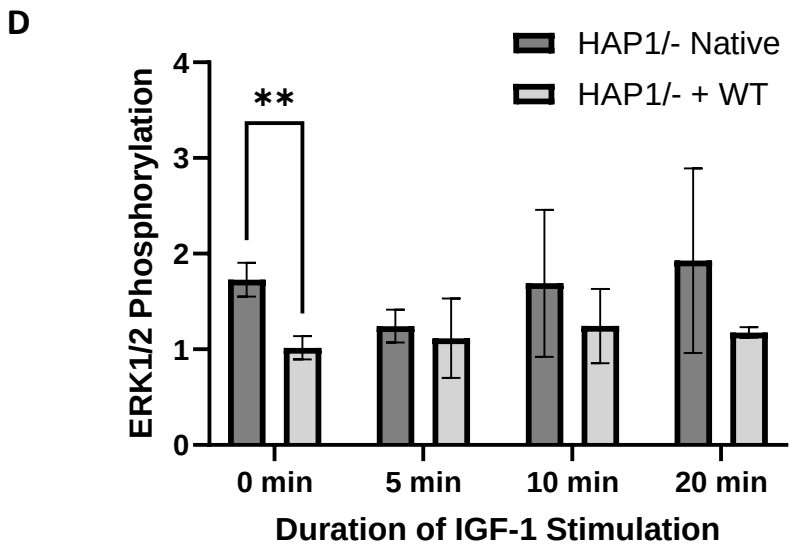

Figure 3.15. Growth factor stimulation of HAP1/- MEKK2 add-back cells. A) HAP1/- native and HAP1/- + WT MEKK2 cells were each cultured in five 100mm dishes and grown to 75% confluency. Cells were incubated with 100ng/ml IGF-1 for either 0, 5, 10, or 20 minutes. Cell lysis was performed immediately following the end of the desired stimulation duration. Whole-cell lysates were total-protein normalized using BCA Protein Assay Kit. FLAG-immunoprecipitated proteins were separated by SDS-PAGE and immunoblotted with anti-FLAG, anti-phospho-Thr-263, anti-phospho-Thr-283, anti-ERK1/2, and anti-phospho-ERK1/2. Fluorescent secondary antibodies were detected by Odyssey infrared imaging. Band quantification was performed using ImageJ. Total FLAG MEKK2 signal was isolated by subtracting the averaged value corresponding to background signal from the HAP1/- native lanes from each total FLAG signal from each of the HAP1- + WT MEKK2 lanes. MEKK2 phosphorylation to total MEKK2 ratios were normalized to the unstimulated HAP1/- + WT MEKK2 condition. ERK1/2 phosphorylation to total ERK1/2 ratios were normalized to the unstimulated HAP1/- native condition. B) HAP1/- native and HAP1/- + WT MEKK2 cells were each cultured in two 100mm dishes and grown to 75% confluency. Stimulation and IP was performed as described in A. Proteins were immunoblotted with anti-MEKK2, anti-phospho-Thr-263, anti-ERK1/2, and anti-phospho-ERK1/2. Signal quantification and analysis was performed as described in A. C) Western Blot analysis performed as described in B. Proteins were immunoblotted with anti-MEKK2, anti-ERK1/2, and anti-phospho-ERK1/2. D) Two-way ANOVA followed by Šídák's multiple comparisons test was performed using GraphPad Prism. Data reported as Mean±SD, n=3; (**) $p \leq 0.01$. Significance was set to $p \leq 0.05$.

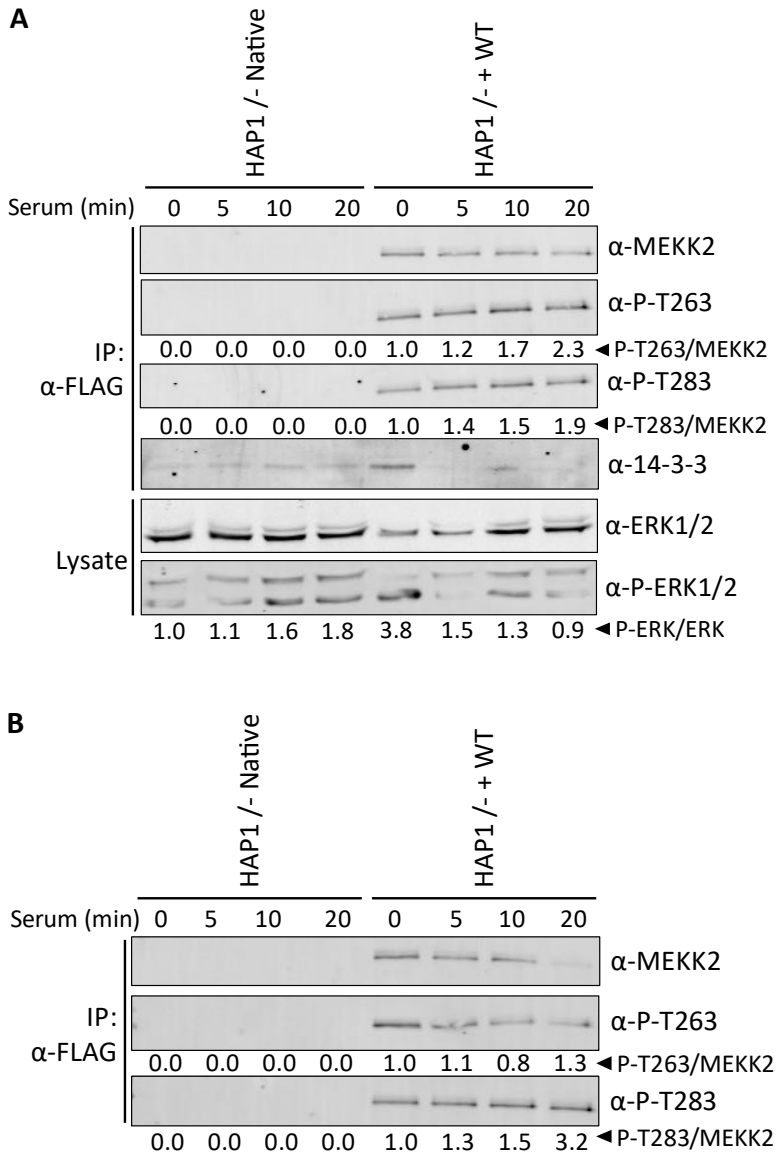

Figure 3.16. Serum stimulation of HAP1/- MEKK2 add-back cells. A) HAP1/- native and HAP1/- + WT MEKK2 cells were each cultured in two 100mm dishes and grown to 75% confluency. Cells were incubated with 550ul FBS for either 0, 5, 10, or 20 minutes. Cell lysis was performed immediately following the end of the desired stimulation duration. Whole-cell lysates were total-protein normalized using BCA Protein Assay Kit. FLAG-immunoprecipitated proteins were separated by SDS-PAGE and immunoblotted with anti-MEKK2, anti-phospho-Thr-263, anti-phospho-Thr-283, anti-ERK1/2, and anti-phospho-ERK1/2. Fluorescent secondary antibodies were detected by Odyssey infrared imaging. Band quantification was performed using ImageJ. MEKK2 phosphorylation to total MEKK2 ratios were normalized to the unstimulated HAP1/- + WT MEKK2 condition. ERK1/2 phosphorylation to total ERK1/2 ratios were normalized to the unstimulated HAP1/- native condition. B) Western Blot analysis was performed as in A. Proteins were immunoblotted with anti-MEKK2, anti-phospho-Thr-263, and anti-phospho-Thr-283.

Chapter 4: Discussion, Future Directions, and Conclusion

4.1 T263 and T283 Constitute the 14-3-3 Bipartite Binding Site

MEKK2 (MAP3K2) is a mitogen-activated protein kinase belonging to the MAP3K family of S/T-kinases and is a crucial contributor to the regulation of MAPK signalling pathways that are responsible for normal cell proliferation and function.[38] MEKK2 activates downstream MAPK proteins in response to various stress and mitogenic stimuli.[63] Aberrant regulation of these intricate cellular pathways have profound implications for cellular function and overall human health.[138]

Matitau et al. have demonstrated that MEKK2 interacts with 14-3-3 through a phosphorylation-dependent association at T283.[63] 14-3-3 proteins are phosphoserine and phosphothreonine binding modules involved in all major cellular signalling pathways.[109] This interaction has been shown through Western Blotting methods to prevent trans-autophosphorylation of S519 with in the activation loop, resulting in inactivation of MEKK2 and reduced ERK5 activation. 14-3-3 is characterized as a regulator of MEKK2 as it controls MEKK2 input to several MAPK pathways.[63]

Following the identification of a threonine residue 20 amino acids upstream from T283, a known MEKK2 phosphosite, T263 was assessed for phosphorylation through Western Blot analysis. The complete abolishment of T263 phosphorylation signal following T263A mutagenesis of MEKK2, phosphorylation-resistant, together with the loss of phosphorylation-dependent 14-3-3 association upon T263A mutation and competition with T263-phosphorylated peptides, depicts T263 as a novel MEKK2 phosphorylation site and site of 14-3-3 interaction. Furthermore, phosphorylation-resistant mutations at either T263 or T283 resulted in significantly reduced

phosphorylation signal at both sites, demonstrating a co-dependence between T263 and T283 phosphorylation. 14-3-3 phosphoadapter proteins have been documented to protect their targets from dephosphorylation.[114,115] Furthermore, the loss of 14-3-3 binding following T to A phosphorylation-resistant mutations at either site may potentially increase susceptibility of the remaining phosphosite to dephosphorylation by protein phosphatases, resulting in reduced phosphorylation as demonstrated.

Our data suggests that T263 and T283 of MEKK2 serve as the bipartite binding group for phosphoadapter protein 14-3-3. Each monomeric unit within a 14-3-3 complex can bind to one phosphosite, enabling a 14-3-3 dimer to bind two phosphosites simultaneously.[114] 14-3-3 was confirmed through Western Blot analysis to not interact with either T263A or T283A MEKK2, suggesting that MEKK2 must be phosphorylated at T263 and T283 simultaneously to promote 14-3-3 association. Further, this data suggests that 14-3-3 monomers do not independently interact with either phosphosite individually. Therefore, since 14-3-3 only binds MEKK2 when phosphorylated at both T263 and T283, and each 14-3-3 monomer binds one phosphosite, 14-3-3 must dimerize to simultaneously interact with both phosphosites within the bipartite binding group. Further, since 14-3-3 proteins predominately exist as dimers, a dimeric 14-3-3 protein complex likely cooperatively binds MEKK2 in a phosphorylation-dependent manner.[110,114] In this context, phosphorylation at both binding sites is necessary to increase the binding affinity for each monomeric unit of the 14-3-3 dimeric complex to interact with each site. Lastly, we can infer from our data that kinase activity does not influence the association of 14-3-3 with the MEKK2 bipartite binding site, as 14-3-3 co-immunoprecipitation levels in the kinase dead K385M MEKK2 mutant remained consistent with WT MEKK2 levels.

4.2 MEKK2 is the Sole Target of SMYD3 within the MAPK Family

Using protein array technology, MEKK2 was identified as the only target of SMYD3 methylation among thousands of potential substrates, including various members of the MAPK pathway.[95,139] The presence of a phenylalanine residue at the -2 position relative to K260 confers selective substrate preference for MEKK2.[132] Despite high sequence homology between MEKK3 (MAP3K3) and MEKK2, MEKK3 showed no methylation signal at the homologous K271 residue when screened for di- and tri-methylation using Western Blot procedures. Furthermore, we have demonstrated K260 as the sole locus of SMYD3-mediated methylation of MEKK2, shown by the complete abolishment of di- and tri-methylation signal following K260R and F258R mutagenesis. Taken together, these findings further support the existing data that K260 of MEKK2 is the sole target of SMYD3 within the MAPK family and the upstream phenylalanine residue, F258, is required for SMYD3-mediated methylation at K260 of MEKK2. Therefore, SMYD3 selectively upregulates MEKK2 signalling and directs signal specificity downstream of oncogenic Ras signalling, making MEKK2 the sole therapeutic target of the MAP3K family for PDAC and LAC treatment.

4.3 T263 Phosphorylation is Required for K260 Methylation

Considering the role of K260 methylation in promoting progression of K-Ras driven tumorigenesis, several experiments were conducted to investigate the potential influence on neighbouring phosphorylation at T263. Recent studies have recognized the significance of "methyl switches" in regulating post-translational modifications (PTMs) of neighbouring residues, characterized by stimulation or inhibition of neighbouring modifications as a result of methylation at one lysine residue.[129] Furthermore, lysine methylation has been recognized as a method of regulating kinase and phosphatase activity, as methylation has been shown to alter the

conformation of kinase proteins.[140] As this recent data suggests, we hypothesized that K260 methylation would alter phosphorylation status of the neighbouring T263 phosphosite. Therefore, K260 methylation was hypothesized to also regulate the phosphorylation-dependant bipartite association of 14-3-3 with MEKK2.

Interestingly, our data suggests the opposite mechanism of regulation between the neighbouring PTMs, whereby T263 phosphorylation regulates methylation status at K260. Our phosphorylation analyses of K260R and F258R MEKK2 mutants, methylation-resistant, demonstrate no significant alterations in T263 phosphorylation status following loss of K260 methylation. Additionally, BAY-6035-mediated endogenous SMYD3-inhibition also demonstrated no significant effect on T263 or T283 phosphorylation. Multiple replicates of this data suggest with high confidence that K260 methylation does not exert regulatory control over T263 and T283 phosphorylation.

Conversely, it was concluded through Western Blot analysis that K260 methylation is significantly reduced following T263A, T283A, and T2A mutagenesis of MEKK2. These findings suggest that phosphorylation at both phosphosites is required to promote efficient SMYD3-mediated methylation at K260, thereby serving as a regulatory mechanism to control K260 methylation. This data suggests T263 and T283 as therapeutic targets in the treatment of PDAC and LAC, where the development and progression of these cancers have been correlated with aberrant K260-methylation resulting in upregulated MEKK2 activity and input downstream of oncogenic Ras signalling.[95]

Given the distal proximity of T283 relative to K260 and T263, it was interesting to also observe a loss of K260 methylation upon abolishment of T283 phosphorylation. Whether T283 can be considered a neighbouring amino acid to K260 is dependent on its spatial proximity in the three-

dimensional structure of MEKK2.[141] Hence, assuming that T283 may not be within range to exert crosstalk control via PTMs, alternative explanations may exist for the observed reduction in K260 methylation upon loss of T263 and T283 phosphorylation. Phosphorylation can create a docking site for a methyltransferase enzyme or protein complex that promotes methylation at a nearby methylation site.[142] Additionally, phosphorylation could induce a conformational change in the protein structure that exposes or enhances the accessibility of adjacent methylation sites to methyltransferases.[143] Furthermore, loss of T263 and T283 phosphorylation results in complete loss of the 14-3-3 binding dimer, and thus SMYD3 could require 14-3-3 to efficiently methylate K260, either directly, or by maintaining T263 phosphorylation.

4.4 14-3-3 Interaction Potentially Facilitates K260 Methylation

When exploring the mechanism of interaction between MEKK2 and SMYD3, Van Aller et al. resolved a co-crystal structure of SMYD3 bound to a substrate MEKK2 peptide, which revealed that the backbone amide of T263 is required to hydrogen-bond with SMYD3.[94] These finding indicate that a direct interaction at T263 must be established to facilitate SMYD3-mediated methylation of K260. Additionally, our data provides some evidence of a direct interaction between MEKK2 and SMYD3, as suggested by an enrichment in MEKK2 co-IP signal upon SMYD3 expression. However, this signal enrichment was observed in both phosphorylation and methylation resistant MEKK2 mutants, inferring that phosphorylation status nor methylation capability influences the interaction between the two proteins. Therefore, we explored other potential mechanisms by which T263 and T283 phosphorylation promotes K260 methylation.

Catalytic efficiency of SMYD3-mediated K260 methylation is dependent on phosphorylation at both T263 and T283, suggesting phosphorylation at the MEKK2 bipartite binding sites as a regulatory mechanism to control methylation at K260. Furthermore, together with our findings

that 14-3-3 regulates T263 and T283 dephosphorylation, 14-3-3 may indirectly facilitate K260 methylation by maintaining the necessary phosphorylation at neighbouring phosphosites.

As mentioned, 14-3-3 phosphoadapter proteins have been documented to protect their targets from dephosphorylation, thereby influencing the activity and interactions of their target proteins.[114,115] T263-phosphorylated peptides were repeatedly observed to out-compete MEKK2 to bind 14-3-3, following multiple peptide competition assays. This resulted in a significant reduction in T263 phosphorylation, corresponding to abolishment of 14-3-3 co-IP. Our data demonstrated that loss of 14-3-3 association resulted in T263 dephosphorylation, suggesting that 14-3-3 regulates MEKK2 phosphorylation status and activity by binding the T263 and T283 bipartite binding group on MEKK2 and shielding these sites from exposure to phosphatases. Further, our data shows that 14-3-3 only binds MEKK2 when phosphorylated at T263 and T283 and that dual phosphorylation at these sites is required for SMYD3-mediated K260 methylation. Since SMYD3-mediated K260 methylation is dependent on T263 and T283 phosphorylation and 14-3-3 has been implicated in preserving phosphorylation at these sites, 14-3-3 may contribute to the progression of K-Ras-driven tumorigenesis and should be implicated as an additional therapeutic target in the treatment of PDAC and LAC.

4.5 Agonist Stimulation of HAP1/- + WT MEKK2 Cells was Inconclusive

Stable-expressing HAP1/- + WT MEKK2 cells were generated to explore the impact of endogenous MEKK2 activation on T263 phosphorylation and subsequent downstream signalling. Through our preliminary experiments, we were able to demonstrate that TNF-α stimulation may induce a short-term increase in ERK1/2 activation in HAP1/- + WT MEKK2 cells, with no observed significant change in T263 and T283 phosphorylation. However, due to the lack of replicate data, significance was not determined. When analyzing the apparent increase in T263

and T283 phosphorylation following IGF-1 stimulation in HAP1/- + WT MEKK2 cells, the use of anti-MEKK2 direct antibody, opposed to anti-FLAG, greatly increased MEKK2 detection and therefore allowed for more accurate signal quantification. Thus, our secondary observation that T263 and T283 phosphorylation is not significantly altered following IGF-1 stimulation is more likely to be accurate than the prior preliminary experiment. IGF-1 stimulation data was produced in triplicates, where no significant change in ERK1/2 activation was observed following stimulation. There was a significant reduction in ERK1/2 activity observed in HAP1/- + WT MEKK2 cells, relative to HAP1/- native cells, prior to IGF-1 stimulation. However, this observation was not evident prior to stimulation with TNF-α or FBS (serum), raising concerns regarding the reliability of these findings. The FBS stimulation experiments generally indicate a positive correlation between T263 and T283 phosphorylation and duration of stimulation in HAP1/- + WT MEKK2 cells, however significance was not determined. Overall, TNF-α and IGF-1 stimulation of endogenous MEKK2, as described in Section 3.8 generally appeared to have no significant influence on T263 and T283 phosphorylation and subsequent ERK1/2 activation, however further investigations are required.

4.6 Limitations & Future Directions

4.6.1 Exploring a Regulatory Role of PP2A in Oncogenic MEKK2 Activity

Western Blots were conducted to explore T263 as a target of dephosphorylation by PP2A. The experimental design included duplicate transient transfections of WT MEKK2, T263A MEKK2, and K260R MEKK2 in the presence and absence of SMYD3 co-expression. As a result of repeated unsuccessful attempts to immunoblot PP2A subunits A, B, and C for co-IP detection using a PP2A antibody kit (Cell Signalling 9780), the experiment was abandoned. The heterotrimeric PP2A complex is composed of the structural PPP2R1A subunit (A), the regulatory

PPP2R2A subunit (B), and the catalytic PPP2CA subunit (C). Mazur et al. established that amino acids 249-273 of MEKK2 constitutes the binding region for the PP2A complex and methylation at K260 inhibits this interaction, therefore inferring that aberrant MEKK2 activation is due to the inability of PP2A to negatively regulate activating phosphorylation events on MEKK2 and MEKK2 downstream targets.[95] They have also established that the regulatory PPP2R2A subunit directly interacts with MEKK2 when unmethylated at K260. Given that T263 is within this binding range, it was hypothesized that PP2A negatively regulates oncogenic MEKK2 activity by dephosphorylating T263, thereby reducing SMYD3-mediated K260 methylation. Since PP2A binds to MEKK2, dephosphorylation could additionally occur at S519, within the activation loop, thereby providing an additional potential mechanism whereby PP2A inactivates MEKK2.[63,95] Overall, due to the lack of Western Blot data we are unable to draw any conclusions regarding the regulatory role of PP2A, however we postulate a mechanism by which SMYD3 overexpression leads to large quantities of methylated MEKK2, preventing the PP2A complex from dephosphorylating T263 and S519, thereby resulting in oncogenic MEKK2 input to the Ras pathway in PDAC and LAC.

4.6.2 Improving Stable-Expressing MEKK2 Cell Lines and Stimulation

The generation of stable-expressing MEKK2 add-back cell lines played a crucial role in our strategy to investigate the impact of T263 phosphorylation on endogenous MEKK2 activation and downstream signalling. Given the limited reliability and ambiguous understanding of its relevance, the stimulation data is inconclusive and requires additional reproduction to verify the validity of these findings. Vital to this strategy was the generation of mutant MEKK2 stable-expressing add-back cell lines, including T263A, T283A, T2A, F258R, K260R, and K385M MEKK2. The lack of data from the failed generation of these cell lines contributes to the

ambiguous interpretation of the data produced by the stimulation experiments, since the only point of reference is HAP1/- MEKK2-null cells. MEKK2-MEK5-ERK5 and MEKK2-MEK1/2-ERK1/2 pathway activation were the intended pathways of observation in this study, as we aimed to determine whether phosphorylation at T263 and T283 exerts regulatory control over K260 methylation and subsequent ERK1/2 activation, as observed in our transient experiments in HEK 293T cells.

Another factor that could have contributed to the lack of substantial data following stimulation of HAP1 add-back cells could have been the use of the use of improper concentrations of stimuli or the use of stimuli that do not consistently and reliably activate MEKK2 across all conditions. For instance, the use of Epidermal Growth Factor-1 (EGF-1), which has been demonstrated to strongly correlate with the activation of MEKK2 and MAPK pathways in various cellular contexts.[144] Future investigations involving the generation of mutant MEKK2 add-back stable cell lines would require substantial time and resources. The production of significant protein quantities from stable cell lines is imperative to yield discernible and relevant observations. The use of a different host cell line could be considered to support MEKK2 expression, as well as the use of lentiviral plasmid possessing more than one FLAG epitope, to improve FLAG-MEKK2 detection.

The use of HAP1 cells as our host cell could be another limitation contributing to the lack of significant ERK1/2 activation and the accuracy of these findings in the context of PDAC and LAC. While isolating PDAC and LAC cells directly from patient tissue samples might have yielded more reliable and clinically relevant data, the limited accessibility to these cells posed a significant challenge. Additionally, isolating sufficient quantities of cells for multiple series of

experiments, particularly when observing endogenous changes in post-translational modifications, would be substantial access to resources.

4.6.3 Future studies

For future investigations, genetic manipulation techniques such as CRISPR/Cas9 gene editing could potentially be used to induce relevant activating mutations in *KRAS* and overexpression of *smyd3* in HEK 293T cells. Alternatively, the use of human PDAC cell lines such as Capan-1, MIA PaCa-2, and Panc-1, which harbour K-Ras driver mutations, could also provide valuable models for studying pancreatic cancer and generating data with clinical relevance.[145] These cell lines closely mimic the genetic alterations observed in human pancreatic cancers, and therefore could enhance the translational relevance of research findings, making them useful tools for drug development and preclinical studies. Additionally, investigations could be conducted to identify the target loci of PP2A-mediated dephosphorylation on MEKK2. These experiments would determine whether P-T263 and P-S519 are targets of PP2A-mediated negative regulation of MEKK2, further characterizing these residues as regulatory phosphorylation sites and potentially identifying a mechanism by which SMYD3-mediated K260 methylation promotes oncogenic MEKK2 activity.

4.7 Conclusion

In summary, we have demonstrated that T263 and T283 of MEKK2 form the bipartite binding group for 14-3-3 phosphoadapter proteins and that this interaction occurs in a phosphorylation-dependent manner. Mazur et al. have demonstrated that SMYD3-mediated methylation of MEKK2 at K260 results in MEKK2 input downstream of oncogenic K-Ras signalling, leading to worsened prognosis of PDAC and LAC in mouse models.[95] Recent studies have shown that expression of SMYD3 is robustly elevated in diverse human cancers, suggesting its role as a putative oncogene.[127] Therefore, investigating the role of SMYD3 in cancer progression provides opportunities for developing targeted chemotherapeutics. Furthermore, inhibition of SMYD3 activity could be explored as a treatment for cancers marked by SMYD3 overexpression, making research on the oncogenic function of SMYD3 critical for therapeutic development.

In this study we've characterized T263 and T283 as the bipartite phospho-binding sites for dimeric 14-3-3 and discovered a regulatory role of T263 and T283 phosphorylation in controlling SMYD3-mediated methylation at K260 methylation, depicting T263 and T283 as potential therapeutic targets in mediating oncogenic activation of MEKK2. Additionally, we've implicated 14-3-3 as another potential therapeutic target as its interaction with the phosphosites may contribute to sustained phosphorylation, therefore facilitating K260 methylation and MEKK2 oncogenic function. Figure 4.1 provides an overview of our findings and implications. Our findings have discovered novel regulatory targets in the oncogenic function of SMYD3, paving the way for further exploration in the treatment of the treatment of PDAC and LAC.

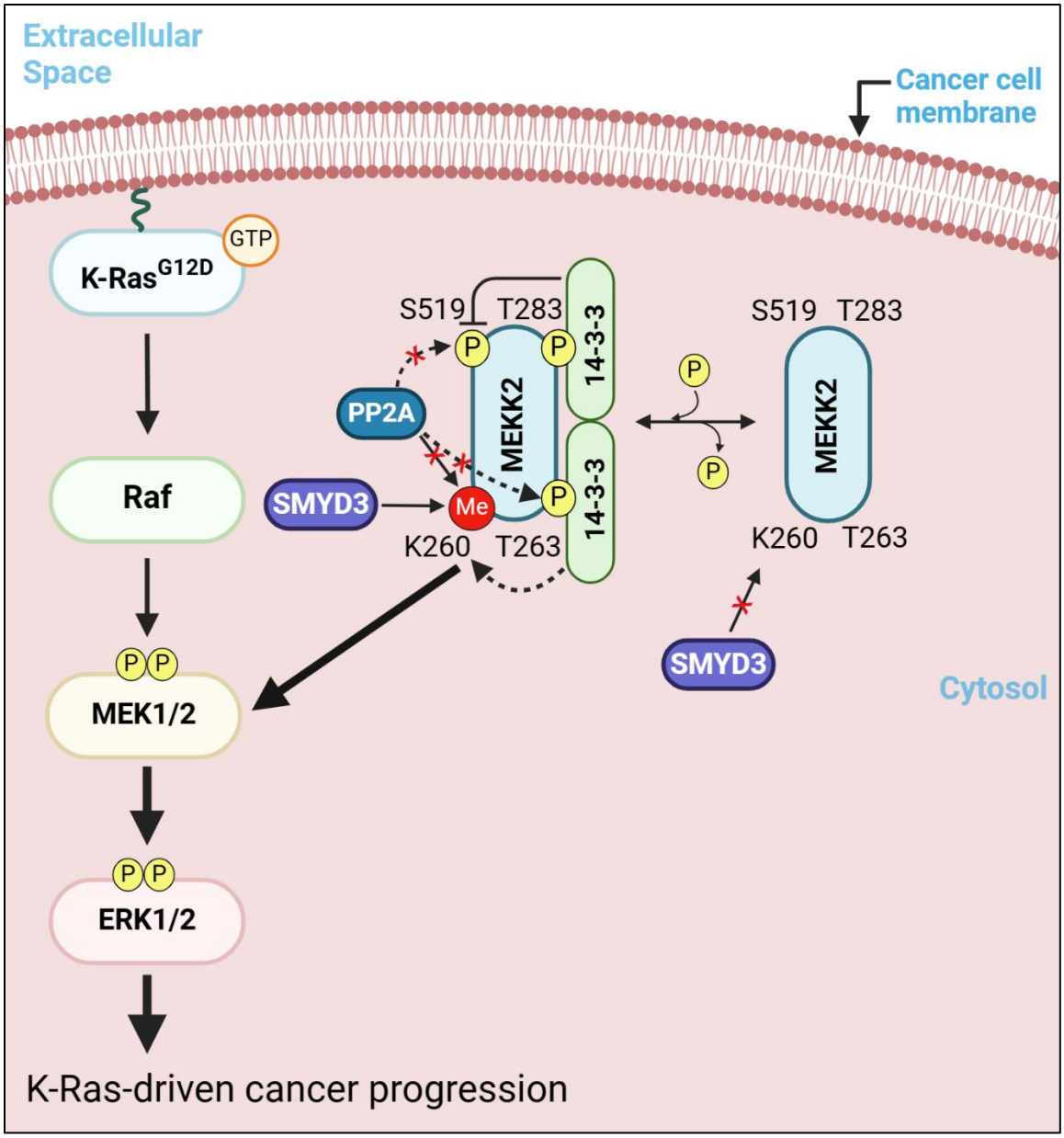

Figure 4.1. MEKK2, 14-3-3, and SMYD3 model depicting MEKK2 oncogenic function. Within the cancer cell, mutated K-Ras initiates oncogenic activation of ERK1/2. Upon phosphorylation of MEKK2 at T263 and T283, a 14-3-3 dimer binds and presumably sustains phosphorylation, promoting SMYD3-mediated K260 methylation. 14-3-3 binding has also been demonstrated to negatively regulate S519 phosphorylation and MEKK2 activity (Matitau et al. 2013). Methylation prevents PP2A association and negative regulation of MEKK2, potentially by preventing dephosphorylation at T263 and S519, overall resulting in increased input to MEK1/2 downstream of oncogenic K-Ras signalling and progression of tumorigenesis (Mazur et. al 2014). Unphosphorylated MEKK2 does not associate with 14-3-3 and prevents SMYD3-mediated K260 methylation. Thickness of arrow indicates strength of signal. Created with BioRender.com.

References

1. Ramazi, S. & Zahiri, J. Post-translational modifications in proteins: resources, tools and prediction methods. *Database* **2021**, (2021).
2. Pan, S. & Chen, R. Pathological implication of protein post-translational modifications in cancer. *Mol. Aspects Med.* **86**, (2022).
3. Bogoyevitch, M. A. & Kobe, B. Uses for JNK: the Many and Varied Substrates of the c-Jun N-Terminal Kinases. *Microbiol. Mol. Biol. Rev.* **70**, 1061 (2006).
4. Deribe, Y. L., Pawson, T. & Dikic, I. Post-translational modifications in signal integration. *Nat. Struct. Mol. Biol. 2010 176* **17**, 666–672 (2010).
5. Biggar, K. K. & Li, S. S. C. Non-histone protein methylation as a regulator of cellular signalling and function. *Nat. Rev. Mol. Cell Biol.* **16**, 5–17 (2015).
6. Kupai, A., Vaughan, R. M., Dickson, B. M. & Rothbart, S. B. A Degenerate Peptide Library Approach to Reveal Sequence Determinants of Methyllysine-Driven Protein Interactions. *Front. Cell Dev. Biol.* **8**, 241 (2020).
7. Guo, H. J. & Tadi, P. Biochemistry, Ubiquitination. *StatPearls* (2022).
8. Callis, J. The Ubiquitination Machinery of the Ubiquitin System. *Arabidopsis Book* **12**, e0174 (2014).
9. Soares-Silva, M., Diniz, F. F., Gomes, G. N. & Bahia, D. The mitogen-activated protein kinase (MAPK) pathway: Role in immune evasion by trypanosomatids. *Front. Microbiol.* **7**, 183 (2016).
10. Wei, Z. & Liu, H. T. MAPK signal pathways in the regulation of cell proliferation in mammalian cells. *Cell Res. 2002 121* **12**, 9–18 (2002).
11. Morrison, D. K. MAP Kinase Pathways. *Cold Spring Harb. Perspect. Biol.* **4**, (2012).
12. Cargnello, M. & Roux, P. P. Activation and Function of the MAPKs and Their Substrates, the MAPK-Activated Protein Kinases. *Microbiol. Mol. Biol. Rev.* **75**, 50 (2011).
13. Cuevas, B. D., Abell, A. N. & Johnson, G. L. Role of mitogen-activated protein kinase kinase kinases in signal integration. *Oncogene 2007 2622* **26**, 3159–3171 (2007).
14. Chang, F. *et al.* Signal transduction mediated by the Ras/Raf/MEK/ERK pathway from cytokine receptors to transcription factors: Potential targeting for therapeutic intervention. *Leukemia* **17**, 1263–1293 (2003).
15. Chen, Z. *et al.* MAP kinases. *Chem. Rev.* **101**, 2449–2476 (2001).
16. Robbinssq, D. J. *et al.* THE JOURNAL OF BIOLOGICAL CHEMISTRY Regulation and Properties of Extracellular Signal-regulated Protein Kinases 1 and 2 in Vitro*. **268**, 5097–5106 (1993).
17. Hagemann, C. & Blank, J. L. The ups and downs of MEK kinase interactions. *Cell.*

Signal. **13**, 863–875 (2001).

18. Tanoue, T. & Nishida, E. Molecular recognitions in the MAP kinase cascades. *Cell. Signal.* **15**, 455–462 (2003).

19. BARDWELL, L. & THORNER, J. A conserved motif at the amino termini of MEKs might mediate high-affinity interaction with the cognate MAPKs. *Trends Biochem. Sci.* **21**, 373–374 (1996).

20. Barr, R. K. & Bogoyevitch, M. A. The c-Jun N-terminal protein kinase family of mitogen-activated protein kinases (JNK MAPKs). *Int. J. Biochem. Cell Biol.* **33**, 1047–1063 (2001).

21. Degirmenci, U., Wang, M. & Hu, J. Targeting Aberrant RAS/RAF/MEK/ERK Signaling for Cancer Therapy. *Cells* **9**, (2020).

22. Guo, Y.-J. *et al.* ERK/MAPK signalling pathway and tumorigenesis. *Exp. Ther. Med.* **19**, 1997 (2020).

23. Waters, A. M. & Der, C. J. KRAS: The Critical Driver and Therapeutic Target for Pancreatic Cancer. *Cold Spring Harb. Perspect. Med.* **8**, (2018).

24. Prior, I. A., Hood, F. E. & Hartley, J. L. The frequency of ras mutations in cancer. *Cancer Res.* **80**, 2669–2974 (2020).

25. Takács, T. *et al.* The effects of mutant Ras proteins on the cell signalome. *Cancer Metastasis Rev.* **39**, 1051 (2020).

26. Huang, L., Guo, Z., Wang, F. & Fu, L. KRAS mutation: from undruggable to druggable in cancer. *Signal Transduct. Target. Ther. 2021 61* **6**, 1–20 (2021).

27. Margolis, B. & Skolnik, E. Y. Activation of ras by receptor tyrosine kinases. *J. Am. Soc. Nephrol.* **5**, 1288–1299 (1994).

28. Hubbard, S. R. & Miller, W. T. Receptor tyrosine kinases: mechanisms of activation and signaling. *Curr. Opin. Cell Biol.* **19**, 117 (2007).

29. Du, Z. & Lovly, C. M. Mechanisms of receptor tyrosine kinase activation in cancer. *Mol. Cancer 2018 171* **17**, 1–13 (2018).

30. Chen, D., Waters, S. B., Holt, K. H. & Pessin, J. E. SOS phosphorylation and disassociation of the Grb2-SOS complex by the ERK and JNK signaling pathways. *J. Biol. Chem.* **271**, 6328–6332 (1996).

31. Terrell, E. M. & Morrison, D. K. Ras-Mediated Activation of the Raf Family Kinases. *Cold Spring Harb. Perspect. Med.* **9**, (2019).

32. Martinez Fiesco, J. A., Durrant, D. E., Morrison, D. K. & Zhang, P. Structural insights into the BRAF monomer-to-dimer transition mediated by RAS binding. *Nat. Commun. 2022 131* **13**, 1–14 (2022).

33. Tran, T. H. *et al.* KRAS interaction with RAF1 RAS-binding domain and cysteine-rich domain provides insights into RAS-mediated RAF activation. *Nat. Commun. 2021 121* **12**,

1–16 (2021).

34. Li, L. *et al.* The Ras/Raf/MEK/ERK signaling pathway and its role in the occurrence and development of HCC. *Oncol. Lett.* **12**, 3045 (2016).

35. Barbosa, R., Acevedo, L. A. & Marmorstein, R. The MEK/ERK Network as a Therapeutic Target in Human Cancer. doi:10.1158/1541-7786.MCR-20-0687.

36. Roskoski, R. ERK1/2 MAP kinases: structure, function, and regulation. *Pharmacol. Res.* **66**, 105–143 (2012).

37. Burack, W. R. & Sturgill, T. W. The activating dual phosphorylation of MAPK by MEK is nonprocessive. *Biochemistry* **36**, 5929–5933 (1997).

38. Roberts, P. J. & Der, C. J. Targeting the Raf-MEK-ERK mitogen-activated protein kinase cascade for the treatment of cancer. *Oncogene 2007 2622* **26**, 3291–3310 (2007).

39. Neuzillet, C. *et al.* MEK in cancer and cancer therapy. *Pharmacol. Ther.* **141**, 160–171 (2014).

40. Menu, E. *et al.* Specific roles for the PI3K and the MEK–ERK pathway in IGF-1-stimulated chemotaxis, VEGF secretion and proliferation of multiple myeloma cells: study in the 5T33MM model. *Br. J. Cancer 2004 905* **90**, 1076–1083 (2004).

41. Wortzel, I. & Seger, R. The ERK Cascade: Distinct Functions within Various Subcellular Organelles. *Genes Cancer* **2**, 195 (2011).

42. Ducker, C. *et al.* De-ubiquitination of ELK-1 by USP17 potentiates mitogenic gene expression and cell proliferation. *Nucleic Acids Res.* **47**, 4495–4508 (2019).

43. Murphy, L. O., Smith, S., Chen, R. H., Fingar, D. C. & Blenis, J. Molecular interpretation of ERK signal duration by immediate early gene products. *Nat. Cell Biol.* **4**, 556–564 (2002).

44. Whitmarsh, A. J. & Davis, R. J. Transcription factor AP-1 regulation by mitogen-activated protein kinase signal transduction pathways. *J. Mol. Med. (Berl).* **74**, 589–607 (1996).

45. Shaulian, E. & Karin, M. AP-1 in cell proliferation and survival. *Oncogene* **20**, 2390–2400 (2001).

46. Tchakarska, G. & Sola, B. The double dealing of cyclin D1. *Cell Cycle* **19**, 163 (2020).

47. Mebratu, Y. & Tesfaigzi, Y. How ERK1/2 Activation Controls Cell Proliferation and Cell Death Is Subcellular Localization the Answer? *Cell Cycle* **8**, 1168 (2009).

48. Sugiura, R., Satoh, R. & Takasaki, T. ERK: A Double-Edged Sword in Cancer. ERK-Dependent Apoptosis as a Potential Therapeutic Strategy for Cancer. *Cells* **10**, (2021).

49. Bolomsky, A. *et al.* MCL-1 inhibitors, fast-lane development of a new class of anti-cancer agents. *J. Hematol. Oncol.* **13**, 173 (2020).

50. Stine, Z. E., Walton, Z. E., Altman, B. J., Hsieh, A. L. & Dang, C. V. MYC, Metabolism, and Cancer. *Cancer Discov.* **5**, 1024 (2015).

51. Lee, T., Yao, G., Nevins, J. & You, L. Sensing and Integration of Erk and PI3K Signals by Myc. *PLOS Comput. Biol.* **4**, e1000013 (2008).

52. Zuo, Z. *et al.* ERK and c-Myc signaling in host-derived tumor endothelial cells is essential for solid tumor growth. *Proc. Natl. Acad. Sci. U. S. A.* **120**, e2211927120 (2023).

53. Dittmer, J. The Biology of the Ets1 Proto-Oncogene. *Mol. Cancer 2003 21* **2**, 1–21 (2003).

54. Plotnik, J. P., Budka, J. A., Ferris, M. W. & Hollenhorst, P. C. ETS1 is a genome-wide effector of RAS/ERK signaling in epithelial cells. *Nucleic Acids Res.* **42**, 11928 (2014).

55. Stamenkovic, I. Matrix metalloproteinases in tumor invasion and metastasis. *Semin. Cancer Biol.* **10**, 415–433 (2000).

56. Das, A., Monteiro, M., Barai, A., Kumar, S. & Sen, S. MMP proteolytic activity regulates cancer invasiveness by modulating integrins. *Sci. Reports 2017 71* **7**, 1–13 (2017).

57. Jiang, L. *et al.* Overexpression of MEKK2 is associated with colorectal carcinogenesis. *Oncol. Lett.* **6**, 1333 (2013).

58. Cheng, J. *et al.* Mip1, an MEKK2-Interacting Protein, Controls MEKK2 Dimerization and Activation. *Mol. Cell. Biol.* **25**, 5955–5964 (2005).

59. Matitau, A. E. & Scheid, M. P. Phosphorylation of MEKK3 at threonine 294 promotes 14-3-3 association to inhibit nuclear factor κB activation. *J. Biol. Chem.* **283**, 13261–13268 (2008).

60. Chang, X. *et al.* The Kinases MEKK2 and MEKK3 Regulate Transforming Growth Factor-β-Mediated Helper T Cell Differentiation. *Immunity* **34**, 201–212 (2011).

61. Naor, Z., Benard, O. & Seger, R. Activation of MAPK Cascades by G-protein-coupled Receptors: The Case of Gonadotropin-releasing Hormone Receptor. *Trends Endocrinol. Metab.* **11**, 91–99 (2000).

62. Lu, J. *et al.* MEKK2 and MEKK3 suppress Hedgehog pathway-dependent medulloblastoma by inhibiting GLI1 function. *Oncogene* **37**, 3864–3878 (2018).

63. Matitau, A. E., Gabor, T. V., Gill, R. M. & Scheid, M. P. MEKK2 kinase association with 14-3-3 protein regulates activation of c-Jun N-terminal kinase. *J. Biol. Chem.* **288**, 28293–28302 (2013).

64. Zhang, D. *et al.* Identification of MEKK2/3 serine phosphorylation site targeted by the Toll-like receptor and stress pathways. *EMBO J.* **25**, 97–107 (2006).

65. Takeda, A. *et al.* Ubiquitin-dependent regulation of MEKK 2/3- MEK 5- ERK 5 signaling module by XIAP and c IAP 1 . *EMBO J.* **33**, 1784–1801 (2014).

66. Roux, P. P. & Blenis, J. ERK and p38 MAPK-Activated Protein Kinases: a Family of Protein Kinases with Diverse Biological Functions. *Microbiol. Mol. Biol. Rev.* **68**, 320 (2004).

67. Fritz, A. *et al.* Phosphorylation of serine 526 is required for MEKK3 activity, and

association with 14-3-3 blocks dephosphorylation. *J. Biol. Chem.* **281**, 6236–6245 (2006).

68. Park, M. H. & Hong, J. T. Roles of NF-κB in Cancer and Inflammatory Diseases and Their Therapeutic Approaches. *Cells* **5**, (2016).

69. Lu, Z. & Xu, S. ERK1/2 MAP kinases in cell survival and apoptosis. *IUBMB Life* **58**, 621–631 (2006).

70. Chayama, K. *et al.* Role of MEKK2-MEK5 in the regulation of TNF-α geneexpression and MEKK2-MKK7 in the activation of c-Jun N-terminalkinase in mast cells. *Proc. Natl. Acad. Sci. U. S. A.* **98**, 4599 (2001).

71. T, M. *et al.* A novel SAPK/JNK kinase, MKK7, stimulated by TNFalpha and cellular stresses. *EMBO J.* **16**, 7045–7053 (1997).

72. Lin, A. Activation of the JNK signaling pathway: breaking the brake on apoptosis. *Bioessays* **25**, 17–24 (2003).

73. Sun, W. *et al.* MEK Kinase 2 and the Adaptor Protein Lad Regulate Extracellular Signal-Regulated Kinase 5 Activation by Epidermal Growth Factor via Src. *Mol. Cell. Biol.* **23**, 2298 (2003).

74. Cook, S. J. & Lochhead, P. A. ERK5 Signalling and Resistance to ERK1/2 Pathway Therapeutics: The Path Less Travelled? *Front. Cell Dev. Biol.* **10**, (2022).

75. Paudel, R., Fusi, L. & Schmidt, M. The MEK5/ERK5 Pathway in Health and Disease. *Int. J. Mol. Sci.* **22**, (2021).

76. Nishimoto, S. & Nishida, E. MAPK signalling: ERK5 versus ERK1/2. *EMBO Rep.* **7**, 782 (2006).

77. Rose, B. A., Force, T. & Wang, Y. Mitogen-Activated Protein Kinase Signaling in the Heart: Angels Versus Demons in a Heart-Breaking Tale. *Physiol. Rev.* **90**, 1507–1546 (2010).

78. Nakamura, K. & Johnson, G. L. PB1 domains of MEKK2 and MEKK3 interact with the MEK5 PB1 domain for activation of the ERK5 pathway. *J. Biol. Chem.* **278**, 36989–36992 (2003).

79. Nakamura, K., Uhlik, M. T., Johnson, N. L., Hahn, K. M. & Johnson, G. L. PB1 domain-dependent signaling complex is required for extracellular signal-regulated kinase 5 activation. *Mol. Cell. Biol.* **26**, 2065–2079 (2006).

80. Jiang, W. *et al.* Extracellular signal regulated kinase 5 promotes cell migration, invasion and lung metastasis in a FAK-dependent manner. *Protein Cell* **11**, 825 (2020).

81. Lu, J. *et al.* MEKK2 and MEKK3 orchestrate multiple signals to regulate Hippo pathway. *J. Biol. Chem.* **296**, 100400 (2021).

82. Raucci, A., Laplantine, E., Mansukhani, A. & Basilico, C. Activation of the ERK1/2 and p38 Mitogen-activated Protein Kinase Pathways Mediates Fibroblast Growth Factor-induced Growth Arrest of Chondrocytes. *J. Biol. Chem.* **279**, 1747–1756 (2004).

83. Meloche, S. & Pouysségur, J. The ERK1/2 mitogen-activated protein kinase pathway as a master regulator of the G1- to S-phase transition. *Oncogene 2007 2622* **26**, 3227–3239 (2007).

84. Cuadrado, A. & Nebreda, A. R. Mechanisms and functions of p38 MAPK signalling. *Biochem. J.* **429**, 403–417 (2010).

85. Ono, K. & Han, J. The p38 signal transduction pathway: activation and function. *Cell. Signal.* **12**, 1–13 (2000).

86. Remy, G. *et al.* Differential activation of p38MAPK isoforms by MKK6 and MKK3. *Cell. Signal.* **22**, 660–667 (2010).

87. Kolch, W. Meaningful relationships : the regulation of the Ras/Raf/MEK/ERK pathway by protein interactions. *Biochem. J* **351**, 289–305 (2000).

88. Chuang, H. C., Wang, X. & Tan, T. H. MAP4K Family Kinases in Immunity and Inflammation. *Adv. Immunol.* **129**, 277–314 (2016).

89. Hamm, H. E. How activated receptors couple to G proteins. *Proc. Natl. Acad. Sci. U. S. A.* **98**, 4819–4821 (2001).

90. Rosenbaum, D. M., Rasmussen, S. G. F. & Kobilka, B. K. The structure and function of G-protein-coupled receptors. *Nature* **459**, 356 (2009).

91. Goldsmith, Z. G. & Dhanasekaran, D. N. G Protein regulation of MAPK networks. *Oncogene 2007 2622* **26**, 3122–3142 (2007).

92. Cheng, J. *et al.* Dimerization through the catalytic domain is essential for MEKK2 activation. *J. Biol. Chem.* **280**, 13477–13482 (2005).

93. Sun, W. *et al.* Protein Phosphatase 2A Acts as a Mitogen-activated Protein Kinase Kinase Kinase 3 (MEKK3) Phosphatase to Inhibit Lysophosphatidic Acid-induced IκB Kinase β/Nuclear Factor-κB Activation. *J. Biol. Chem.* **285**, 21341 (2010).

94. Van Aller, G. S. *et al.* Structure-Based Design of a Novel SMYD3 Inhibitor that Bridges the SAM-and MEKK2-Binding Pockets. *Structure* **24**, 774–781 (2016).

95. Mazur, P. K. *et al.* SMYD3 links lysine methylation of MAP3K2 to Ras-driven cancer. *Nature* **510**, 283–287 (2014).

96. Hasan, R. *et al.* Mitogen activated protein kinase kinase kinase 3 (MAP3K3/MEKK3) overexpression is an early event in esophageal tumorigenesis and is a predictor of poor disease prognosis. *BMC Cancer* **14**, (2014).

97. Mirza, A. A., Kahle, M. P., Ameka, M., Campbell, E. M. & Cuevas, B. D. MEKK2 regulates focal adhesion stability and motility in invasive breast cancer cells. *Biochim. Biophys. Acta - Mol. Cell Res.* **1843**, 945–954 (2014).

98. Cazares, L. H. *et al.* Imaging mass spectrometry of a specific fragment of mitogen-activated protein kinase/extracellular signal-regulated kinase kinase kinase 2 discriminates cancer from uninvolved prostate tissue. *Clin. Cancer Res.* **15**, 5541–5551 (2009).

99. Hoang, V. T. *et al.* MEK5-ERK5 Signaling in Cancer: Implications for Targeted Therapy. *Cancer Lett.* **392**, 51 (2017).

100. Chen, X., Duan, N., Zhang, C. & Zhang, W. Survivin and Tumorigenesis: Molecular Mechanisms and Therapeutic Strategies. *J. Cancer* **7**, 314 (2016).

101. Cao, X. Q., Lu, H. S., Zhang, L., Chen, L. L. & Gan, M. F. MEKK3 and survivin expression in cervical cancer: association with clinicopathological factors and prognosis. *Asian Pac. J. Cancer Prev.* **15**, 5271–5276 (2014).

102. Lu, H. *et al.* The expression and role of MEKK3 in renal clear cell carcinoma. *Anat. Rec. (Hoboken).* **298**, 727–734 (2015).

103. Robinson, R. L. *et al.* Comparative STAT3-regulated gene expression profile in renal cell carcinoma subtypes. *Front. Oncol.* **9**, 72 (2019).

104. Samanta, A. K., Huang, H. J., Bast, R. C. & Liao, W. S. L. Overexpression of MEKK3 confers resistance to apoptosis through activation of NFkappaB. *J. Biol. Chem.* **279**, 7576–7583 (2004).

105. Zhang, Y. *et al.* Overexpression of MAP3K3 promotes tumour growth through activation of the NF-κB signalling pathway in ovarian carcinoma. *Sci. Reports 2019 91* **9**, 1–13 (2019).

106. He, Y. *et al.* MAP3K3 expression in tumor cells and tumor-infiltrating lymphocytes is correlated with favorable patient survival in lung cancer. *Sci. Reports 2015 51* **5**, 1–13 (2015).

107. Pennington, K., Chan, T., Torres, M. & Andersen, J. The dynamic and stress-adaptive signaling hub of 14-3-3: emerging mechanisms of regulation and context-dependent protein–protein interactions. *Oncogene* **37**, 5587–5604 (2018).

108. Pozuelo-Rubio, M. 14-3-3 Proteins are Regulators of Autophagy. *Cells* **1**, 754 (2012).

109. Obsilova, V. & Obsil, T. Structural insights into the functional roles of 14-3-3 proteins. *Front. Mol. Biosci.* **9**, (2022).

110. Stevers, L. M. *et al.* Modulators of 14-3-3 Protein−Protein Interactions. *J. Med. Chem.* **61**, 3755–3778 (2017).

111. Madeira, F. *et al.* 14-3-3-Pred: Improved methods to predict 14-3-3-binding phosphopeptides. *Bioinformatics* **31**, 2276–2283 (2015).

112. Johnson, C. *et al.* Bioinformatic and experimental survey of 14-3-3-binding sites. *Biochem. J.* **427**, 69–78 (2010).

113. Sluchanko, N. N. & Gusev, N. B. Oligomeric structure of 14-3-3 protein: What do we know about monomers? *FEBS Lett.* **586**, 4249–4256 (2012).

114. Gogl, G. *et al.* Hierarchized phosphotarget binding by the seven human 14-3-3 isoforms. *Nat. Commun. 2021 121* **12**, 1–12 (2021).

115. Kundu, A. *et al.* 14-3-3 proteins protect AMPK-phosphorylated ten-eleven translocation-2

(TET2) from PP2A-mediated dephosphorylation. *J. Biol. Chem.* **295**, 1754 (2020).

116. Fanger, G. R. *et al.* 14-3-3 Proteins Interact with Specific MEK Kinases. *J. Biol. Chem.* **273**, 3476–3483 (1998).

117. Bernard, B. J., Nigam, N., Burkitt, K. & Saloura, V. SMYD3: a regulator of epigenetic and signaling pathways in cancer. *Clin. Epigenetics* **13**, (2021).

118. Roeder, S. *et al.* SAM levels, gene expression of SAM synthetase, methionine synthase and ACC oxidase, and ethylene emission from N. suaveolens flowers. *Plant Mol. Biol.* **70**, 535 (2009).

119. Sun, J., Shi, F. & Yang, N. Exploration of the Substrate Preference of Lysine Methyltransferase SMYD3 by Molecular Dynamics Simulations. *ACS Omega* **4**, 19573–19581 (2019).

120. Wagner, T., Robaa, D., Sippl, W. & Jung, M. Mind the Methyl: Methyllysine Binding Proteins in Epigenetic Regulation. *ChemMedChem* **9**, 466–483 (2014).

121. Giakountis, A., Moulos, P., Sarris, M. E., Hatzis, P. & Talianidis, I. Smyd3-associated regulatory pathways in cancer. *Semin. Cancer Biol.* **42**, 70–80 (2017).

122. Bottino, C., Peserico, A., Simone, C. & Caretti, G. SMYD3: An Oncogenic Driver Targeting Epigenetic Regulation and Signaling Pathways. *Cancers (Basel).* **12**, (2020).

123. Kannan, S., Shaik Syed Ali, P. & Sheeza, A. Short report - Lethal and aggressive pancreatic cancer: molecular pathogenesis, cellular heterogeneity, and biomarkers of pancreatic ductal adenocarcinoma. *Eur. Rev. Med. Pharmacol. Sci.* **26**, 1017–1019 (2022).

124. Sarantis, P., Koustas, E., Papadimitropoulou, A., Papavassiliou, A. G. & Karamouzis, M. V. Pancreatic ductal adenocarcinoma: Treatment hurdles, tumor microenvironment and immunotherapy. *World J. Gastrointest. Oncol.* **12**, 173 (2020).

125. Xue, J. & Zhang, F. LncRNA LINC00511 plays an oncogenic role in lung adenocarcinoma by regulating PKM2 expression via sponging miR-625-5p. *Thorac. cancer* **11**, 2570–2579 (2020).

126. Sanese, P., Fasano, C. & Simone, C. Playing on the Dark Side: SMYD3 Acts as a Cancer Genome Keeper in Gastrointestinal Malignancies. *Cancers (Basel).* **13**, (2021).

127. Wang, Y. *et al.* Amplification of SMYD3 promotes tumorigenicity and intrahepatic metastasis of hepatocellular carcinoma via upregulation of CDK2 and MMP2. *Oncogene 2019 3825* **38**, 4948–4961 (2019).

128. Moore, K. E. & Gozani, O. An Unexpected Journey: Lysine Methylation Across the Proteome. *Biochim. Biophys. Acta* **1839**, 1395 (2014).

129. Lanouette, S., Mongeon, V., Figeys, D. & Couture, J. F. The functional diversity of protein lysine methylation. *Mol. Syst. Biol.* **10**, 724 (2014).

130. Gradl, S. *et al.* Discovery of the SMYD3 Inhibitor BAY-6035 Using Thermal Shift Assay (TSA)-Based High-Throughput Screening. *SLAS Discov.* **26**, 947–960 (2021).

131. Johari, Y. B. *et al.* Engineering of the CMV promoter for controlled expression of recombinant genes in HEK293 cells. *Biotechnol. J.* **17**, (2022).

132. Fu, W. *et al.* Structural basis for substrate preference of SMYD3, a SET domain-containing protein lysine methyltransferase. *J. Biol. Chem.* **291**, 9173–9180 (2016).

133. Chen, Z., Zhou, Y., Zhang, Z. & Song, J. Towards more accurate prediction of ubiquitination sites: a comprehensive review of current methods, tools and features. *Brief. Bioinform.* **16**, 640–657 (2015).

134. Blount, J. R., Libohova, K., Silva, G. M. & Todi, S. V. Isoleucine 44 Hydrophobic Patch Controls Toxicity of Unanchored, Linear Ubiquitin Chains through NF-κB Signaling. *Cells* **9**, (2020).

135. Mengstie, M. A. & Wondimu, B. Z. Mechanism and Applications of CRISPR/Cas-9-Mediated Genome Editing. *Biologics* **15**, 353 (2021).

136. Merten, O. W., Hebben, M. & Bovolenta, C. Production of lentiviral vectors. *Mol. Ther. Methods Clin. Dev.* **3**, 16017 (2016).

137. Guo, C., Fordjour, F. K., Tsai, S. J., Morrell, J. C. & Gould, S. J. Choice of selectable marker affects recombinant protein expression in cells and exosomes. *J. Biol. Chem.* **297**, (2021).

138. Yang, M. & Huang, C. Z. Mitogen-activated protein kinase signaling pathway and invasion and metastasis of gastric cancer. *World J. Gastroenterol.* **21**, 11673 (2015).

139. Levy, D. *et al.* A proteomic approach for the identification of novel lysine methyltransferase substrates. *Epigenetics and Chromatin* **4**, 1–12 (2011).

140. Cornett, E. M., Ferry, L., Defossez, P. A. & Rothbart, S. B. Lysine methylation regulators moonlighting outside the epigenome. *Mol. Cell* **75**, 1092 (2019).

141. Liu, S., Xiang, X., Gao, X. & Liu, H. Neighborhood Preference of Amino Acids in Protein Structures and its Applications in Protein Structure Assessment. *Sci. Rep.* **10**, (2020).

142. Kumari, M., Arora, P. & Trivedi, R. Epigenetic and metabolic changes in traumatic brain injury. *Epigenetics and Metabolomics* 97–106 (2021) doi:10.1016/B978-0-323-85652-2.00010-5.

143. Ardito, F., Giuliani, M., Perrone, D., Troiano, G. & Muzio, L. Lo. The crucial role of protein phosphorylation in cell signaling and its use as targeted therapy (Review). *Int. J. Mol. Med.* **40**, 271 (2017).

144. Fanger, G. R., Johnson, N. L. & Johnson, G. L. MEK kinases are regulated by EGF and selectively interact with Rac/Cdc42. *EMBO J.* **16**, 4961–4972 (1997).

145. Koujima, T. *et al.* Oncolytic Virus-Mediated Targeting of the ERK Signaling Pathway Inhibits Invasive Propensity in Human Pancreatic Cancer. *Mol. Ther. - Oncolytics* **17**, 107–117 (2020).